DISSERTATIONES
NEUROSCIENTIAE
UNIVERSITATIS
TARTUENSIS
47

KEERTHANA CHITHANATHAN

Distinct roles of miR-146a and miR-146b in neurons and microglia

DISSERTATIONES NEUROSCIENTIAE UNIVERSITATIS TARTUENSIS
47

DISSERTATIONES NEUROSCIENTIAE UNIVERSITATIS TARTUENSIS
47

KEERTHANA CHITHANATHAN

Distinct roles of miR-146a and miR-146b in neurons and microglia

UNIVERSITY OF TARTU
Press
1632

Department of Pharmacology, Institute of Biomedicine and Translational Medicine, University of Tartu, Tartu, Estonia

The dissertation was accepted for the commencement of the degree of Doctor of Philosophy in Neurosciences on April 15th 2025 by the council for the Curriculum of Neurosciences

Supervisors: Professor Emeritus Aleksandr Žarkovski PhD,
Department of Pharmacology, Institute of Biomedicine and Translational Medicine, University of Tartu

Monika Jürgenson, PhD (Neurosciences),
Department of Pharmacology, Institute of Biomedicine and Translational Medicine, University of Tartu

Professor Ana Rebane, PhD,
Department of Biomedicine, Institute of Biomedicine and Translational Medicine, University of Tartu

Professor Li Tian, PhD,
Department of Physiology, Institute of Biomedicine and Translational Medicine, University of Tartu

Reviewers: Indrek Koppel, PhD,
Professor, Head of Department – Department of Genetic ˇ Engineering and Biomedicine, Institute of Chemistry and Biotechnology, Tallinn University of Technology, Tallinn

Aili Tagoma, PhD,
Department of Immunology, Institute of Biomedicine and Translational Medicine, University of Tartu

Opponent: Tomi Rantamäki, Professor (molecular pharmacology), PhD (Pharm.)
Head of Division, Laboratory of Neurotherapeutics, Division of Pharmacology & Pharmacotherapy, Drug Research Program
Faculty of Pharmacy, University of Helsinki, Finland

Commencement: June 9th 2025

This study was supported by the Estonian Research Council personal research funding team grants PRG878 and PRG1259, European Regional Development Fund (Project No. 2014-2020.4.01.15-0012) and Estonian Research Council-European Union Regional Developmental Fund Mobilitas Pluss Program No. MOBTT77.

ISSN 1736-2792 (print)
ISBN 978-9916-27-874-1 (print)
ISSN 2806-2418 (pdf)
ISBN 978-9916-27-875-8 (pdf)

University of Tartu Press
www.tyk.ee

TABLE OF CONTENTS

LIST OF ORIGINAL PUBLICATIONS

I. **Chithanathan K**, Somelar K, Jürgenson M, Žarkovskaja T, Periyasamy K, Yan L, Magilnick N, Boldin MP, Rebane A, Tian L, Zharkovsky A. Enhanced cognition and neurogenesis in miR-146b deficient mice. *Cells.* 2022 Jun 22;11(13):2002.

II. **Chithanathan K**, Jürgenson M, Guha M, Yan L, Žarkovskaja T, Pook M, Magilnick N, Boldin MP, Rebane A, Tian L, Zharkovsky A. Paradoxical attenuation of neuroinflammatory response upon LPS challenge in miR-146b deficient mice. *Frontiers in Immunology*. 2022 Oct 31;13:996415.

III. **Chithanathan K**, Jürgenson M, Ducena K, Remm A, Kask K, Rebane A, Tian L, Zharkovsky A. Elocalcitol mitigates high-fat diet-induced microglial senescence via miR-146a modulation. *Immunity & Ageing*. 2024 Dec; 21(1): 1–21.

Contributions of the author to the original publications:

I. The author has participated in the study design, behavioral experiments, carried out flow cytometry experiments, image and data analysis of immunohistochemistry, performed RT-qPCR, prepared the figures, wrote the original draft of the manuscript and participated in manuscript revision.

II. The author participated in the study design, behavioral experiments, carried out flow cytometry experiments, image and data analysis of immunohistochemistry, performed RT-qPCR, participated in protein expression analysis, prepared the figures, wrote the original draft of the manuscript, and participated in manuscript revision.

III. The author has participated in study design and performed RT-qPCR, flow cytometry, image and data analysis of immunohistochemistry, participated in protein expression analysis, prepared the figures, wrote the original draft of the manuscript and participated in manuscript revision.

ABBREVIATIONS

AB	Antibody
AD	Alzheimer's disease
AGO	Argonaute
AMPA	α-amino-3-hydroxy-5-methyl-4-isoxazolepropionic acid
APOE	Apolipoprotein E
APP	Amyloid precursor protein
ASD	Autism spectrum disorder
BACE1	Beta-site amyloid precursor protein cleaving enzyme 1
BDNF	Brain-derived neurotrophic factor
BrdU	Bromodeoxyuridine
CalB	Calbindin
C/EBPβ	CCAAT-enhancer-binding protein beta
Chr	Chromosome
Ccl5	C-C motif ligand 5
CFC	Contextual fear conditioning
CNS	Central nervous system
Cx3cr1	Chemokine (C-X3-C motif) receptor 1
DCX	Doublecortin (marker for immature neurons)
DROSHA	Drosha ribonuclease III
DGCR8	DiGeorge syndrome critical region 8
EV	Extracellular vesicles
Elo	Elocalcitol
FC	Frontal cortex
FOXO1	Forkhead box O1
GBM	Glioblastoma
GFAP	Glial fibrillary acidic protein
GLAST	Glutamate aspartate transporter
HP	Hippocampus
HT	Hypothalamus
Iba1	Ionized calcium binding adaptor molecule 1
IHC	Immunohistochemistry
IL	Interleukin
IRAK1	Interleukin-1 receptor-associated kinase 1
IRF	Interferon regulatory factor
KLF4	Krüppel-like factor 4
LFD	Low-fat diet
LPS	Lipopolysaccharide
MDD	Major depressive disorder
MHCII	Major histocompatibility complex class II
Mir146a-/-	miR-146a knockout mice
Mir146b-/-	miR-146b knockout mice
miR-146a/b	miR-146a and miR-146b

NeuN	neuronal nuclear antigen
NF-κB	Nuclear factor kappa-light-chain-enhancer of activated B cells
NMDAR	N-methyl-D-aspartate receptor
NAFLD	non-alcoholic fatty liver disease
NORT	Novel object recognition test
NOS3	Nitric oxide synthase 3
nt	Nucleotide
OPC	Oligodendrocyte precursor cell
PD	Parkinson's disease
pri-miRNA	primary miRNA
pre-miRNA	precursor miRNA
p16	Cyclin-dependent kinase inhibitor 2A
p21	Cyclin-dependent kinase inhibitor 1
RT	Room temperature
RT-qPCR	Reverse transcription quantitative polymerase chain reaction
RISC	RNA-induced silencing complex
SASP	Senescence-associated secretory phenotype
SIRT1	Sirtuin 1
SMAD4	Sterile alpha motif domain containing 4A
SNpc	Substantia nigra pars compacta
STAT	Signal transducer and activator of transcription
TGFβ	Transforming growth factor beta
TLR	Toll-like receptor
TNF	Tumor necrosis factor
TNRC6	Trinucleotide Repeat Containing 6
TRAF6	Tumor necrosis factor receptor-associated factor
Vglut2	Vesicular glutamate transporter 2
UTR	Untranslated region
WT	Wild type
XPO5	Exportin-5
ZFP36	Zinc finger protein 36

1. INTRODUCTION

MicroRNAs (miRNAs) are small, non-coding RNAs that are typically about 18-22 nucleotides (nt) in length. These small RNA molecules play a crucial role in regulating gene expression by binding to the 3′ untranslated region (UTR) of their target mRNAs, and inducing mRNA degradation and/or translation inhibition and thereby influence various cellular processes (1,2). Numerous studies show that miRNAs are involved in regulating central nervous system (CNS) processes, such as neural cell proliferation and differentiation (3,4), apoptosis (5), neuroinflammation (6) and synaptic plasticity (7,8), animal behaviors (9), and in several brain pathologies, including neurodevelopmental (10), neurodegenerative (11,12) and psychiatric disorders (13,14).

The miR-146 family consists of two miRNAs, miR-146a-5p (later miR-146a) and miR-146b-5p (later miR-146b), and has gained attention for its role in modulating immune responses in a wide variety of conditions (15–17). These two miRNAs differ only by two nucleotides and are encoded by distinct genes located in different chromosomes (Chr) (18). The expression of miR-146a is mainly induced via nuclear factor kappa B (NF-κB) pathway in canonical inflammation (19), while signal transducer and activator of transcription (STAT)1 and STAT3 have been shown to drive miR-146b expression (20,21). Both miR-146a and miR-146b (miR-146a/b) are known to negatively regulate immune responses and are predicted to target the same or similar sets of genes (18). Two key miRNAs targets are tumor necrosis factor receptor-associated factor 6 (TRAF6) and interleukin-1 receptor-associated kinase (IRAK)1, which are important signaling mediators in the NF-κB pathway (22).

In miR-146 family, miR-146a is well studied in numerous brain pathologies due its predominant role on neuroinflammation (23–26), and high expression in the microglia cells (27). miR-146a regulates inflammation and microglial polarization by downregulating pro-inflammatory cytokines through IRAK1/TRAF6/NF-κB pathways (28), and the miR-146a deficient mice are more vulnerable to inflammatory marker expression upon lipopolysaccharide (LPS) induction (27). Apart from microglial roles, miR-146a has been identified as a significant regulator of cognitive functions (29,30). While miR-146a has been extensively studied, the function of miR-146b remains less explored in the brain. Like miR-146a, miR-146b is also involved in the inhibition of inflammatory responses via suppression of NF-κB signaling (31). However, the crosstalk between miR-146a and miR-146b in the regulation of neuroinflammation has yet to be investigated. Furthermore, the functions of miR-146a/b are mostly studied in the microglial cells, but less in non-immune cells of the brain. Previous research has established a link between NF-κB signaling, aging, and senescence-related mechanisms in the brain (32,33), suggesting a potential interaction with the miR-146 family, but its specific role in senescence remains poorly understood. In our studies, we employed behavioral assays, molecular biology techniques, flow cytometry, and proteomics methods to further characterize the multiple roles of miR-146 family in the brain functions.

2. REVIEW OF LITERATURE

2.1 Introduction to miRNAs and their functions

2.1.1 miRNAs – discovery and biological functions

miRNAs are small, non-coding RNA molecules, usually 18 to 22 nt long. They play a crucial role in gene expression regulation and are found in a wide range of organisms, including plants, animals, and protozoans. Mature miRNAs are involved in the post-transcriptional regulation of gene expression through the repression of the translation or via degradation of target mRNA (Figure 1). Functionally, miRNAs bind to their target mRNAs through partial complementarity, typically within the 3' UTR, where a single miRNA can suppress the expression of multiple mRNAs, and conversely, a single mRNA may be regulated by multiple miRNAs (1,34). Although the highest number of miRNA binding sites have been verified in the 3' UTR of target mRNAs, there is evidence suggesting that miRNAs can also bind to other regions, such as the 5' UTR or the coding sequence (35–37). The predominance of binding in the 3′ UTR likely reflects its role in regulating mRNA stability and translation, as well as the abundance of complementary binding sites in this ribosome-free region (38,39).

The seed sequence, 7–8 nt of the miRNA is highly conserved among homologous metazoan miRNAs, providing perfect complementarity to 3' UTR elements of the target mRNA. Additionally, other supplementary miRNA sequences can also bind to the target mRNA, contributing to the regulatory complexity (40). There are several tools, such as TargetScan and MiRanda, available for prediction of target mRNAs based on miRNA seed sequence and additional features, such as thermodynamic stability and site conservation. However, as the binding region of miRNAs is very short, not all of the predicted targets can be proven experimentally, indicating that they are either very weakly or not influenced in cellular context (41).

The first miRNA, lin-4 was identified in *C. elegans* larvae, where scientists discovered that lin-4 gene does not encode a protein but instead produces small RNA transcripts complementary to the 3' UTR of the lin-14 mRNA (42). Moreover, it was shown that lin-4 reduces the LIN-14 protein level (43). Later, let-7 miRNA was found to control the timing of fate specification of neuronal and hypodermal cells during larval development in *C. elegans* (44,45). Unlike lin-4, which is not conserved in other species, let-7 was found to be evolutionarily conserved across multiple species, including humans, marking a significant discovery in the field of miRNA research (46).

Currently, the miRBase database (www.mirbase.org, version 22) contains 1917 annotated different mature human and 1234 mouse miRNA sequences (accessed on February 1st 2025) (47). However, the function of many of them remains to be discovered. Current knowledge indicates that miRNAs are implicated

in a variety of cellular processes, including differentiation, apoptosis, proliferation, embryonic development, immune response regulation, inflammation, aging, and stress response (48–52).

2.1.2 Biogenesis of miRNAs

miRNAs can be encoded by their own genes with dedicated promotor sequences or in the intronic regions of protein-coding genes. Approximately half of the identified miRNAs, which predominantly originate from introns, are known as intragenic (53). In case of own genes, several miRNAs can be encoded from a single primary transcript. These miRNAs are often related and share their mRNA targets, reflecting their cooperative roles in regulating gene networks (54). In addition, miRNAs can be grouped into families based on their targeting properties, which depend primarily on the identity of their seed region. Members of the same seed family are usually evolutionarily related and often target the same set of genes (1).

The biogenesis of miRNA is a complex process that involves multiple steps from transcription in the nucleus to maturation of miRNA in the cytoplasm. The miRNA biogenesis occurs via two pathways: canonical and non-canonical, involving distinct mechanisms and components. Both pathways start in the nucleus, where RNA Polymerase II transcribes the primary miRNA (pri-miRNA) transcript, which forms a stem-loop structure (55). In canonical pathway, this structure is recognized by the microprocessor complex that consists of Drosha ribonuclease III (DROSHA), an RNase III enzyme responsible for cleaving the pri-miRNA into a precursor miRNA (pre-miRNA), and DiGeorge Syndrome Critical Region 8 (DGCR8), a double-stranded RNA-binding protein that acts as a co-factor for DROSHA (56). The microprocessor complex cleaves the pri-miRNA recognizing RNA secondary structure, generating a ~80 nucleotide pre-miRNA with stem-loop structure, a 5′ phosphate, and a ~2 nt 3′ overhang (57). The pre-miRNA is actively transported from the nucleus to the cytoplasm by exportin-5 (XPO5) bound to Ran-GTP (58). In the cytoplasm, the pre-miRNA is further processed by DICER into miRNA duplex. The miRNA duplex is then loaded onto of the argonaute (AGO1-4) proteins, most often AGO2. AGO2 preferentially binds one of the strands of the duplex known as the guide strand, forming the RNA induced silencing complex (RISC), while the other passenger strand is released and degraded (59,60). The guide strand, together with AGO2 and trinucleotide repeat-containing protein 6 (TNRC6), forms RISC, facilitates post-transcriptional gene silencing by binding to complementary sequences on target mRNAs, usually within their 3'UTRs. If the complementarity between the miRNA and the mRNA is near-perfect, AGO2 cleaves the mRNA. When the complementarity is imperfect, TNCR6 induces mRNA degradation by initiating mRNA deadenylation and suppression of translation (60). Several studies have shown that deadenylation-mediated mRNA decay is the most common mechanism of miRNA-mediated gene regulation (61,62). When mRNA degradation is

completed, the miRNA remains often intact and can guide the recognition and destruction of additional mRNA molecules (63).

The non-canonical miRNA biosynthesis pathways are either DROSHA (64) or DICER independent. In vertebrates, most of the miRNAs follow canonical biogenesis pathway (65). Despite these alternative processing routes, the fundamental function of miRNAs in gene regulation remains unchanged, as mature miRNAs generated via non-canonical pathways are still incorporated into the RISC complex to mediate post-transcriptional gene silencing (66).

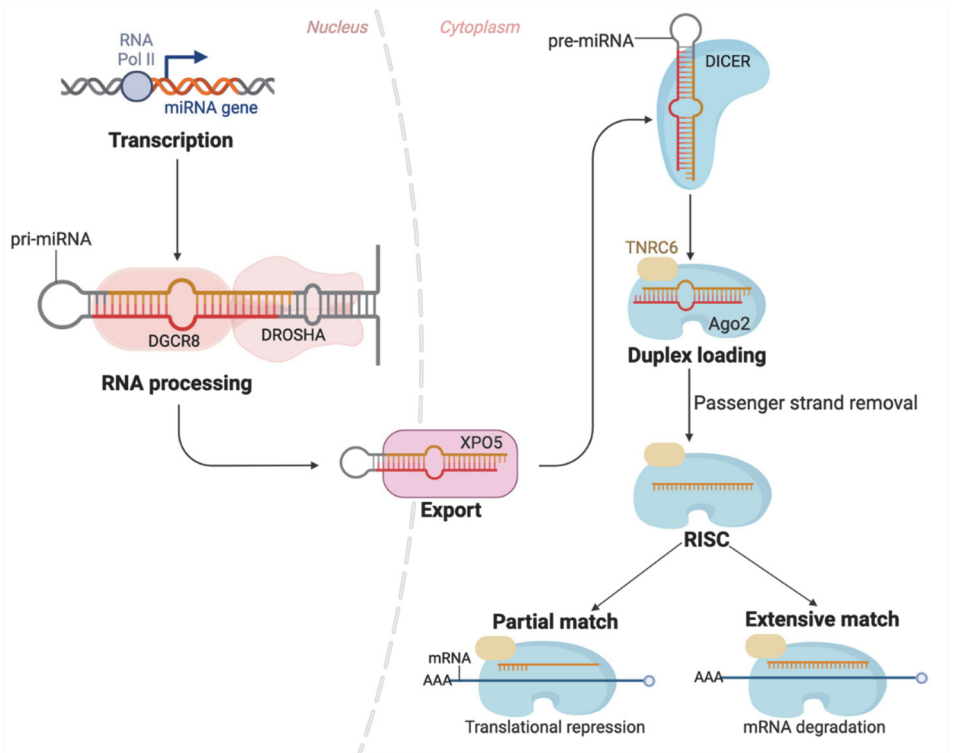

Figure 1: Canonical miRNA biogenesis pathway and biological function. miRNAs are transcribed as pri-miRNA by RNA Polymerase II and processed in the nucleus by the microprocessor complex, composed of DROSHA and DGCR8. The resulting pre-miRNA is exported to the cytoplasm by XPO5, further processed by DICER, generating miRNA duplex. The miRNA duplex is loaded onto AGO2, which preferentially binds to the guide strand, while the passenger strand is degraded. In association with TNRC6, AGO2 forms the RISC complex, which is guided by miRNA to recognize and regulate the target mRNAs. When RISC binds to target mRNA with partial complementarity, TNRC6 facilitates mRNA deadenylation and translational repression, followed by gradual mRNA degradation. In contrast, when RISC binds with high complementarity, AGO2 directly cleaves the mRNA, leading to rapid degradation.

The figure was modified from (60).

2.2 Role of miRNAs in neuronal and microglial cells

2.2.1 The expression of miRNAs in the brain

In the central nervous system (CNS), approximately 70% of all known miRNAs are expressed, suggesting that about 1600 different miRNAs may be present. Brain miRNAs exhibit distinct expression patterns that vary across different cell types, brain regions and developmental stages, highlighting their importance in neurodevelopment and function (67). This diversity is crucial for the specialized functions of various neuronal and non-neuronal cell types within the CNS. For example, already an early study showed that miR-124 is predominantly expressed in neurons and miR-23, -26, and -29 are specifically expressed in astrocytes (68). Some miRNAs, such as miR-155 and miR-146a, have been identified to be highly expressed in microglial cells (69,70). In addition to cell-specific expression, miRNAs may exhibit region-specific expression pattern. For example, miR-132 is particularly enriched in the hippocampus (71), while miR-326 is predominantly expressed in microglia within the brainstem, but is largely absent from spinal microglia, indicating that miR-326 may influence immune responses differently across neuroanatomical structures (72). Along with cell specific expression, neurons also display differential intraneuronal miRNA distribution. For example, miR-125b and miR-132 are enriched in synaptic compartments (73). Other studies have demonstrated that the expression of certain miRNAs changes during development. For instance, in a recent study by Todorov *et al.* a small RNA sequencing of cerebral cortex samples at various developmental stages (E14, E17, and postnatal day P0) demonstrated that the expression of approximately 57% of miRNAs significantly changed during development. This research provided a detailed map of longitudinal changes in miRNA expression patterns during corticogenesis, emphasizing the dynamic regulatory roles of miRNAs in shaping brain development (74).

2.2.2 miRNAs in neurons and microglia and their impact on brain health

miRNAs play crucial roles in the regulation of gene expression and cellular functions in both neurons and microglia. In neuronal cells, miRNAs exhibit unique expression patterns and are critical for neuron development and function. For example, a study analyzing miRNA distribution across different CNS cell types revealed that neuron-enriched miR-376a and miR-434 promote the differentiation of neural stem cells into neurons, while glia-enriched miRNAs, like miR-223 and miR-146a, inhibit this process (75). A unique feature of neuronal miRNAs is their presence not only in the cell body but also in dendrites and axons, enabling them to regulate peripheral protein synthesis in response to synaptic activity. For example, miR-134 restricts dendritic spine growth by repressing Limk1, a key modulator of actin dynamics. This localized and

stimulus-driven miRNA activity highlights their pivotal role in fine-tuning neuronal networks during learning and memory (76).

Microglia cells exhibit a distinct set of miRNAs compared to other CNS cell types. A recent study identified nearly 300 miRNAs upregulated in microglial cell, of which miR-146a, miR-223 and miR-142 were identified as most highly expressed. This unique miRNA signature is crucial for defining microglial identity and function (77). For example, miR-155 and miR-124 have been identified as 'master regulators' of activated and quiescent microglia (78–80), while miR-146a and miR-155 have been shown to regulate immune activation and polarization between pro-inflammatory and anti-inflammatory states, which is essential for resolving inflammation and protecting neuronal health (81,82). Microglial miRNAs also influence phagocytosis, exosome-mediated communication, and the release of cytokines (83).

Given their central regulatory roles, dysregulation of miRNAs in neurons and microglia is recognized factor in CNS pathologies, including Alzheimer's disease (AD), Parkinson's disease (PD), multiple sclerosis, and neuropsychiatric disorders. Specific examples, along with their associated conditions and roles, are summarized in Table 1.

Table 1: Dysregulated miRNAs in neurons and microglia contributing to CNS Pathologies

Disease	miRNA	Function	References
Alzheimer's disease	miR-124	Targets BACE1 mRNA in neurons, contributes to AD	(84)
	miR-155, miR-146a	Modulates microglial response to amyloid beta and influences synaptic pruning	(85,86)
	miR-140-3p and miR-122-5p	Upregulated in AD, reduces neuroprotective protein sAPPα via targeting ADAM10 resulting cognitive decline and impaired microglial function	(87)
Parkinson's disease	miR-126	Upregulated in SNpc dopaminergic neurons; increases vulnerability to neurotoxins	(88)
	miR-146a	Upregulated in response to inflammation; involved in the regulation of Parkin levels	(89)
Schizophrenia	miR-19a	Dysregulated in schizophrenia; associated with cognitive deficits and treatment resistance, found in neuron-derived EVs	(90)
Autism spectrum disorder (ASD)	miR-130a	Inhibits neurite growth and reduces dendritic spine density	(91)
	miR-146a	Overexpression leads to neurite outgrowth and enrichment of ASD-linked genes	(92)

Disease	miRNA	Function	References
Major depressive disorder	miR-124-3p	Downregulates Gria3 and Gria4 receptors, affecting AMPA receptor leading to synaptic dysfunction in neurons	(93)
	miR- 146a/b, 425-3p and 24-3p	Markers of antidepressant response	(14)

Abbreviations used in the table: BACE: Beta-site amyloid precursor protein cleaving enzyme; APP: Amyloid precursor protein; ADAM10: A disintegrin and metalloproteinase domain-containing protein 10; SNpc: Substantia nigra pars compacta; EV: Extracellular vesicles; AMPA: α-amino-3-hydroxy-5-methyl-4-isoxazolepropionic acid.

2.3 The miR-146 family and CNS associated functions

2.3.1 The miR-146 family

Among other miRNAs implicated in brain functions, the miR-146 family has gained significant attention due to its critical role in neuroinflammation, immune regulation, and microglial activity. miR-146a (named as miR-146) was identified first in a study by Mariana Lagos-Quintana *et al.* published in 2002, through a systematic approach involving the cloning of small RNAs from various mouse tissues, particularly cardiac tissue (94). In the subsequent study by Cai *et al.* in 2005, the researchers utilized cDNA libraries prepared from size-selected small RNAs derived from the human BC-1, body cavity-based lymphoma-1 cell line. They classified the sequences using analyses of the GenBank database and the Sanger miRNA registry, identifying 34 cellular miRNAs, including miR-146a. This study emphasized that miR-146a is also conserved in human (95). In 2006, Taganov *et al.* discovered that miR-146 family comprises of miR-146a and miR-146b, which are induced in human monocytes upon exposure to endotoxins and pro-inflammatory cytokines and found that miR-146a/b function as negative regulators in immune signaling via downregulation of IRAK1 and TRAF6 protein levels in monocytes (96). Further studies have identified toll-like receptor 4 (TLR4) as an additional target of miR-146a/b, reinforcing their role in regulating innate immune responses (97,98). Following, the foundational work of Taganov *et al.* miR-146a has gained enormous interest in various immune system diseases and conditions, but also in neurobiology.

2.3.2 Genomic location and structure

The genomic organization of the *MIR146A* and *MIR146B* genes has been reported to be distinct across species. In humans, the *MIR146A* gene is found within area encoding a larger long noncoding RNA in chr5, while *MIR146B* is located in human chr10. In mouse, miR-146a is encoded by chr11, and miR-146b by chr19. The mature miRNA sequences of miR-146a/b is highly conserved across species

and share their seed sequence that's allows them to target similar mRNAs. However, they differ by two nucleotides in their supplementary region, which may affect their specificity and binding affinity for some targets (Figure 2). From two strands, the 5p strand is considered as the guide strand, responsible for the regulatory functions of the miR-146a, while the 3p strand is the passenger strand that is usually degraded and less frequently studied (99).

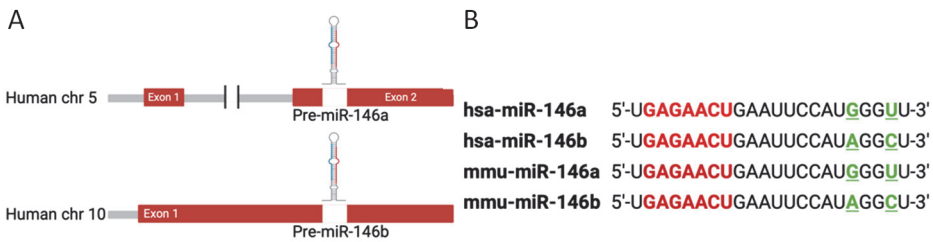

Figure 2: Genomic organization human *MIR146A* and *MIR146B* genes and sequences of mature miR-146a/b. (A) The human pre-miR-146a encoding region is located on human chr5 within exon 2, while pre-miR-146b encoding region is located in an intergenic region of human chr10. (B) The sequences of mature miR-146a/b from human (hsa) and mouse (mmu) are shown. The seed region is highlighted in red and bases 2–8 from the 5' end. Differences in the 3' ends of miR-146a/b are highlighted in green.

2.3.3 Transcriptional regulation of miR-146a/b

In the original study by Taganov, the *MIR146A* and *MIR146B* genes were found to be induced by LPS and miR-146a was proven to be NF-κB dependent. The authors identified three putative binding sites for the NF-κB upstream of the first exon of *MIR146A* and verified in luciferase assay that two of them are important for miR-146a expression. Additionally, two IRF3/IRF7 binding sites were predicted in the MIR146A promoter region. However, mutating these sites did not significantly affect miR-146a induction in reporter assays, suggesting that IRF3/7 does not play a primary role in miR-146a transcription *in vitro* (96). The study by Liu *et al.* indicated that FOXP3 binds directly to the promoter region of *MIR146A*, but not to that of *MIR146B*, indicating that FOXP3 induces the expression of miR-146a, which then negatively regulates the NF-κB activation through the inhibition of IRAK1 and TRAF6 (100). In addition, the transcription factor Ets-1 contributed to the regulation of miR-146a. Interestingly, genetic variant (rs57095329) in the *MIR146A* promoter was shown to reduce Ets-1 binding and was suggested to decrease expression of miR-146a in systemic lupus erythematosus (SLE) patients, which then may lead to the abnormal activation of the type I interferon pathway associated with SLE (101). In melanoma cells, it has been found that increased BRAF-MEK-ERK signaling results in activation and recruitment of MYC to the miR-146a promoter, which stimulates miR-146a transcription (102).

Less is known about the regulation of miR-146b expression, however, a study by Curtale *et al.* demonstrated that IL-10 induces recruitment of polymerase II to the miR-146b promoter most probably via transcription factor STAT3 (103). In addition, it has been shown that miR-146b is transcriptionally regulated by the C/EBPβ transcription factor C/EBPβ LAP2 isoform, which positively influences its expression in esophageal squamous cell carcinoma (104), and transcription factor SP1 in colorectal cancer cells (105).

2.4 Role of miR-146a in brain functions

miR-146a is one of the most widely studied miRNAs in the brain, and recent literature suggests that miR-146a is a wide-reaching neuroinflammatory regulator. miR-146a is primarily recognized for its role as a negative regulator of inflammatory responses in the CNS and has been implicated in various neurological disorders. Again, also in the brain, miR-146a has been shown to target IRAK1 and TRAF6, which helps to attenuate the secretion of pro-inflammatory cytokines, thereby protecting neurons from inflammation-induced damage (106,107). A substantial body of evidence suggests that miR-146a plays a significant role almost all major neurological disorders, encompassing cerebrovascular diseases, neurodegenerative conditions, neuroautoimmune disorders, CNS viral infections, peripheral neuropathy, and brain tumors (108). However, our focus is on the role of miR-146a, specifically its impact on neuroinflammation and metabolic stress-induced microglial senescence.

2.4.1 Functions of miR-146a in microglial cells

In the brain, miR-146a is particularly enriched in microglia cells (27), which are antigen presenting cells capable of expressing major histocompatibility complex (MHC) proteins and secretion of both pro-inflammatory cytokines, such as IL-1β, and TNF, and anti-inflammatory cytokines. Like in peripheral immune cells, miR-146a is also significantly upregulated in microglial cells in response to stimulation with LPS followed by negative feedback regulation of neuroinflammation via TLR4/NF-κB signaling pathway (109). Both TLR2 and TLR4 activation were shown to increase miR-146a level in microglia. In response to TLR2 stimulation, miR-146a suppressed inflammatory responses, including NF-κB and JAK-STAT signaling pathways. Two phagocytic mediators of the oxidative burst, cytochrome b-245, alpha polypeptide and nitric oxide synthase 3, were shown to be suppressed by miR-146a (110). In addition, miR-146a can switch microglial phenotypes promoting neuroprotection and reduced cognitive deficits (111). In response to LPS and cuprizone treatment, miR-146a knockout mice exhibited altered inflammatory protein responses and impaired phagocytosis in microglia, suggesting miR-146a is crucial for proper proteomic adaptation during inflammation and demyelination. (27). Microglia also secrete exosomes containing miR-146a, which have been shown to enter to neurons, where miR-146a

targets Krüppel-like factor (KLF) 4, thereby suppressing neurogenesis and contributing to cognitive deficits seen in conditions like depression (112). Zhao *et al.* have reported that miR-146a knockout mice exhibit a mild reduction in exploratory locomotor activity and an increase in anxiety-like behavior, while other cognitive functions remain unaffected. Additionally, the absence of miR-146a led to elevated levels of inflammatory cytokines and markers of oxidative stress in the middle-aged mice brain, indicating that miR-146a is crucial for regulating neuroinflammation and maintaining oxidative balance even without external inflammatory stimuli (113). Interestingly, in glioma progression, miR-146a shows tumor suppressor function via targeting sterile alpha motif domain containing 4A (SMAD4), a key mediator of the transforming growth factor beta (TGF-β) signaling pathway, thereby influencing microglial behavior in the tumor microenvironment (114). Thus, miR-146a is crucial for regulating neuroinflammation and microglial function, with potential therapeutic implications for neuroinflammatory diseases.

2.4.2 Role of miR-146a in metabolic stress-induced senescence

The global rise in obesity rates has become a significant public health concern, closely associated with an increased risk of metabolic disorders such as insulin resistance, cardiovascular diseases, chronic inflammation, cancer, and neuropsychiatric disorders (115–118). miR-146a plays a critical role in the body's response to metabolic stress, both in peripheral systems and the brain. In the periphery, miR-146a expression has been shown to be decreased in high fat-induced non-alcoholic fatty liver disease (NAFLD) mouse model (119). *In vitro*, overexpression of miR-146a mimics suppresses hepatic stellate cell activation and fibrotic signaling pathways, consistent with *in vivo* findings in nonalcoholic fibrosing steatohepatitis models where miR-146a is downregulated and regulates fibrosis-related pathways (120).

In the brain, chronic low-grade inflammation, often associated with obesity and metabolic disorders, leads to the downregulation of miR-146a. This is observed in mice upon chronic high-fat diet (HFD) in the nucleus accumbens, a region involved in metabolism and energy balance (121). In models of chronic type 2 diabetes mellitus, decreased levels of miR-146a negatively correlated with elevated inflammatory mediators (COX-2, TNF-α, IL-1β) and markers of oxidative stress, while reduced antioxidant proteins positively correlated with miR-146a levels in the hippocampus (HP) and cerebral cortex (122). Under high glucose conditions or glucose fluctuations, microglia tend to polarize toward the pro-inflammatory M1 phenotype, which is associated with increased production of pro-inflammatory cytokines and downregulation of miR-146a. However, when miR-146a was overexpressed under glucose stress, BV2 microglial cells shifted toward the anti-inflammatory M2 phenotype, accompanied by an increase in IL-10 levels (82).

It has been reported that obesity leads to the accumulation of senescent cells in the brain (123). Senescent cells display markers, including telomere-associated

DNA damage foci (124), increased activity of lysosomal senescence-associated β-galactosidase (SA-β-gal) (125), and increased expression of the cyclin-dependent kinase inhibitor proteins, p16Ink4a (p16) and p21Cip1 (p21) (126). Additionally, senescent cells secrete several inflammatory cytokines, chemokines, and SASP (the senescence-associated secretory phenotype) (127). Among these, the pro-inflammatory components of SASP contribute to chronic systemic low-grade inflammation, called "inflammaging," which is one of the main risk factors for the development of age-related diseases (128). HFD can also lead to increased lipid content in cells, triggering oxidative stress and senescence in the brain, especially in areas like the HP and amygdala, along with increased microglial priming and impairs phagocytosis (129). The HFD also induces microglial senescence and contributes to increased pro-inflammatory markers, such as IL-6, IL-1β, and TNFα, via the NF-κB signaling pathway (129). miR-146a is also found to be increased in senescent cells (130) and suppress oxidative stress (131). however, the relationship between metabolic stress and microglial senescence that may be influenced by miR-146a in brain remains unexplored.

2.4.3 Functional role of miR-146a in neuronal cells

In the mouse brain, miR-146a is expressed in the cortex, HP, and amygdala as evidenced by *in situ* hybridization. During embryonic development, miR-146a initially exhibits high and widespread expression, which becomes restricted to some cellular layers in postnatal brain regions (132). Another study demonstrates that miR-146a is essential for the differentiation of neural stem cells, promoting the transition from progenitor cells to mature neurons by targeting pathways, such as Notch1, which is crucial for cell cycle exit and neuronal identity (133). In embryonic stages, miR-146a loss impairs the differentiation of radial glial cells and disrupts the neurogenesis process. More specifically, the absence of miR-146a leads to significant developmental defects, including impaired neurite extension detected at embryonic day 14.5 (E14.5). However, these effects do not persist into later developmental stages, as there is no observed change in neuronal ratios in the adult brain. Interestingly, behavioral assessments reveal that mice lacking miR-146a exhibit notable learning and memory deficits at three months of age, suggesting that miR-146a is essential for early neural lineage determination and maintaining cognitive functions thorough adulthood. miR-146a modulates the expression of Klf4 and thereby influence adult hippocampal neurogenesis and cognitive functions in the mouse model of AD (134). Additionally, overexpression of miR-146a in primary hippocampal neurons leads to downregulation of N-methyl-D-aspartate receptor (NMDA) subunits, GluN2A and GluN2B, further injecting miR-146 into rat hippocampus caused cognitive deficits and decreased protein levels of NMDA receptor subunits (30). A study identified miR-146a, as a negative regulator of glial cell line-derived neurotrophic factor (Gdnf) via interaction with its 3'UTR (135). Gdnf is an essential neurotrophic factor implicated in dopaminergic neuron survival and neuroprotection, maintaining the nigrostriatal dopamine system, protection against neurotoxic

damage in Parkinson's disease models (136). This regulation highlights a potential mechanism by which miR-146a influences neuronal survival and function, particularly in conditions affecting the dopaminergic system.

2.5 Role of miR-146b in brain functions

The function of miR-146b in the nervous system has been less explored compared to miR-146a, with most existing literature focusing on its roles in glioma and neuroinflammation. Like miR-146a, miR-146b has been shown to be upregulated upon LPS treatment in microglial cells. Notably, transfection of miR-146b into microglial cells significantly reduced LPS-induced microglial activation, downregulated IRAK1, and prevented cognitive deficits in models of perinatal inflammation (137). Similarly, overexpression of miR-146b modulated inflammatory responses by suppressing NF-κB signaling in the brain in rat encephalopathy models (31). Furthermore, miR-146b was shown to be upregulated in other neuroinflammatory conditions, such as brain white matter lesions from multiple sclerosis patients and experimental autoimmune encephalomyelitis model in mice (138), as well as in microglia from amyotrophic lateral sclerosis (6). These findings collectively highlight the immunomodulatory and neuroprotective potential of miR-146b in various pathological contexts.

Besides possible function in neuroinflammation, miR-146b may play a significant role in neuronal function and neurodegenerative processes. It has been shown to be expressed at significantly higher levels in the rat HP (139), but lower levels in mature neurons, where it is associated with critical neuronal processes, such as axon guidance in rats (140). The brain-derived neurotrophic factor (BDNF) Val66Met genetic variant leads to lower levels of miR-146b in the HP of mice, accompanied with increased expression of neuronal genes like *Per1* and *Npas4* at mRNA level (141). Given the essential role of BDNF survival and phenotypic maintenance of mature, fully developed neurons, its dysregulation may contribute to neurodegenerative diseases by disrupting these pathways (142). In rats, miR-146b overexpression via lentiviral vectors inhibited the proliferation of primary hippocampal neural stem cells, emphasizing its regulatory role in neurogenesis (143). In neurodegenerative diseases, miR-146b is implicated in AD and PD. miR-146b levels were significantly altered in cerebrospinal fluid extracellular vesicles in AD, influenced by sex and apolipoprotein E (APOE) genotype, with distinct differences between males and females. Pathway analysis linked miR-146b dysregulation to neurodegenerative mechanisms, such as autophagy and senescence (144). Similarly, serum miR-146b levels were markedly decreased in patients with early-stage PD, distinguishing them from healthy controls and highlighting its potential as a biomarker for early detection of the disease (145). Another study demonstrated that low levels of miR-146b, alongside other miRNAs, could effectively differentiate PD from multiple system atrophy (146). miR-146b also may play a pivotal role in neuronal repair and regeneration, particularly in peripheral nerves. Inhibition of miR-146b increased

the proliferation and migration of Schwann cells by enhancing the expression of Klf7, a transcription factor critical for axonal growth. Silencing of miR-146b in rat promoted axonal outgrowth, improved nerve conduction, and enhanced the expression of neuronal markers such as neurofilaments and myelin proteins, underscoring its potential in neuronal repair following sciatic nerve injury (147). In the context of acute ischemic stroke, serum levels of miR-146b are significantly elevated within 24 h after stroke onset (148). In line with this, overexpression of miR-146a/b improved endothelial progenitor cells function and vascular repair by downregulation of IRAK1 and TRAF6, promoting a more favorable environment for cell proliferation and angiogenesis in mice (149). Furthermore, miR-146b has been shown to exert protective effects in rat cerebral infarction models by modulating the SIRT1/FOXO1 signaling pathway, and reducing oxidative stress and neuronal apoptosis (150).

In gliomas, miR-146b is downregulated across all grades, contributing to increased cell proliferation and decreased apoptosis by targeting TRAF6 (151). Other studies highlight that miR-146b negatively regulates glioblastoma cell invasion and migration by targeting matrix metalloproteinases (152) and that miR-146b downregulation is associated with resistance to temozolomide therapy (153). Conversely, there are observations of upregulation of miR-146b in recurrent glioblastoma multiforme cases, where it may contribute to immune suppression and tumor recurrence (154). This suggests a complex role for miR-146b in glioma, where its expression can vary depending on the tumor stage and context.

2.6 Vitamin D analogs and miR-146a

Vitamin D is naturally acquired primarily through ultraviolet B-irradiation induced synthesis in the skin (vitamin D3), and to a lesser extent by food (vitamin D2 and D3) (155). The primary supplemental form of vitamin D3 is also known as cholecalciferol. This form serves as a precursor to the biologically active form of vitamin D, which is 1,25-dihydroxyvitamin D3 (1α,25(OH)2D3) or calcitriol. Calcitriol mediates its biological effects by binding to and activating the vitamin D receptor, a member of the steroid hormone nuclear receptor family that functions as a transcription factor upon activation (156). Calcitriol is also known to impact protein expression, oxidative stress, inflammation, and cellular metabolism through various genomic and non-genomic mechanisms (157). It should be noted that supplemental vitamin D3 exerts its immunomodulatory actions at supraphysiological concentrations, which similarly to the administration of calcitriol, leads to hypercalcemia, hypercalciuria, and renal dysfunctions (158). In the periphery, vitamin D3 treatment induces miR-146a expression in hepatic stellate cells and during skin wound healing in diabetic mice (159). Additionally, vitamin D3 has demonstrated anti-inflammatory effects in TNF-α-stimulated adipocytes and the adipose tissue of inflammatory mouse models, partly by regulating miR-146a expression (160). In the brain, vitamin D has emerged as a neurosteroid hormone and has been shown to act as a regulator of a variety of

brain functions, such as neuroprotection, anti-epileptic and anti-calcification effects, neuro-immunomodulation, and interplay with neurotransmitters and hormones (161). Vitamin D also promotes neuronal differentiation, provides trophic support and improves cognition (162), prevents oxidative stress (163), and is neuroprotective on dopaminergic neurons by attenuating inflammation through shifting microglial polarization from M1 to M2 in PD mouse model (164). Today, more than 3000 synthetic vitamin D analogs have been developed by various pharmaceutical companies and academic research groups, with the main goal to identify compounds with a lower calcemic effect (165). One such analog, Elocalcitol (BXL-628 or Ro-26-9228, referred to as Elo), is a synthetic vitamin D analog derived from calcitriol. The key modification in Elo occurs at the side chain of calcitriol, it features a 2-substituted (2-(5-hydroxy-5,5-dimethylpentyl)) side chain, which alters the interaction with the vitamin D receptor (166,167). Elo has been known for its anti-inflammatory, anti-proliferative, and bone-protective properties in both preclinical and clinical studies (168,169). Although miR-146a and vitamin D are both known to exhibit anti-inflammatory activity, it remains unknown whether the immunomodulatory effects of vitamin D and analogs are mediated through miR-146a.

2.7 Summary of review of literature

Previously, versatile actions of miR-146a have been extensively studied in relation to neuroinflammation, brain tumors, neuron development and some roles in metabolic stress. miR-146a is primarily recognized as a negative regulator of neuroinflammation in the brain and extends its various roles in developmental disorders, like autism, neurodegenerative disorders, like AD, and in brain tumors. Depending on the cellular or pathological environment, miR-146a levels fluctuates. Its expression is mostly upregulated in acute inflammation and downregulated in chronic metabolic stress or neurodegenerative conditions. In microglial cells, miR-146a acts as a negative regulator of immune response, regulates phagocytosis, and promotes microglial polarization to provide neuroprotection. miR-146a is also found in the exosomes secreted by microglia and thereby mediates intercellular communication. It also plays critical roles in neuronal development and more importantly in embryonic development, where its higher expression controls radial glia differentiation and neurogenesis. Loss of miR-146a also affects cognition later in life. In the context of metabolic stress, miR-146a was downregulated in animal HFD and diabetes models, while inflammatory mediators and markers of oxidative stress were elevated. Interestingly, miR-146a knockout mice exhibit increased oxidative stress without any external stimuli. It is also known that factors that influence HFD linked brain damage are oxidative stress and inflammation, of which oxidative stress is the inducer of cellular senescence indicating that neuroinflammation may be closely linked to metabolic dysfunction, underscoring the importance of studies on molecular mechanisms of HFD induced changes in microglia. While miR-146a role in

regulating neuroinflammation and oxidative stress is well-documented, its function in HFD-induced microglial senescence remains unclear.

Besides miR-146a, miR-146b is emerging as a significant player in neuroinflammation, neurodegeneration, and glioma, although its functions remain less explored compared to miR-146a. miR-146b is upregulated in neuroinflammatory conditions and similarly to miR-146a, it targets genes from the NF-κB pathway. Overexpression of miR-146b has been shown to reduce microglial activation, improve cognitive deficits in perinatal inflammation models, and attenuates inflammatory responses in rat encephalopathy models. miR-146b also is expressed in HP and targets genes involved in neuronal processes like axon guidance and neuronal repair. miR-146b is downregulated in case of genetic variants in *BDNF*, and this is associated with dysregulation of neuronal gene expression, while its overexpression inhibits hippocampal neural stem cell proliferation. Although miR-146b has been shown to influence inflammatory pathways and neural stem cells in the brain, the downstream effects on brain cells, as well as to cognitive and behavior phenotypes are not fully elucidated. This leaves a critical gap in understanding how the miR-146b affects neural circuits, inflammatory responses, and cognitive functions. Also, several previous studies have primarily used miR-146b overexpression in disease models, yet the consequences of miR-146b deficiency on neuroinflammation and associated outcomes have not been adequately addressed. This thesis aimed to address these gaps by investigating the distinct roles of miR-146b in cognition, neurogenesis, and inflammation, as well as to study the influence of miR-146a in cellular senescence under conditions of HFD-induced metabolic stress. To achieve this, we used miR-146b and miR-146a knockout mice and interventions, such as systemic LPS, HFD with or without vitamin D analogue, Elo, performed behavioral studies, and examined cellular functions in the brain.

3. AIMS OF THE STUDY

The aim of the study was to elucidate the regulatory roles of the miR-146a/b in cognition, neuroinflammation, and microglial senescence using miR-146b and miR-146a knockout mouse models.

Specific aims of the study were the following:

1. To measure the CNS cell specific expression of miR-146a/b in the mouse brain and to characterize and evaluate the cognitive behavior, brain cell alterations and adult hippocampal neurogenesis using miR-146b deficient mouse model (publication I).
2. To evaluate the impact of microglial expression of miR-146a/b and their crosstalk in the neuroinflammation induced by LPS in miR-146b knockout mice (publication II).
3. To define the role of miR-146a in the hypothalamic cellular senescence upon HFD challenge using miR-146a knockout mice with or without elocalcitol intervention (publication III).

4. MATERIALS AND METHODS

4.1 Experimental design (Publications I–III)

Experimental approach used in the thesis is provided in Figures 3–5.

Publication I:

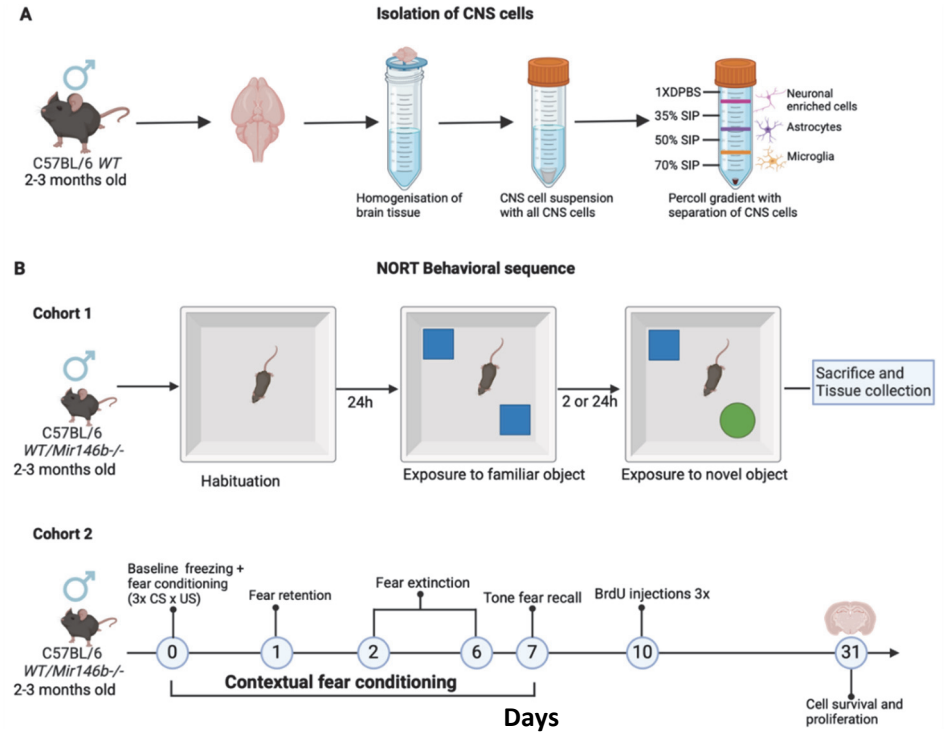

Figure 3: Experimental strategy for publication I. (A) To measure the expression of miR-146a/b in different CNS cell types, *WT* male mouse brains (n = 3) were subjected to percoll gradient centrifugation to isolate microglia, astrocytes and neuronal enriched cell populations. (B) To characterize the *Mir-146b-/-* mice, we used two cohorts: the first cohort (male WT n = 12, *Mir-146b-/-* n = 15) was used for novel object recognition test (NORT) followed by flow cytometry or qPCR, and the second cohort (male WT n = 10, *Mir-146b-/-* n = 11) was used in contextual fear conditioning (CFC) model to evaluate adult hippocampal neurogenesis. In CFC, conditioned stimulus (CS, tone) and was paired with an unconditioned stimulus (US, foot shock) to induce associative learning. The second cohort received three bromodeoxyuridine (BrdU) injections in a total dosage of 300 mg/kg with 2 h intervals, to determine the survival/differentiation of neurons, the animals were killed after three weeks at day 31. Figure is created with BioRender.

Publication II:

Figure 4: Experimental strategy for publication II. Male *WT* (n = 40) and *Mir146b-/-* mice (n = 44), were randomly assigned to experimental groups. The Body weight was measured and 1.5 mg/kg of LPS was administrated at 0 hr. Assessment of sickness behavior, such as locomotor activity and tail suspension test were carried out after 20 h and body weights were recorded after 24h, followed by collection of tissues. The animals were tested for LPS-induced changes in microglial profile, as well as mRNA (qPCR) and protein expression (IHC) of microglial cells. Figure is created with BioRender.

Publication III:

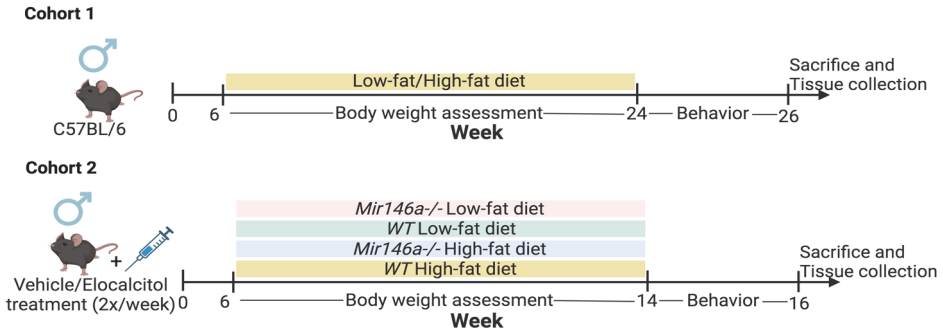

Figure 5: Experimental design for the publication III. The first cohort of 6-week-old male C57BL/6J mice (obtained from Envigo RMS B.V., Horst, Netherlands) was used to study the effects of a HFD on body weight and miR-146a expression. Mice were divided into: (1) Low-fat diet (LFD) group (n = 19), and (2) HFD group (n = 19) and were fed these diets for 18 weeks. The second cohort was used to study the impact of miR-146a deficiency and Elo treatment. Male *WT* (n = 40) and miR-146a knockout mice (*Mir146a-/-*) (n = 40) were randomly assigned to one of eight experimental groups (n = 10 in each group): (1) *WT* LFD, (2) *WT* HFD, (3) *Mir146a-/-* LFD, (4) *Mir146a-/-* HFD, (5) *WT* LFD + Elo, (6) *WT* HFD + Elo, (7) *Mir146a-/-* LFD + Elo, and (8) *Mir146a-/-* HFD + Elo. Elo (30 µg/kg, SML23-95, Sigma Aldrich, Germany) was administered intraperitoneally twice a week, while control groups received vehicle. Following an 8-week dietary and treatment period, behavioral experiments were conducted, after which the animals were euthanized for tissue collection and further analyses. Created in BioRender.

4.2 Animal models and housing conditions

All mouse lines were maintained and bred in the Laboratory Animal Centre at the Institute of Biomedicine and Translational Medicine, University of Tartu, following institutional regulations and the principles of laboratory animal care (Directive 2010/63/EU). The mice were group-housed under a 12-h light/dark cycle, with food and water provided ad libitum. All the behavioral experiments were performed between 9 am to 6 pm in the light phase. Before starting the behavioral experiments, animals were allowed to habituate in the experimental room for about 30 mins and conducted blinded to the animal groups.

4.2.1 *Mir146b-/-* mouse line (Publications I, II)

The *Mir146b-/-* mouse line on C57BL/6J background was generated by deletion of miR-146b encoding gene from mouse Chr19 as previously described in (170). *Mir146b-/-* and corresponding *WT* mice used for this study were obtained by crossing *Mir146b+/-* heterozygous mice. 2–3 months old male littermates were used for all experiments. The Animal Experimentation Committee at the Estonian Ministry of Agriculture approved the experimental protocol (no. 183, 2021). Mice were genotyped using the primer sequence:
146b locus 5′ forward primer- 5′ CTCACACTCTTGTTCTTACCCAGTTCTT 3′;
146b locus 3′ reverse primer- 5′ CAAACAAACAAACAAAAGGTTCAGCTAAG 3′;
146b locus internal reverse primer-5′ACACACAGGGCATATGAGATCAGTTGGTT 3′.

4.2.2 *Mir146a-/-* mouse line (Publication II, III)

Publication III: The *Mir146a-/-* mice originally purchased from Jackson Laboratory (Bar Harbor, US)), were housed and bred in the laboratory animal facility of University of Tartu. The C57BL/6J *WT* and *Mir146a-/-* cohorts were crossbred during maintenance, and to generate *Mir146a-/-* and corresponding *WT* mice *Mir146a+/-* heterozygous mice were crossed. The experimental protocol was approved by the Animal Experimentation Committee at the Estonian Ministry of Agriculture (No. 177, 2020 and 1.2–17/166, 2023). Genotyping was performed using the following primers:
146a forward primer- 5’ ACCAGCAGTCCTCTTGATGC 3’;
146a reverse primer- 3’ GACGAGCTGCTTCAAGTTCC 5’.
Publication II: *Mir146a/b* double knockout mice were generated by crossing *Mir146a-/-* and *Mir146b-/-* lines. These mice were used in a single experiment evaluating LPS-induced sickness behavior and pro-inflammatory cytokine expression.

4.2.3 Diet and drug treatment (Publications I–III)

In publication I, *WT* and *Mir146b-/-* mice received three BrdU injections (100 mg/kg, i.p, Sigma Aldrich, Berlington, MA, USA) for a total dosage of 300 mg/kg, given at 2h to assess evaluate cell survival and differentiation. In publication II, *WT*, *Mir146b-/-* mice were injected intraperitoneally (i.p.) with 1.5 mg/kg bodyweight of LPS (derived from *E. coli* serotype O55:B5; Sigma-Aldrich, St. Louis, MO, USA) solution in 0.9% NaCl (saline) and control group received injection of an equal volume of saline. In publication III, the animals received either LFD, fat constituting 10% of total energy (3.61 kcal/g) or HFD, fat constituting 45% of total energy (4.65 kcal/g). The main source of fat in both diets was lard (Ssniff Spezialdiäten GmbH). The animals were fed this diet starting at six weeks of age for a duration of eight weeks and Elo (30 µg/kg, SML23-95, Sigma Aldrich, Germany) was administered intraperitoneally twice a week to the respective groups, while others received vehicle.

4.3 Behavioral experiments (Publications I–III)

4.3.1 Novel object recognition test (Publications I)

NORT was performed as described by (171) in wood open chamber 50 cm × 50 cm × 50 cm (L × W × H). The objects utilized were glass cups with comparable textures and colors but differing in size and shape. They were sufficiently heavy to ensure that the mice could not move them. In the habituation phase, the animals were given 5 min to explore the arena without any objects present. Twenty-four h later, during the training phase, two identical objects were positioned diagonally (each placed 10 cm from a corner), and each mouse was given 5 min to explore the field. The time spent by each mouse exploring both objects was recorded. In the retention phase, conducted either 2 or 24 h later, the mice explored the arena containing one familiar object and one novel object to assess short-term recognition memory (STM) and long-term recognition memory (LTM), respectively. The preference ratio for each mouse was calculated as the percentage of time spent exploring the novel object: (Tnew ×100)/(Tf + Tnew), where Tf and Tnew represent the time spent exploring the familiar and novel objects, respectively. An observer, who was "blind" to the genotypes, recorded the exploration times during and between trials. To maintain consistency, the objects were cleaned with a 5% ethanol solution after each trial. Exploration was defined as sniffing or making contact with the object using the nose or forepaws.

4.3.2 Contextual fear conditioning and tone fear recall (Publication I)

The procedure was adapted from (172,173). The setup consisted of an experimental chamber measuring 22 cm × 22 cm × 35 cm (L × W × H), housed within a larger noise-attenuating box. A built-in ventilation fan provided background

noise. The chamber's floor was composed of stainless-steel rods suitable for mice and connected to a scrambled shock generator (TSE Systems), which included a speaker for emitting audible tones. The CFC experiment was conducted over seven consecutive days. On day 0, the mice were given 3 min to freely explore the conditioning chamber, during which baseline freezing behavior was recorded. Following this, a conditioned stimulus – a tone (75 dB, 2 kHz, lasting 30 seconds) – was paired with an unconditioned stimulus – a foot shock (1 second, 0.50 mA, constant electric current). This pairing was automatically administered three times at 1 min intervals through the grid floor. After the conditioning session, the mice were returned to their home cages. On day 1, contextual fear retention was evaluated 24 h after conditioning by placing the mice in the conditioned context for 3 min without the tone or foot shock, during which their freezing duration was recorded. Contextual fear memory extinction was assessed from days 2 to 6 by placing the mice in the same context for 3 min each day and measuring their freezing time. On day 7, tone fear recall was tested by placing the mice in a novel context for 3 min to record baseline freezing. Following this, a tone (75 dB, 2 kHz, 30 seconds) was presented, and freezing time was measured over the subsequent 3 min.

4.3.3 Body weight and locomotor activity assessment (Publications II and III)

In publication II, body weight was measured before and 24 h post LPS or saline injection in *WT* and *Mir146b-/-* mice. The effect of LPS on locomotor activity was monitored for 60 or 30 min by using PhenoTyper apparatus (Noldus, Leesburg, VA) with Ethovision XT live video tracking software (Version 8.0, Noldus Information Technologies, Leesburg, VA). Total distance traveled in the whole arena was measured.

In publication III, body weight was monitored throughout the duration of the dietary and pharmacological interventions, starting from week 0 and continuing until week 16.

4.3.4 Tail suspension test (Publication II)

Tail suspension test was performed as previously described (174). Each mouse was suspended by its tail using adhesive tape attached to a wooden beam, with each placed in a separate compartment of the wooden test apparatus. The total duration of immobility during the 6-min testing period was manually recorded with a stopwatch. Immobility was defined as the complete absence of movement, except for respiration, minor forelimb movements, or swinging resulting from prior activity.

4.4 Flow cytometry (Publications I–III)

Mice were euthanized using CO2, and their brains were dissected and mechanically dissociated through 70 µm cell strainers (352350, BD Bioscience, San Jose, CA, USA) in ice-cold flow buffer (phosphate-buffered saline (PBS) with 1% fetal calf serum). The isolated cells were then blocked with either 10% rat serum or ice-cold flow buffer for 1 h at 4°C. FcR blocking was performed using a mouse FcR blocking reagent (BD Pharmingen™ Purified Rat Anti-Mouse CD16/CD32, Mouse BD Fc Block™). The cells were stained with the appropriate antibodies or corresponding isotype control antibodies in flow buffer for 1 h, as detailed in Table 3. After staining, cells were fixed with 4% paraformaldehyde (PFA), permeabilized with PBS containing 0.05% TritonX-100 at 4°C for 30 min and incubated with an antibody for intracellular staining or the Cell Event Senescence Green flow cytometry assay kit (Thermofisher Scientific, Waltham, MA, USA) following the manufacturer's instructions. The cells were then washed, resuspended, and acquired using a LSRFortessa™ flow cytometer (BD Bioscience). Data analysis was conducted using Kaluza v2.1 software (Beckman Coulter).

Table 3: Summary of antibodies and kits used for surface and intracellular staining in flow cytometry experiments.

Category	Antibody	Target	Fluorophore	Cat. Number	Source	Isotype Control
Surface staining	Glast	Astrocyte marker	APC	130-123-555	Miltenyi	Mouse IgG2a-APC (#400219)
	Cd11b	Microglial/macrophage marker	BV421 / PerCP-Cy5.5	101251 / 101228	Biolegend	Rat IgG2b-BV421 (#400639), PerCP-Cy5.5 (#400631)
	o4	Oligodendrocyte marker	PE	130-117-357	Miltenyi	Mouse IgM-PE (#401611)
	Cd45	Microglial marker	BV650 / APC	103151 / 103112	Biolegend	Rat IgG2b-BV650 (#400651), APC (#400611)
Intracellular Staining	Vglut2	Vesicular glutamate transporter	FITC	MAB5504A4	Millipore	mAb-Alexa488 (#400132)
	Cell Event Senescence Kit	Senescence marker (SA-β-gal)	FITC	-	Thermo Fisher Scientific	-

4.4.1 Gating strategy for flow cytometry

Publication I:

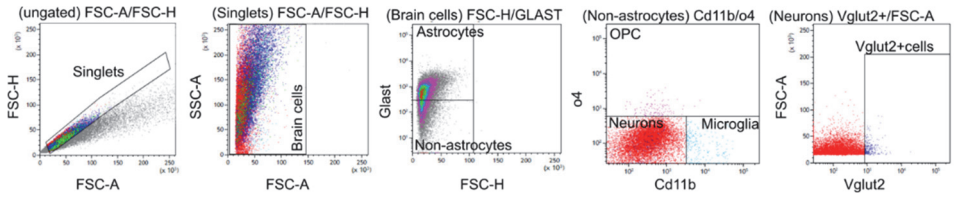

Figure 6: Gating strategy for determining brain cell abundancy. The astrocytes were first identified by flow cytometry based on Glast expression. The remaining non-astrocyte fraction was then analyzed to distinguish microglia, oligodendrocyte precursor cells (OPCs), and neurons. Microglia were identified by Cd11b expression, while OPCs were gated based on o4 expression. Neurons were isolated through negative selection. Intracellular staining for Vglut2, a marker of glutamatergic neurons, was performed among the neuron population. Representative dot plots illustrating the gating strategy for these brain cell populations are shown.

Publication II

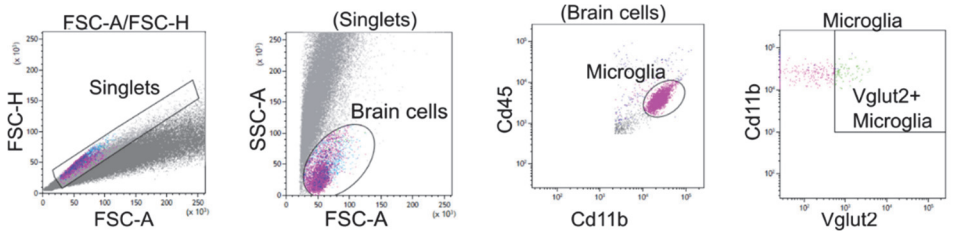

Figure 7: Gating strategy for microglial phagocytosis analysis. Brain-resident cells were selected based on FSC-A vs SSC-A. Microglia were then identified as Cd11b+ Cd45low cells. Within this microglial population, intracellular staining for Vglut2 was used to quantify the proportion of Vglut2+ microglia, representing phagocytosis activity.

Publication III:

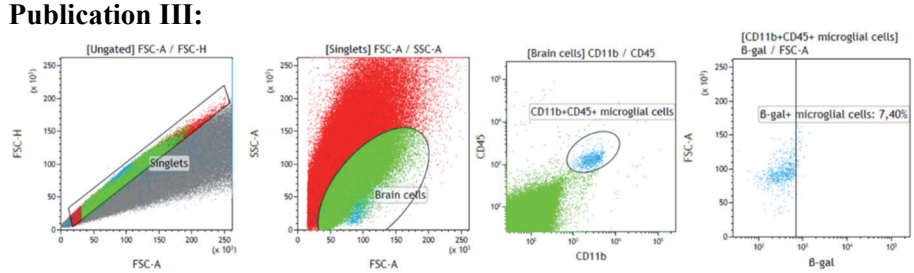

Figure 8: Gating strategy to measure SA-β-gal in microglial cells. The microglial cells were gated based on the expression levels of Cd11b and Cd45 markers. Within the Cd11b+Cd45 population, we gated Cd11b+Cd45 intermediate as microglia and we used Cell Event Senescence Green flow cytometry assay kit to detect SA-β-gal in microglial cells.

4.5 Isolation of brain cells (Publications I and II)

Tissues were homogenized and passed through a 70 μm nylon cell strainer (352350, BD Bioscience) using approximately 10–15 mL of 1X DPBS supplemented with 0.2% glucose. To prepare isotonic Percoll, stock Percoll (GE Healthcare, 17-0891-01, Chicago, IL, USA) was diluted at a 9:1 ratio with 10X PBS to create stock isotonic Percoll (SIP), considered to be 100% SIP. Percoll layers were created by diluting the 100% SIP with 1X Dulbecco's Phosphate Buffered Saline (DPBS) to generate 70%, 50%, and 35% SIP solutions. The homogenate was then centrifuged at 600× *g* for 6 min at room temperature (RT), and the pellet was resuspended in 6 mL of 70% SIP. This resuspended homogenate was transferred to a 15 mL tube, and 3 mL of 50% SIP was carefully layered on top, followed by 3 mL of 35% SIP, and 2 mL of 1X DPBS was added on top of the 35% SIP. The tubes were then centrifuged at 2000× *g* for 20 min at RT. After centrifugation, three distinct layers were formed. Microglial cells were collected from the interface between the 70–50% SIP layers, while astroglial cells were obtained from the 50–35% SIP interface. The top layer, consisting of myelin and other cells, was collected and used for characterizing neuronal marker. All isolated cells were resuspended in sterile 1X DPBS and centrifuged at 600× *g* for 6 min at RT to remove any remaining Percoll. The washed cells were then evaluated for purity using qPCR and flow cytometry, with Glast used to verify astrocyte purity, *Cx3cr1* and *Slc17a6* to confirm microglial and neuronal purity, respectively.

4.6 Quantification of miRNA expression (Publications I–III)

Total RNAs were extracted using TRI Reagent® (TR 118) (Molecular Research Center, Inc., Cincinati, OH, USA) and quantification of miRNA expression was carried out using TaqMan® MicroRNA Assays hsa-miR-146a (Assay ID: 000468, Life technologies) and TaqMan® MicroRNA Assays hsa-miR-146b (Assay ID: 001097, Life technologies) according to the manufacturer's instructions. For cRNA synthesis, TaqMan® MicroRNA reverse transcription kit (4366596, Thermo Scientific) and for qPCR, 5× HOT FIREPol® Probe qPCR Mix Plus (ROX) (Solis BioDyne) were used, respectively. U6 snRNA (Assay ID: 001973, Life Technologies) was used for the normalization of RT-qPCR. Absolute quantification was carried out according to the manufacturer's instructions (Qiagen) using miRCURY LNA RT Kit (Cat. No. 339340) for cDNA synthesis and miRCURY LNA PCR Assays (Assay IDs: YP00204688, YP02119310) in combination with QI Acuity EG PCR Kit (Cat. No. 250111) for detection of miR-146a and miR-146b. The samples were run and analyzed on QIAcuity One dPCR System using QIAcuity 26k Nanoplates (all from Qiagen).

4.7 Immunohistochemistry (IHC) and image analysis (Publications I–III)

Animals were deeply anesthetized with chloral hydrate (300 mg/kg, i.p.) and transcardially perfused with 0.9% saline followed by 4% PFA in PBS (pH = 7.4). After the brain was fixed in PFA for 24 h, 40 µm-thick sections were cut using a Leica VT1000S vibro-microtome (Leica Microsystems Pvt Ltd., Wetzlar, Germany) and stored at −20°C in a cryoprotectant solution (30% ethylene glycol, 30% glycerol in PBS; pH 7.4). The sections were washed in PBS and treated with a 2% H2O2 solution for 20 min, followed by incubation in 0.01 M citrate buffer (pH 6.0) at 85°C for 30 min in a water bath, then left for 30 min at RT. The sections were washed again, blocked with 5% goat serum, 0.5% Tween-20, and 0.25% Triton X-100 in 100 mM PBS for 1 h, and incubated with the respective primary antibodies in blocking buffer. The antibodies used in this study, along with the regions investigated and detection methods, are listed in Table 4. After incubation with primary antibodies, the sections were washed three times with PBS, followed by secondary antibody treatment. For negative control, the primary antibody incubation step was omitted.

4.7.1 Image analysis

Ionized calcium binding adaptor molecule 1 (Iba-1) and neuronal nuclear antigen (NeuN) analysis: the counts of Iba-1- or NeuN-positive cells were obtained from images according to the algorithm described previously in (175). Briefly, images were converted to 8-bit format, background was subtracted, and the obtained images were thresholded, binarized and counted using “analyze particles” command in ImageJ software.

Microglial morphology: the morphological characteristics of Iba1+ microglia (cell size, cell body size, size dendritic processes), were analyzed using image analysis software (ImageJ 1.48v, http://imagej.nih.gov/ij), an algorithm previously described (176) was used. Briefly, images were converted into binarized 8-bit format and “adjusted threshold” and “analyze particles” functions were used to apply intensity thresholds and size filter. To measure the total cell size, the threshold was maintained at the level that was automatically provided by the ImageJ program, and size filter of 150 pixels was applied. To measure the total cell body size, the threshold was lowered by 40 points and no size filter was applied (Publications I–III).

4.7.2 Assessment of neurogenesis

Neuronal cell proliferation and survival assessment was performed according to (177). In brief, mice were administered three BrdU injections (100 mg/kg, i.p., Sigma Aldrich, Burlington, MA, USA) for a total dose of 300 mg/kg, with 2h intervals between injections. For the survival and differentiation studies, the animals were sacrificed three weeks after the injections, and their brains were

sectioned and stored in a cryoprotectant solution. Ki67-, NeuN-, DCX-, BrdU- and Iba1-positive cells were visualized using peroxydase method and the sections were dried, cleared with xylol and cover-slipped with mounting medium (Vector Laboratories, Newark, CA, USA). For BrdU + calbindin and BrdU + GFAP co-localization confocal microscope (LSM 710 Duo, Carl Zeiss Microscopy GmbH, Oberkochen, Germany) equipped with an argon laser was used to visualize fluorescent signals. 3D images were constructed from series of scans taken at 1.5 μm intervals from the dentate gyri, using 40× objective and 2× digital zoom. Ki67 and BrdU-positive cells were counted in every sixth section within the dentate gyrus (DG). Total number of doublecortin-positive cells in a given region was obtained from every 24 h section. To determine the phenotype of the newly generated cells, two sections from each animal were analyzed for co-expression of BrdU and neuronal (calbindin, a marker for mature neurons) or glial (glial fibrillary acidic protein, GFAP, a marker for astrocytes) markers. Confocal microscope (LSM 710 Duo, Carl Zeiss Microscopy GmbH, Oberkochen, Germany) was used to visualize fluorescent signals. 3D images were constructed from series of scans taken at 1.5 μm intervals from the dentate gyri, using 40× objective and 2× digital zoom. (Publication I).

Table 4: Details of IHC markers and antibodies used in the study.

Marker	Purpose	Section selection criteria	Primary AB	Secondary AB	Regions Studied	Detection Method	Publication
Ki67	Marker for proliferating cells	Every 6th section	Rabbit monoclonal AB (SP6), 1:200, Abcam (#ab16667) incubated for 24 h at 4 °C	Goat anti-rabbit biotinylated IgG (H+L), 1:400, Vector Laboratories incubated at RT for 1 h	HP	Peroxidase method (ABC system, DAB chromogen)	I
NeuN	Neuronal marker	Every 6th section	Rabbit anti-NeuN, 1:200, Cell Signaling Technology (#D4G40) incubated for 48 h at 4 °C	Goat anti-rabbit biotinylated IgG (H+L), 1:400, Vector Laboratories incubated at RT for 1 h	FC	Peroxidase method (ABC system, DAB chromogen)	I
Iba1	Microglial marker	Every 6th section	Rabbit anti-Iba1, 1:700, FUJIFILM Wako Chemicals (#CAF6806) incubated for 72 h at 4 °C	Goat anti-rabbit biotinylated IgG (H+L), 1:700, Vector Laboratories incubated at RT for 1 h	HP, HT	Peroxidase method (ABC system, DAB chromogen)	I, II, III
BrdU	To trace neurogenesis and cell survival	Every 6th section	Rat monoclonal AB to BrdU, 1:300, Bio-Rad (#RF04-2) incubated for 24 h at 4 °C	Rabbit anti-rat biotinylated IgG (H+L), 1:400, Vector Laboratories R1121 or goat anti-rat Alexa-594 AB, 1:800, Invitrogen (# A11007) incubated at RT for 1 h	HP	Peroxidase (ABC system, DAB chromogen), Confocal microscopy	I
Double-cortin	Marker for immature neurons	Every 24th section	Rabbit anti-Doublecortin, 1:500, Abcam (#ab18723) incubated for 48 h at 4 °C	Goat anti-rabbit biotinylated IgG (H+L), 1:1000, Vector Laboratories, BA- 1000, incubated at RT for 2 h	HP	Peroxidase method (ABC system, DAB chromogen)	I
Calbindin	Marker for mature neurons	2 sections from each animal	Rabbit anti-Calbindin, 1:800, Chemicon International (#AB1778) incubated for 72 h at 4 °C	Goat anti-rabbit Alexa-488, 1:700, Invitrogen (# A11034) incubated at RT for 1 h	HP	Immunofluorescence (Confocal microscopy for colocalization with BrdU)	I
GFAP	Marker for astrocytes	2 sections from each animal	Rabbit anti-GFAP, 1:800, Dako (#Z0334) incubated for 24 h at RT	Goat anti-rabbit Alexa-488, 1:700, Invitrogen (# A11034) incubated at RT for 1 h	HP	Immunofluorescence (Confocal microscopy for colocalization with BrdU)	I

AB – antibody, HP – hippocampus, FC – frontal cortex, HT – hypothalamus and RT – room temperature

4.8 RNA Extraction and RT-qPCR (Publications I–III)

Total RNAs were extracted from brain tissues (hippocampus or hypothalamus (HT)) by using TRI Reagent® (TR 118) (Molecular Research Center, Inc., Cincinati, OH, USA). To measure mRNA expression, cDNA was synthesized using RevertAid First Strand cDNA Synthesis Kit (Thermo Fisher Scientific) followed by qPCR using 5 × HOT FIREPol® EvaGreen® qPCR Supermix (Solis BioDyne, Tartu, Estonia) on a QuantStudio 12KFlex instrument (Thermo Fisher Scientific) according to the instructions of the respective manufacturers. Primer sequences for target genes are shown in the table 5. To analyze relative mRNA expression, ΔΔCt calculations was used. *Gapdh* was used as housekeeping gene for normalization. The data were analyzed relative to the mean value of one of the samples as a calibrator, which was normalized to 1.

Table 5: RT-qPCR Primers used in this study

Gene name		Primer Sequence 5'-3'
Cx3cr1	Forward	GAGTATGACGATTCTGCTG
	Reverse	CAGACCGAACGTGAAGACG
Slc17a6 (Vglut2)	Forward	GCTGGAAAATCCCTCGGACAG
	Reverse	TCGCATAGCGGAGCCTTCTT
Gdnf	Forward	CAAAAATCGGGGGTGCGTTT
	Reverse	TCACAGGAACCGCTGCAATA
Bdnf	Forward	CATCTGTTGGGGAGACAAGAT
	Reverse	CTTGTCCGTGGACGTTTACTT
Irak1	Forward	TGTGAGGACACAAGGTGCAA
	Reverse	TAGGCTGGGTGCTTTTCAGG
Gapdh	Forward	GTCATATTTCTCGTGGTTCACACC
	Reverse	CTGAGTATGTCGTGGAGTCTACTG
Il1b	Forward	TGAAGAAGAGCCCATCCTCTG
	Reverse	GGAGCCTGTAGTGCAGTTGT
Tnf	Forward	GTAGCCCACGTCGTAGCAAA
	Reverse	TTGAGATCCATGCCGTTGGC
Il18	Forward	TCAAAGTGCCAGTGAACCCC
	Reverse	GGTCACAGCCAGTCCTCTTAC
Il6	Forward	CTGCAAGAGACTTCCATCCAG
	Reverse	AGTGGTATAGACAGGTCTGTTGG
Irf7	Forward	CGGGGACCTCTTGCTTCAG
	Reverse	CAAGGCTGCGCTCAGGA
Smad4	Forward	TGTCTCACCTGGAATTGATCTC
	Reverse	GACGGCTGTCCTTCAAAGTC

4.9 Western blot (publication II)

Hippocampal tissues were lysed in lysis buffer (#ab113474; Abcam, UK) and protein concentration was determined using the Bradford reagent kit (#B6916; Sigma-Aldrich, Germany). Samples containing 20 µg of total protein were run in 15% sodium dodecyl sulfate polyacrylamide gels (SDS-PAGE) and transferred onto a nitrocellulose membrane (Merck Millipore, US). The membranes were blocked with TBS Blocking Buffer (Li-Cor Biosciences, US) for 60 min at RT, then incubated for 48h at 4°C with the primary antibody for Iba1 (Rb, #ab178846, 1:1000; Abcam, UK) or TLR4 (Ms, #sc-293072, 1:500; Santa Cruz Biotechnology, USA) in TBS. After washing thrice with TBST (50 mmol/L Tris, pH 7.6; 0.9% NaCl; and 0.1% Tween-20), the membranes were incubated with the secondary antibody (IRdye800, aRb, #C40721-02, 1:10000; Li-Cor Biosciences) for 1h at RT. Loading control β-actin (Ms, #039M4768V, 1:10000; Sigma-Aldrich, US) was detected by incubating membranes overnight and followed by incubation with IRDye conjugated secondary antibody (IRdye680LT, aMs, #C60301-03, 1:10000; Li-Cor Biosciences). For determination of NF-κB p65 protein, nuclear extract was prepared from the hippocampal tissues according to manufacturer's protocol (Abcam nuclear extraction kit, ab113474). The anti-rabbit NF-κB p65 (Abcam antibody, ab 16502), anti-rabbit histone-4 (Abcam antibody, ab 10158) and anti-mouse beta-tubulin antibody (MAB1637, Millipore) was used. Secondary antibodies (1:10000, either goat anti-rabbit IRDye 800CW or 680LT or goat anti-mouse IRDye 680LT, all from Licor Biosciences) were used and Odyssey Infrared Imaging System was used in all western blots followed by densitometry analysis by Image studio Ver 2.0.

4.10 Statistical analysis (publications I–III)

In all the publications, GraphPad (8.0.1 and 9.4.1) was used for statistical analyses and graphical presentations. In publication I, statistical analysis was performed using Student's t-test, one-way, or two-way ANOVA with Tukey's test for post-hoc comparisons. For publication II and publication III, data sets were first tested for normality using the Shapiro-Wilk test and for homogeneity of variances using the Brown-Forsythe test (publication II). If the data passed these tests, two-way ANOVA followed by Tukey's test for post-hoc comparisons was applied. If normality or homogeneity was violated, data were transformed using log10 (Y = Log(Y)) and analyzed with Mann-Whitney test (for two groups) or one-way ANOVA with Tukey's test (for multiple groups). For publication II, if homogeneity was not met, Welch's ANOVA followed by Dunnett's test was used. The results were considered statistically significant at $p < 0.05$ when Student's t-test was used, or at corrected $p < 0.05$ (all other analyses). Data are shown as mean ± standard error of the mean (SEM).

5. RESULTS

5.1 Functional roles of miR-146b in neurons (Publication I)

5.1.1 miR-146b is highly expressed in neuronal cells

To better understand the role of miR-146b in the brain, we first measured hippocampal expression of miR-146a and miR-146b and found that they both were expressed at similar levels in the hippocampal tissue ($p = 0.8472$) (Figure 9A). Next, whole brain tissue was processed using a percoll gradient to isolate microglia, astroglia, and other brain cell fractions. Purity was assessed by evaluating *Cx3cr1* mRNA, which was enriched in the microglial fraction, while flow cytometry staining for the astroglial marker GLAST revealed a high number of GLAST+ cells in the astroglial fraction. The remaining cell fraction, defined as neuronal cells, showed elevated expression of *Slc17a6* mRNA, a marker of neuronal cells (178). Within these fractions, miR-146a was found to be enriched in microglial cells ($p = 0.0012$), but almost absent in neuronal cells, and less expressed in astroglial cells (Figure 9B). In contrast, miR-146b was highly expressed in neuronal fractions ($p = 0.0073$), with lower expression in microglial and astroglial fractions (Figure 9C). These results indicate distinct cellular distributions of miR-146a/b in the brain, with miR-146a being primarily associated with microglia and miR-146b predominantly expressed in neurons.

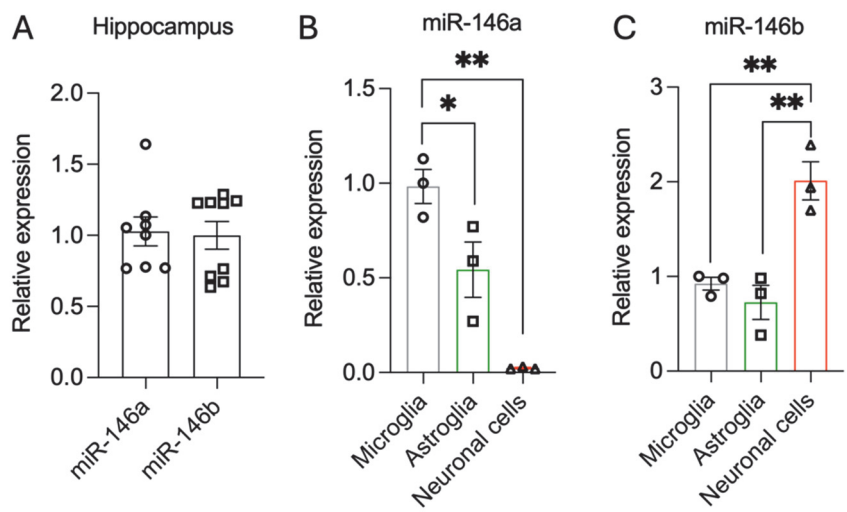

Figure 9: miR-146a/b expression in the hippocampal tissue and in CNS cellular fractions. (A) Hippocampal expression of miR-146a/b in the *WT* mice, N = 8–9, Student's t-test. (B, C) Relative expression of miR-146a/b in microglia, astroglia and neuronal cells. N = 3, one-way ANOVA followed by Tukey's multiple comparison test. Data are represented as mean ± SEM; * $p < 0.05$, ** $p < 0.01$.

5.1.2 Increased number of neurons in the HP and frontal cortex (FC) of *Mir146b-/-* mice

Since miR-146b was highly expressed in neurons, we next examined brain cell abundance in *Mir146b-/-* mice, to investigate whether its loss influences the composition of major brain cell types, including astrocytes, microglia, OPCs, particularly neuronal cells, in the HP. Using flow cytometry, we first identified different brain cells and the gating strategy is illustrated in (Figure 6, Section 4.4.1). Analysis of hippocampal cells in *Mir146b-/-* mice revealed a significant reduction in astrocyte numbers ($p = 0.0010$) (Figure 10A), whereas microglia and OPCs showed no significant changes (Figure 10B, C). In contrast, neuronal cells were significantly increased ($p = 0.0033$) (Figure 10D), as evidenced by increased Vglut2+ glutamatergic neurons in the HP ($p = 0.0019$) (Figure 10E) and an increased density of NeuN+ neurons in the FC of *Mir146b-/-* mice ($p = 0.0084$) (Figure 10F, G). Collectively, these findings indicate that miR-146b deficiency leads to an increase in neuronal populations in both the hippocampus and frontal cortex.

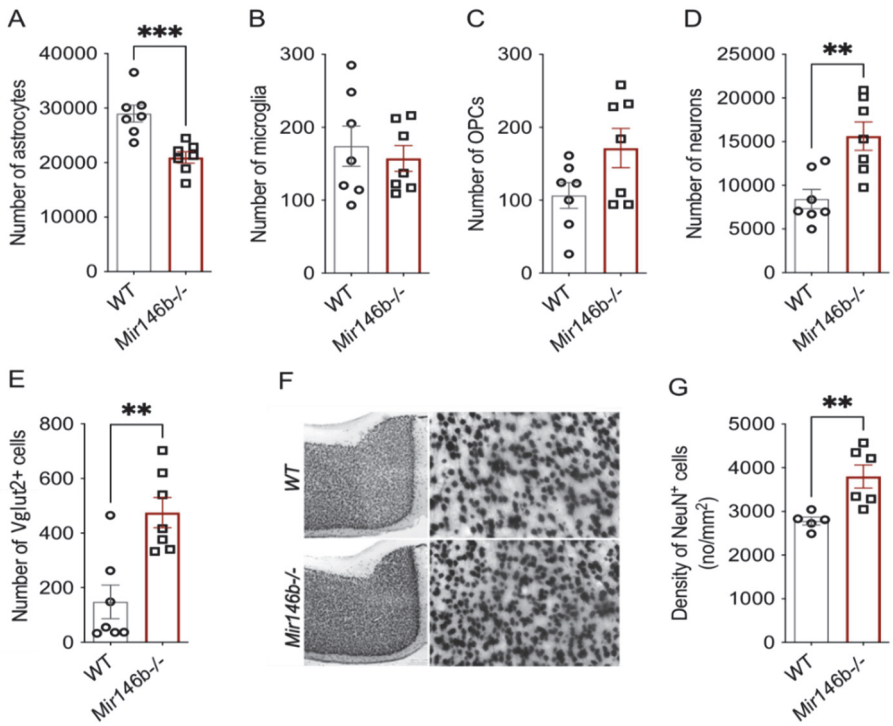

Figure 10: Brain cell abundancy is altered in the HP and FC of *Mir146b-/-* mice. (A) Number of astrocytes among total brain cells. (B) Number of microglia, (C) OPCs and (D) Neurons among non-astrocytes and (E) Vglut2+ cells among neurons in HP. (F) Representative immunohistochemistry of the FC NeuN+ sections at 40× and 200× magnification and (H) Quantification of NeuN-positive cells in the frontal cortex of *WT* and *Mir146b-/-* mice. N = 5–7, Student's t-test. Data represented as mean ± SEM; ** $p < 0.01$, *** $p < 0.001$.

5.1.3 Increased adult hippocampal neurogenesis in *Mir146b-/-* mice

As we observed an increased number of neurons in *Mir146b-/-* mice and previous studies have shown that miR-146b overexpression inhibits the proliferation of primary hippocampal neural stem cells, highlighting its regulatory role in neurogenesis (143), we next investigated adult hippocampal neurogenesis in *Mir146b-/-* mice. To assess different stages of neurogenesis, we used various markers. First, we evaluated cell proliferation, by counting the number of Ki67+ cells in the DG and found a significant increase in *Mir146b-/-* mice compared to *WT* mice ($p = 0.0075$) (Figure 11A, C). For cell survival analysis, we administered BrdU intraperitoneally and collected brains three weeks later for IHC to visualize BrdU+ cells in the DG. Consistent with the proliferation results, *Mir146b-/-* mice exhibited a significantly higher number of surviving BrdU+ cells compared to *WT* mice ($p = 0.0281$) (Figure 11B, D). To assess neuronal differentiation, we examined DCX expression and found a significant increase in *Mir146b-/-* mice compared to *WT* ($p = 0.0252$) (Figure 11E, F). To further investigate the fate of BrdU+ cells, we performed colocalization analysis with the neuronal marker calbindin and the astroglial marker GFAP (Figure 11G). While the percentage of BrdU+ cells co-localized with GFAP showed no significant difference between groups (Figure 11H), the percentage of BrdU+ cells co-localized with calbindin was significantly higher in *Mir146b-/-* mice compared to *WT* ($p = 0.0002$) (Figure 11I). These findings demonstrate that miR-146b deficiency enhances adult hippocampal neurogenesis by promoting the proliferation, survival, and differentiation of progenitor cells into the neuronal lineage.

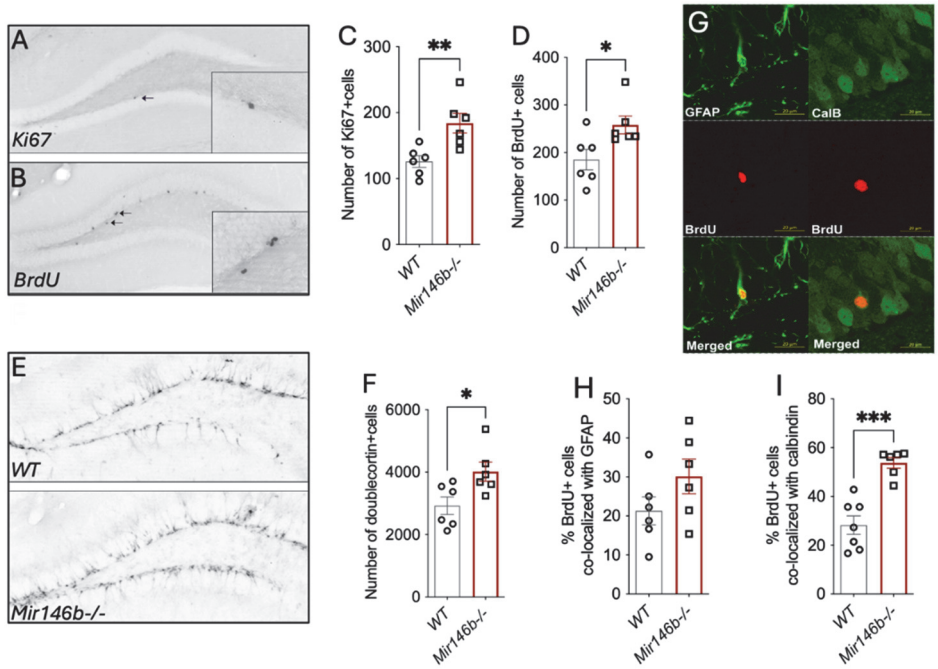

Figure 11: Adult hippocampal neurogenesis is enhanced in *Mir146b-/-* mice. (A) Representative IHC image of the hippocampal Ki67+ cells at 100× magnification and inserted microphotographs at 1000× magnification. (B) Depictive microphotographs of the hippocampal BrdU+ cells at 100× magnification and inserted microphotographs at 1000× magnification. (C-D) Number of Ki67 and BrdU+ cells. (E-F) Representative microphotographs of doublecortin positive cells at 100× magnification and its quantification (G) Illustrative images of BrdU, GFAP and calbindin signal and their co-localization in the HP. (H-I) % of costaining of BrdU+ cells with GFAP (H) or calbindin (I) in the DG. Scale bar = 20 µm. N = 6, Student's t-test. Data are represented as mean ± SEM; * $p < 0.05$, ** $p < 0.01$, *** $p < 0.001$.

5.1.4 Enhanced recognition and associative memory in *Mir146b-/-* mice

As we observed increased neurogenesis in *Mir146b-/-* mice and previous studies suggest that miR-146a may influence cognitive functions (30), we investigated whether miR-146b plays a similar role. To do so, we assessed cognitive behavior by evaluating recognition memory and associative memory using the NORT and CFC, respectively. In NORT, *WT* and *Mir146b-/-* mice were first allowed to explore two identical familiar objects (data not shown), confirming that both genotypes had similar motivation to explore new objects. When one of the familiar objects was replaced with a novel object, *Mir146b-/-* mice showed a significantly stronger preference for the novel object compared to *WT* mice at both the 2h ($p = 0.0027$) (Figure 12A) and 24h ($p < 0.0001$) (Figure 12B) time points, indicating enhanced recognition memory. In the CFC test, baseline

freezing responses on day 0 were similar between the genotypes (data not shown). Following exposure to a tone paired with a foot shock, fear retention was assessed 24h later in the same context. While both genotypes exhibited increased freezing responses, *Mir146b-/-* mice displayed significantly longer freezing time than *WT* mice ($p = 0.0171$) (Figure 12C), suggesting improved fear memory acquisition. Fear extinction, measured from days 2 to 6 in the absence of tone and foot shock, showed no significant differences between the genotypes (Figure 12D). On day 7, during tone fear recall, *Mir146b-/-* mice again demonstrated significantly higher freezing time compared to *WT* mice ($p = 0.0063$) (Figure 12E), further supporting enhanced memory retention. Collectively, these findings suggest that *Mir146b-/-* mice exhibit enhanced recognition and associative memory, as well as greater adaptability compared to *WT* mice.

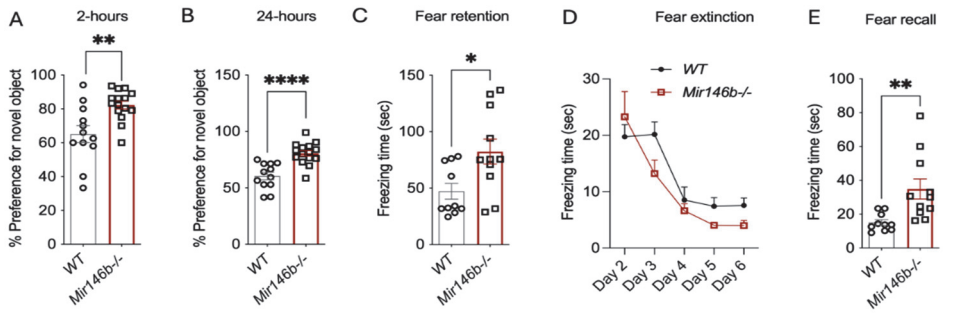

Figure 12: Enhanced cognition in *Mir146b-/-* mice. (A) Preference for novel object at 2h (short-term memory) and (B) 24h (long-term memory) assessed through the NORT. (C) Contextual fear retention, (D) Contextual fear extinction, and (E) Tone fear recall in *WT* and *Mir146b-/-* mice, evaluated using CFC and tone fear recall tests. N = 10–15, student's t-test and two-way ANOVA with Tukey's multiple comparison test. Data are presented as mean ± SEM; *$p < 0.05$, **$p < 0.01$, ****$p < 0.0001$.

5.1.5 *Gdnf* mRNA is upregulated in the hippocampus of *Mir146b-/-* mice

To evaluate the potential of miR-146b targets to influence cognition and neurogenesis, we performed TargetScan (179) analysis in combination with g:Profiler functional enrichment analysis (180), and a literature review for verified targets. When only genes with conserved target sites were selected, we identified 283 genes, of which multiple GO groups associated with neuronal development and function were found to be overrepresented (data not shown). From the identified genes and literature, we selected three genes for further analyses. First, Gdnf, is known to be expressed in neurons (https://www.brainrnaseq.org/ accessed on 1 June 2022) (181), and an earlier study demonstrated that miR-146a suppresses the Gdnf mRNA expression (135). Next, we included Bdnf for analysis due to its established role in miR-146b-related processes. Bdnf is expressed in astrocytes

(https://www.brainrnaseq.org/ accessed on 1 June 2022) (182), and its Val66Met mutation has been linked to altered miR-146b expression and downstream effects (183). Additionally, we selected Irak1, a well-known target of miR-146a/b and abundantly expressed in glial cells (https://www.brainrnaseq.org/ accessed on 1 June 2022) (172). Interestingly, we detected *Gdnf* mRNA levels to be significantly elevated in the HP of *Mir146b-/-* mice compared to *WT* littermates ($p = 0.0477$) (Figure 13A). However, there were no significant changes in *Irak1* expression (Figure 13B) or *Bdnf* mRNA levels (Figure 13C). These findings suggest that miR-146b influences neuronal development by suppressing *Gdnf* expression.

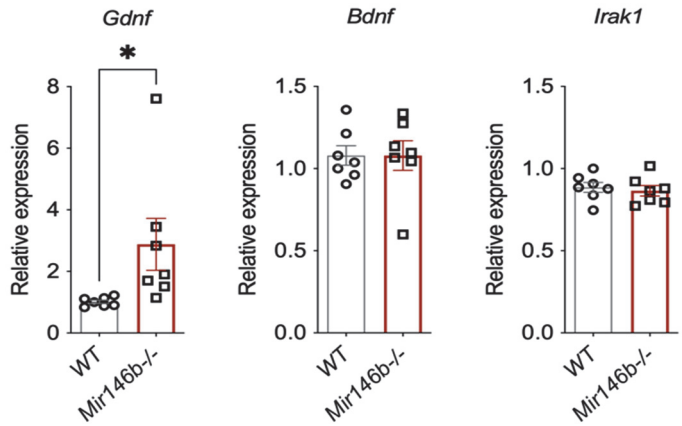

Figure 13: *Gdnf* mRNA is upregulated in *Mir146b-/-* mice. (A-C) Relative mRNA expression of indicated genes in the HP of *WT* and *Mir146b-/-* mice. N = 7, Student's t-test. Data represented as mean ± SEM respectively; * $p < 0.05$.

Thus, together our data show that miR146b can negatively regulate *Gdnf* expression and thereby might retard neuronal generation and cognitive functions. Vice versa, the downregulation of miR146b may lead to disinhibition of neurogenesis and improved cognition via *Gdnf*-dependent mechanisms.

5.2 miR-146b deficiency leads to increased microglial phagocytosis (publication II)

Next, we aimed to determine whether miR-146b deficiency affects microglial function in phagocytosis. Given that *Mir146b-/-* mice exhibit increased neuronal density, we were interested in understanding how microglia respond to this heightened neurogenic environment, as they are key player in synaptic remodeling (184). To investigate this, we examined microglial engulfment of Vglut2, a glutamatergic pre-synapse-specific protein, as a measure of phagocytic activity. Using flow cytometry, we quantified Vglut2+ microglia in *Mir146b-/-* and *WT*

mice (Gating strategy shown in Figure 7, Section 4.4.1). Interestingly, we observed a significantly higher percentage of Vglut2+ microglia in *Mir146b-/-* mice compared to *WT* ($p = 0.0062$) (Figure 14). This suggests that miR-146b negatively regulates microglial- phagocytic activity, offering new insights into its role in shaping synaptic architecture and neuronal network refinement.

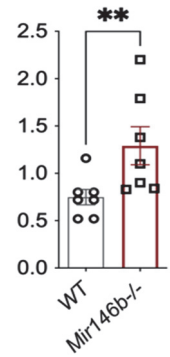

Figure 14: *Mir146b-/-* mice have increased numbers of Vglut2+ microglial cells. N = 6-7, Student's t-test Data represented as mean ± SEM; ** $p < 0.01$.

5.3 Regulation of microglial responses by miR-146a/b under neuroinflammation (publication II)

5.3.1 Increased expression of miR-146a/b in the HP and in microglial cells upon LPS-induced neuroinflammation

Figure 6 shows that miR-146a is highly enriched in microglial cells, whereas miR-146b is expressed at lower levels in microglia. Previous studies have shown that both miR-146a/b are upregulated upon LPS treatment (109,137), but their expression has mostly been examined separately rather than comparatively. To better understand the significance of miR-146a/b in neuroinflammation, we first measured their expression levels in the HP of *WT* mice following LPS administration. At 24h post-LPS treatment, both miR-146a ($p = 0.0013$) and miR-146b ($p = 0.0170$) were significantly upregulated, with miR-146a showing a stronger induction compared to miR-146b ($p = 0.0836$) (Figure 15A). Next, we assessed their expression in microglial cells isolated from *WT* mouse brains, where LPS stimulation also led to a significant upregulation of miR-146a ($p = 0.0340$) and miR-146b ($p = 0.0342$) (Figure 15B). These findings demonstrate that both miR-146a/b are induced in response to LPS in HP and in microglial cells of the mouse brain.

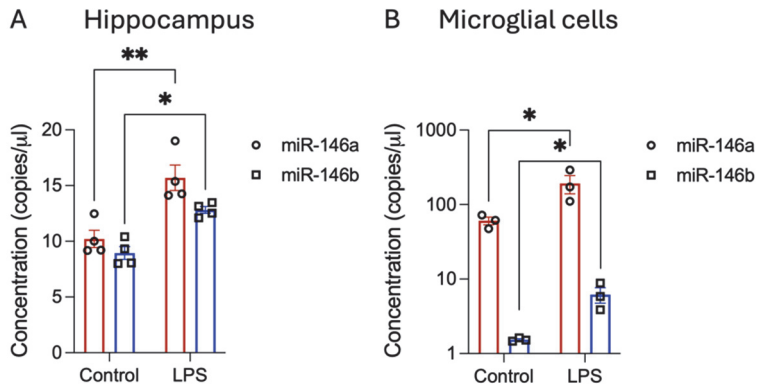

Figure 15: Quantification of miR-146a/b in hippocampal tissue and in microglial cells isolated following LPS treatment. (A) The were mice injected with LPS in saline or equal volume of saline (control). (B) The microglial cells were isolated from *WT* mice brain and subjected to LPS treatment. (A, B) N = 3-4. Two-way ANOVA with Tukey's multiple comparison test; Data are represented as mean ± SEM; * $p < 0.05$, ** $p < 0.01$.

5.3.2 Attenuated LPS-induced sickness behavior in *Mir146b-/-* mice

While several studies have examined the role of miR-146b in neuroinflammatory models or in microglial cells, it is not known about how neuroinflammation is regulated in the absence of miR-146b. To address this, we used *Mir146b-/-* mice and investigated their response to LPS-induced sickness behavior, a condition characterized by weight loss, reduced locomotion, and depression-like behavior (185). Following systemic LPS administration, body weight was measured 24h before and after LPS treatment, revealing a significant weight loss effect in both genotypes ($p < 0.001$). However, *Mir146b-/-* mice exhibited a trend in milder reduction compared to *WT* controls ($p = 0.07$) (Figure 16A). Locomotor activity was significantly reduced in LPS treated *WT* and *Mir146b-/-* mice ($p < 0.0001$), yet the decline was less pronounced in *Mir146b-/-* mice compared to *WT* ($p < 0.01$) (Figure 16B). To evaluate depression-like behavior, we performed the TST, where LPS-treated *WT* mice showed a significant increase in immobility time ($p < 0.0001$), while no enhanced immobility was observed in *Mir146b-/-* LPS mice compared to the untreated group (Figure 16C). Overall, LPS-induced sickness behavior was less severe in *Mir146b-/-* as compared to the respective *WT* controls.

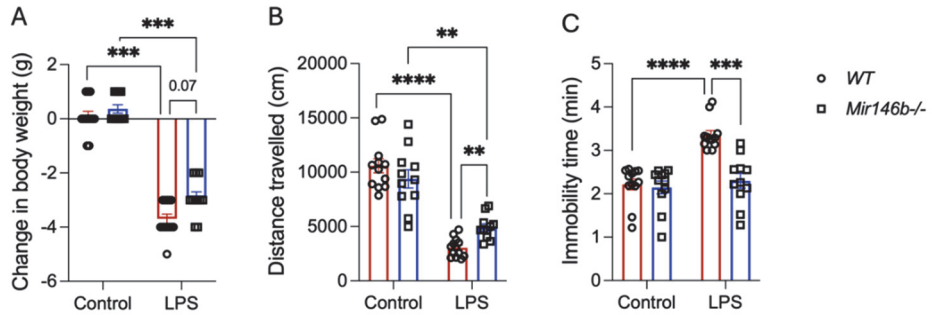

Figure 16: Reduced sickness behavior in *Mir146b-/-* mice upon LPS challenge. The mice were subjected to either equal volume of saline (control) or LPS in saline and then assessed for (A) Change in body weight, (B) Locomotor activity and (C) Immobility time in TST. N = 11-12. Welch's ANOVA with Dunnett's multiple comparisons test; Data are represented as mean ± SEM; ** $p < 0.01$, ***$p < 0.001$, ****$p < 0.0001$.

5.3.3 Reduced microglial activation in *Mir146b-/-* mice upon LPS treatment

LPS treatment is known to trigger microglial activation, characterized by morphological changes and an increase in Iba-1 expression, which is a hallmark of activated microglia (186,187). Hence, to evaluate the role of miR-146b in this process, we assessed microglial activation profiles in *WT* and *Mir146b-/-* mice following LPS treatment. Iba1, a microglial marker, was employed in IHC to measure microglial morphology in the HP (Figure 17A). LPS administration caused significant increases in both microglial cell size (Figure 17B) and cell body size (Figure 17C) in *WT* and *Mir146b-/-* mice. However, these effects were less pronounced in *Mir146b-/-* mice compared to *WT* mice, indicating that miR-146b deficiency leads to lesser microglial activation in response to LPS. We also measured Iba1 protein levels in the HP (Figure 17D), which were significantly increased in LPS-treated *WT* mice (Figure 17E), but no such increase was observed in *Mir146b-/-* mice, suggesting that miR-146b deficiency results in less microglial activation following LPS exposure.

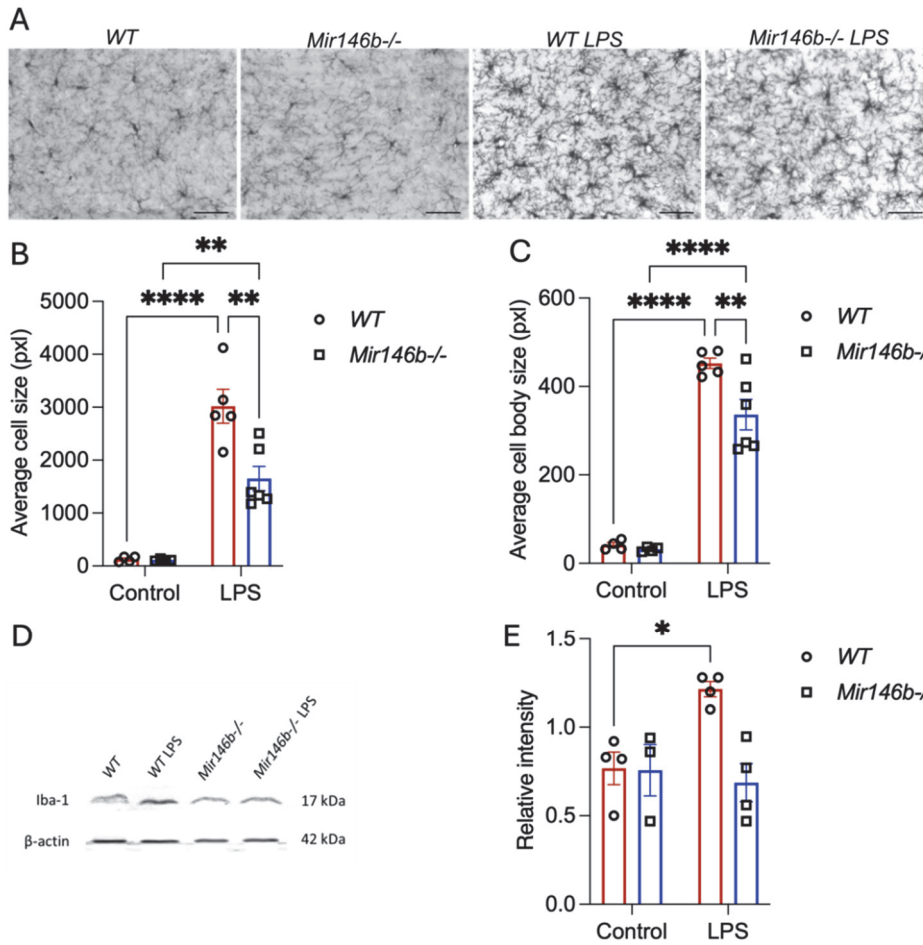

Figure 17: Microglial activation is less pronounced in *Mir146b-/-* mice. (A) Immunohistochemistry microphotographs of the hippocampal Iba1+ cells at 400× magnification, (B) Average cell size and (C) Average cell body size; N = 5-6, Scale bar = 50 µm. (D) Representative western blot of the Iba1 protein and (E) Densitometry quantification of Iba1; N = 3. Two-way ANOVA with Tukey's multiple comparison test (A-C); Welch's ANOVA with Dunnett's multiple comparisons test (D,E); Data are represented as mean ± SEM; *p < 0.05, **p < 0.01, ****p < 0.0001.

5.3.4 LPS-induced cytokine response is blunted in *Mir146b-/-* mice

To investigate whether the reduced neuroinflammatory response observed in *Mir146b-/-* mice following LPS treatment was linked to changes in pro-inflammatory cytokine gene expression, we measured the mRNA levels of *Il1b*, *Il18* and *Tnf* in HP. The baseline mRNA levels of these cytokines were similar between *WT* and *Mir146b-/-* mice. However, LPS administration in *WT* mice induced

elevated *Il1b* (p = 0.0036), while in *Mir146b-/-* mice, *Il1b* mRNA levels remained unchanged (Figure 18A). Similarly, LPS induced a marked increase in *Il18* (p = 0.0019) and *Tnf* (p < 0.0001) mRNA in *WT* mice, while *Il18* levels remained same in *Mir146b-/-* mice, and *Tnf* showed only a modest increase (p = 0.0257) (Figure 18B, C). Together, these results demonstrate that miR-146b plays a role in modulating the LPS-induced production of pro-inflammatory cytokines in HP, with its deficiency leading to a reduction in these cytokines during neuro-inflammation.

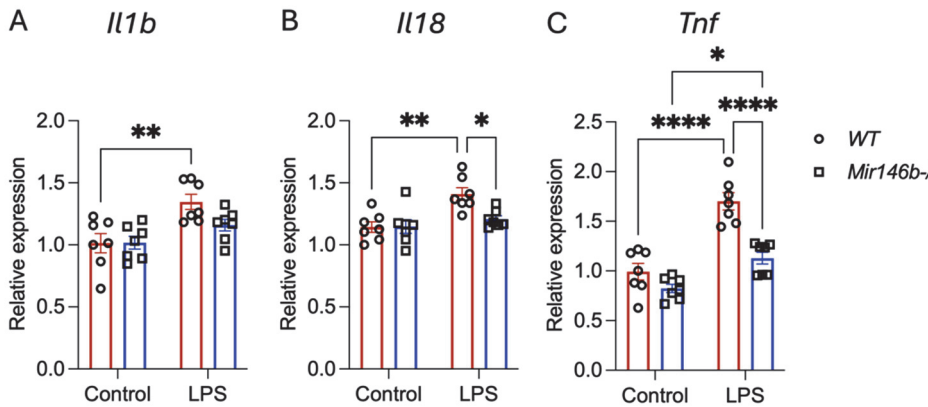

Figure 18: LPS induced cytokine changes in *WT* and *Mir146b-/-* mice. Total RNA was purified from HP of mice injected with LPS in saline or equal volume of saline (control). (A-C) Relative mRNA expression of indicated genes in the HP of *WT* and *Mir146b-/-* mice. N = 7, Data represented as mean ± SEM. two-way ANOVA with Tukey's multiple comparisons test (Data in panels (A–B) and one-way ANOVA with Tukey's multiple comparisons test (C); *p < 0.05, **p < 0.01, ****p < 0.0001.

5.3.5 Loss of miR-146b resulted in elevation of miR-146a

To understand the underlying mechanisms contributing to the reduced LPS-induced neuroinflammation in *Mir146b-/-* mice, we measured miR-146a expression in both hippocampal tissue and in microglial cells. We observed higher expression of miR-146a upon LPS challenge in the hippocampal tissue of *Mir146b-/-* mice as compared to *WT* animals (p = 0.0016) (Figure 19A). The microglial cells isolated from *WT and Mir146b-/-* mice showed overexpression of miR-146a upon LPS administration, whereas *Mir146b-/-* mice demonstrated higher increase (p = 0.0035) in miR-146a levels as compared with *WT* mice upon LPS treatment. In *Mir146b-/-* mice, basal miR-146a expression was also higher than in *WT* mice (p = 0.0005) (Figure 19B). These findings imply that miR-146a may be compensatorily upregulated in response to miR-146b deficiency, which could help mitigate neuroinflammation in these animals.

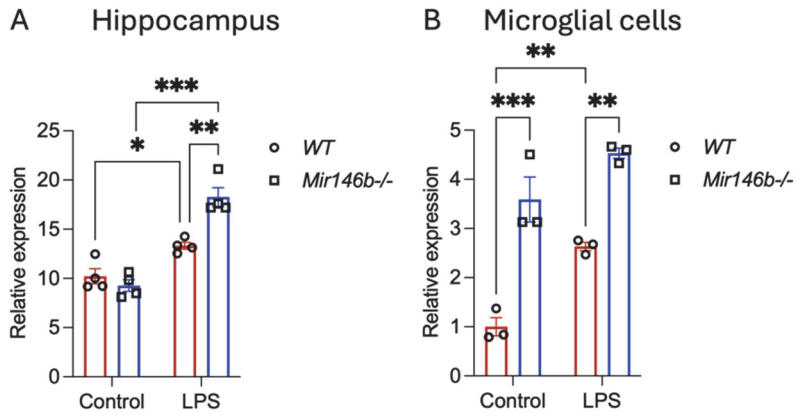

Figure 19: LPS-induced miR-146a expression in the hippocampus (A) and microglia cells (B) of *WT* and *Mir146b-/-* mice. N = 3-4, Data represented as mean ± SEM, two-way ANOVA with Tukey's multiple comparisons test (A) and Welch's ANOVA with Dunnett's multiple comparisons test (B); *p = 0.05, **p < 0.01, ***p < 0.001.

To evaluate whether miR-146a upregulation is responsible for the observed attenuation of neuroinflammation in *Mir146b-/-* mice, additional experiments were performed on *Mir-146a/b-/-* mice. Our results showed that *Mir-146a/b-/-* mice exhibited sickness behavior and elevated expression of *Tnf* and *Ccl5* comparable to *WT* controls. This supports the idea that miR-146a compensates for miR-146b deficiency (Figure 9, Publication II).

5.3.6 *Irf7*-driven upregulation of miR-146a in *Mir-146b-/-* mice contributes to reduced neuroinflammation

To investigate the mechanisms behind miR-146a upregulation following LPS treatment, we focused on NF-κB, a well-established regulator of miR-146a expression. Additionally, we considered IRF7, as previous study identified IRF7 binding sites in the miR-146a promoter region (96). LPS treatment induced an increase in p65 protein levels in the nuclear lysate of HP, indicating activation of NF-κB in *WT* mice ($p = 0.039$), while no such change was observed in *Mir146b-/-* mice (Figure 20A). Next, we examined the mRNA expression of *Irf7*, which was significantly elevated after LPS treatment in both *WT* ($p = 0.0007$) and *Mir146b-/-* mice ($p < 0.0001$), with *Mir146b-/-* mice showing a more pronounced upregulation of *Irf7* ($p = 0.0009$) (Figure 20B). These findings suggest that miR-146a upregulation is likely mediated through *Irf7* in the HP of *Mir146b-/-* mice. To further explore how miR-146a modulates neuroinflammation, we examined components of the NF-κB pathway, including *Irak1* and Tlr4 (97). Interestingly, mRNA expression of *Irak1* was reduced in HP of both *WT* and *Mir146b-/-* mice

in response to LPS. However, the extent of *Irak1* reduction was more prominent in *WT* than *Mir146b-/-* mice (p = 0.0478) (Figure 20C), suggesting an altered response to inflammation in the absence of miR-146b in HP. When we analyzed protein expression, a significant increase in the Tlr4 protein levels upon LPS administration in *WT* animals (p = 0.0352), but not *in Mir146b-/-* mice (Figure 20D) was observed, indicating that overexpressed miR-146a may target TLR4 or indirectly suppress its expression, resulting in attenuation of neuroinflammation in *Mir146b-/-* mice.

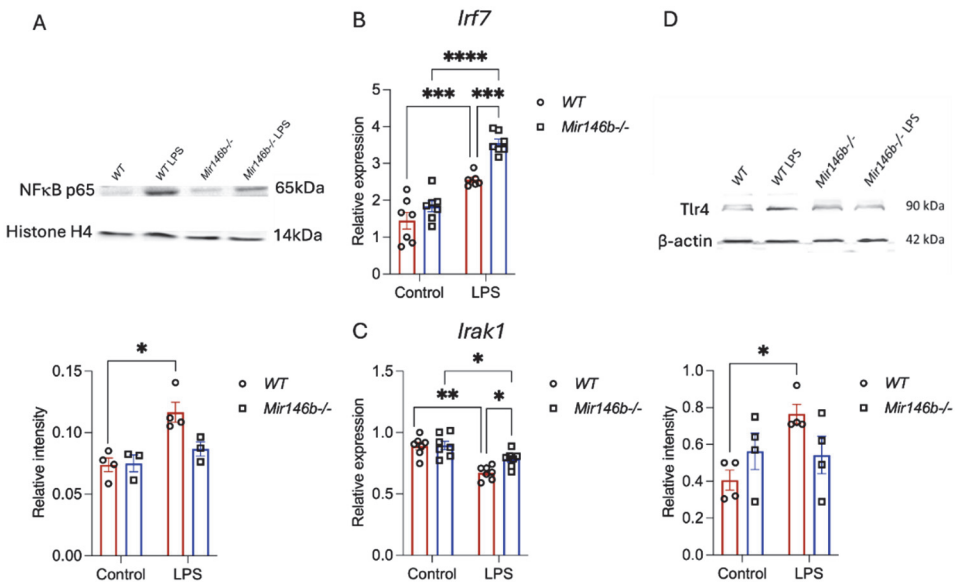

Figure 20: Limited neuroinflammation in *Mir146b-/-* mice. (A,D) Immunoblot and quantification of (A) NF-κB p65 and histone H4 levels nuclear fractions and (D) Tlr4 levels in the HP of saline and LPS treated *WT* and *Mir146b-/-* mice, N = 3-4. (B,C) Relative mRNA expression of indicated genes. N = 6-7 (qPCR). Two-way ANOVA with Tukey's multiple comparison test; Data represented as mean ± SEM; * p < 0.05, ** p < 0.01, *** p < 0.001, **** p < 0.0001.

In summary, these data indicate that the reduced neuroinflammatory response to LPS in *Mir146b-/-* mice may be associated with increased levels of *Irf7* and upregulation of miR-146a.

5.4 Role of miR-146a in HFD induced microglial senescence (publication III)

5.4.1 HFD induced increased body weight and decreased miR-146a expression in HT

HFD-induced obesity has been associated with neuroinflammatory changes, including alterations in microglial function (188). Given the established role of miR-146a in regulating inflammatory responses and enrichment in microglial cells (27), we sought to investigate whether miR-146a expression is affected by HFD. First, to investigate the possible impact of body weight on our HFD-induced obesity model, we subjected mice to either HFD or LFD. A significant increase in body weight of mice exposed to HFD compared to those on the LFD indicated development of obesity in these animals. This difference became evident by the 3rd week ($p = 0.0494$), intensified by the 8th week ($p < 0.0001$), and persisted through the 16-week study period ($p < 0.0001$) (Figure 21A). Next, we measured the expression of miR-146a and found reduction in miR-146a expression in the hypothalamus of HFD-fed mice compared to those on a LFD ($p = 0.0194$) (Figure 21B).

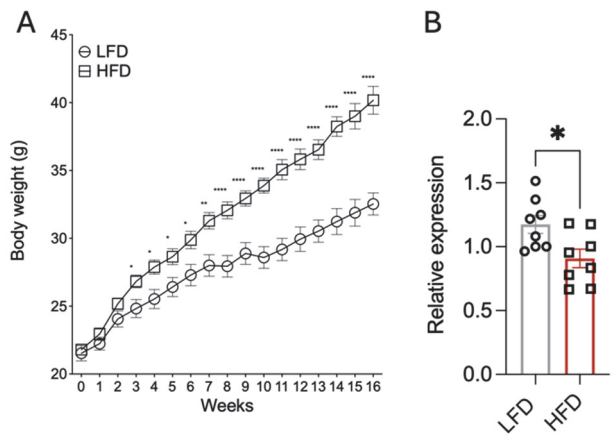

Figure 21: HFD resulted in body weight gain and decreased miR-146a expression in HT. (A) Measurement of body weight. (B) miR-146a expression in HFD and LFD groups. N = 8–10. Two-way ANOVA followed by Tukey's multiple comparisons test and Student's t-test. Data are represented as mean ± SEM; *$p < 0.05$, ** $p < 0.01$, ***$p < 0.001$, **** $p < 0.0001$.

5.4.2 Loss of miR-146a enhances microglial senescence in HFD-induced obesity model

HFD has been previously shown to induce cellular senescence in the brain (189), and miR-146a has been implicated in the regulation of senescence (190). Given the observed downregulation of miR-146a in our HFD-induced obesity model, we aimed to explore its role in microglial senescence by using *Mir146a-/-* mice alongside *WT* controls. Both groups were subjected to either an HFD or LFD, and key markers of senescence and inflammation were assessed in the HT. Assessment of senescence markers revealed that HFD significantly upregulated *p16* and *p21* mRNA expression in both *WT* ($p = 0.0025$, $p = 0.0033$) and in *Mir146a-/-* mice ($p < 0.0001$, $p = 0.0002$). However, this increase was even more pronounced in *Mir146a-/-* mice compared to *WT* HFD group ($p = 0.0031$, $p = 0.0355$) (Figure 22A, B), suggesting an enhanced senescence response in the absence of miR-146a. To specifically identify β-gal + microglial cells additional staining with Cd11b and Cd45 was done before staining with β-gal. The gating strategy for the quantification of microglial percentage is shown in Figure 8, Section 4.4.1. Both *WT* and *Mir146a-/-* mice showed an increase in senescent microglia after HFD exposure in the HT ($p = 0.0445$, $p = 0.0004$), with a more pronounced increase in *Mir146a-/-* mice compared to *WT* mice ($p = 0.0479$) (Figure 22C). Additionally, the mRNA expression of SASP cytokines *Il1b, Il18*, and *Il6* was significantly elevated in the HFD groups compared to the LFD groups in both *WT* ($p = 0.0016$, $p = 0.0064$, $p = 0.0244$) and *Mir146a-/-* mice ($p = 0.0171$, $p = 0.0027$, $p = 0.0159$), with no significant genotypic differences (Figure 22D-F). These findings suggest that miR-146a plays a protective role in limiting HFD-induced microglial senescence.

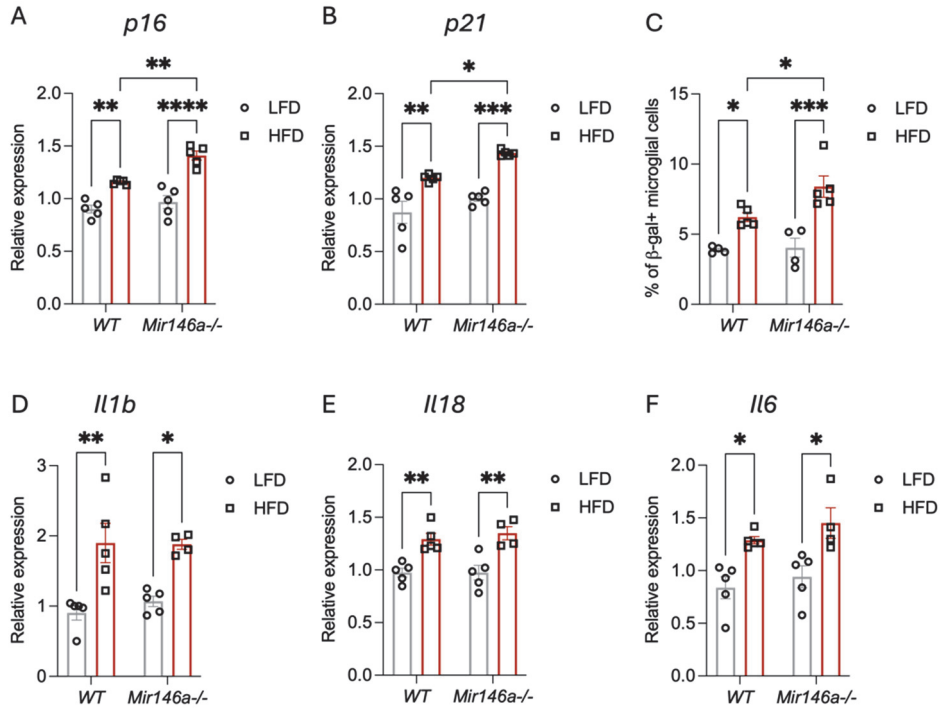

Figure 22: Absence of miR-146a leads to increased microglial senescence in response to HFD. (A-B) *p16* and *p21* mRNA expression, (C) Quantification of β-gal+ microglia, (D-F) mRNA expression of SASP cytokines levels in the HT of *WT* and *Mir146a-/-* mice on HFD and LFD. N = 4–10, two-way ANOVA followed by Tukey's multiple comparisons test (A,B,E,F) and one-way ANOVA with Tukey's multiple comparisons test (C,D). Data are represented as mean ± SEM; *p < 0.05, **p < 0.01, ***p < 0.001,**** p < 0.0001.

5.4.3 Elevated *Smad4* expression in the HT of *Mir146a-/-* mice under HFD

To understand the molecular mechanisms through which miR-146a regulates senescence in response to HFD, we examined the expression of its known direct targets, involved in inflammation and senescence regulation, such as *Irak1* (96) and *Smad4* (191). Our analysis showed that *Irak1* expression remained unchanged across all experimental groups (Figure 23A), suggesting that it may not play a major role in this context. In contrast, *Smad4* expression was elevated in the *WT* HFD group (p = 0.0074) compared to the *WT* LFD group and was further increased in the *Mir146a-/-* HFD group compared to the *Mir146a-/-* LFD group (p = 0.0010) and *WT* HFD group (p = 0.0132), indicating a more pronounced effect in the absence of miR-146a (Figure 23B). These findings suggest that miR-146a may regulate microglial senescence through *Smad4*, as its deficiency leads to *Smad4* upregulation in response to HFD, potentially contributing to enhanced senescence in the hypothalamus.

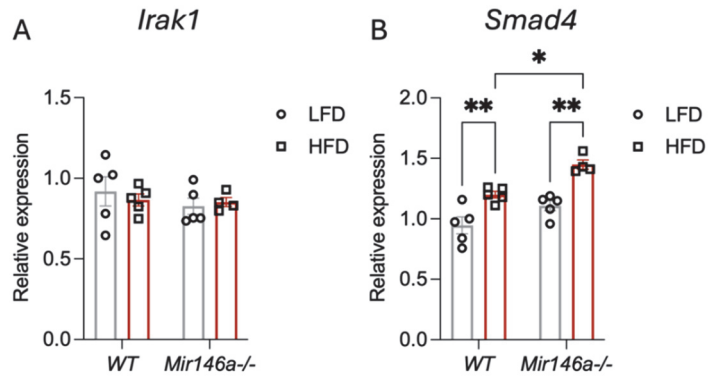

Figure 23*:* Loss of miR-146a leads to enhanced *Smad4* Expression in the HT upon HFD (A-B) Relative mRNA expression of indicated genes in HT, N = 4-6, two-way ANOVA followed by Tukey's multiple comparisons test, Data are represented as mean ± SEM; * $p < 0.05$, ** $p < 0.01$.

5.4.4 Elocalcitol induced miR-146a expression in the hypothalamus

To explore potential strategies for mitigating HFD-induced hypothalamic senescence, we investigated whether restoring miR-146a expression could be effective. Given the known anti-inflammatory properties of vitamin D and its analogue Elo, we assessed their ability to modulate miR-146a levels under HFD conditions. Our analysis revealed that Elo significantly upregulated miR-146a expression in the hypothalamus of HFD-fed mice, whereas vitamin D had no significant effect (Figure 24A). To further validate the impact of Elo, we examined its effect in the absence of HFD and found that Elo treatment alone significantly increased miR-146a levels in the hypothalamus (Figure 24B). These findings suggest that Elo positively regulates miR-146a expression, highlighting its potential as a therapeutic approach for counteracting HFD-induced hypothalamic senescence.

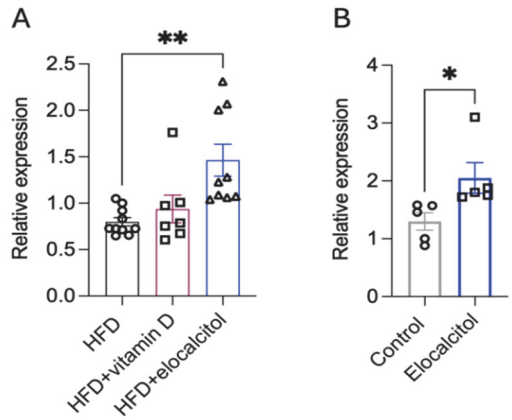

Figure 24: Elocalcitol restores miR-146a expression in HT of HFD-fed mice. miR-146a expression upon HFD with (A) vitamin D or Elo treatment and (B) on Elo treatment. N = 5-10, One-way ANOVA followed by Tukey's multiple comparisons test and Student's t-test, Data are presented as mean ± SEM; * $p < 0.05$, ** $p < 0.01$.

5.4.5 Elocalcitol mitigates HFD-induced senescence changes in *WT* mice but not in *Mir146a-/-* mice

We next performed the experiments to determine whether Elo treatment could counteract HFD-induced cellular senescence, and whether miR-146a is involved in this pathway. For that, we administered Elo to *WT* and *Mir146a-/-* mice on HFD and assessed the senescence markers in the HT compared to mice on HFD without Elo treatment. Interestingly, Elo treatment led to a significant reduction in *p16* and *p21* mRNA levels in *WT* HFD mice ($p = 0.0066$, $p = p < 0.0001$), indicating its ability to mitigate HFD-induced senescence. However, *Mir146a-/-* HFD + Elo mice did not exhibit any significant change in *p16* and *p21* expression compared to *Mir146a-/-* HFD controls (Figure 25A, B). Furthermore, we observed a significant reduction in β-gal-positive microglial cells in the *WT* HFD + Elo group compared to *WT* HFD controls ($p = 0.0125$). However, no such decrease was seen in *Mir146a-/-* HFD + Elo mice ($p = 0.7652$) (Figure 25C). Finally, the levels of SASP cytokines in HT were assessed, revealing that *WT* HFD + Elo mice had a significant reduction in *Il1b* ($p = 0.0057$), *Il18* ($p = 0.0016$), and *Il6* ($p = 0.0390$) compared to *WT* HFD controls, while changes were observed in *Mir146a-/-* HFD + Elo mice (Figure 25D-F). Together, these findings suggest that Elo effectively reduces HFD-induced senescence markers in *WT* mice, but these beneficial effects are absent in *Mir146a-/-* mice, indicating that miR-146a plays a key role in mediating the therapeutic effects of Elo in HFD conditions.

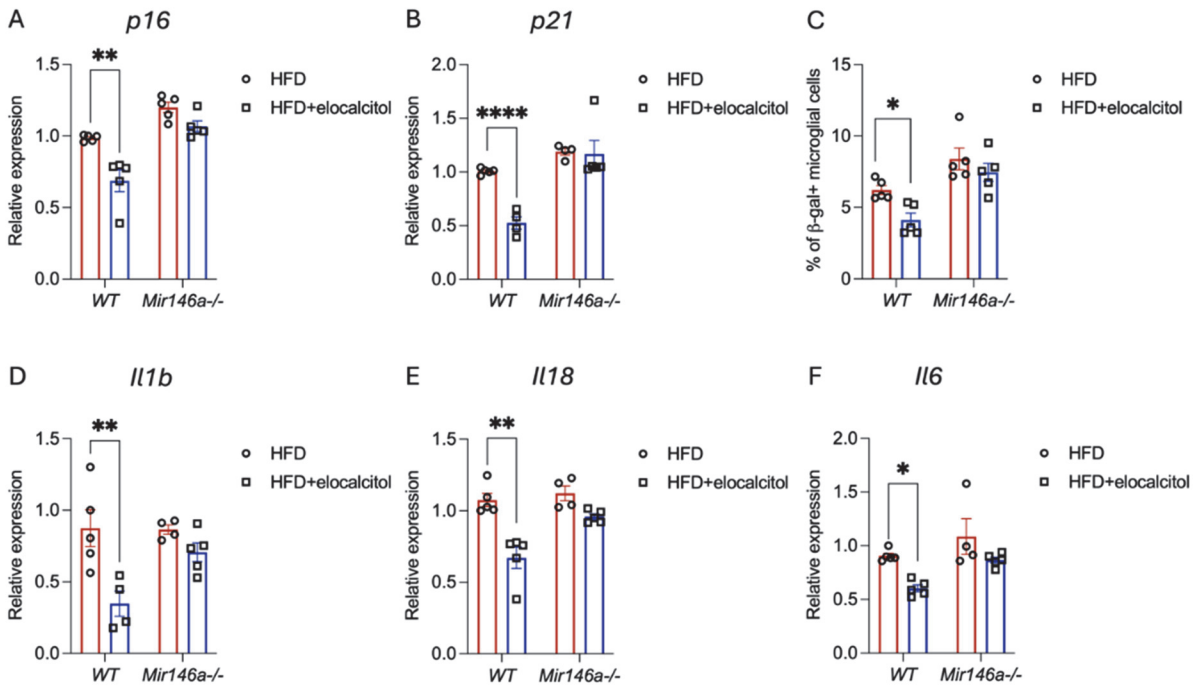

Figure 25: Elocalcitol ameliorates HFD-induced microglial senescence in *WT* but not in *Mir146a-/-* mice. (A-B) *p16* and *p21* mRNA expression. (C) Analysis of β-galactosidase-positive microglial cells. (D-F) mRNA expression of indicated SASP cytokines**.** N = 4-5, one-way ANOVA with Tukey's multiple comparisons test (A, B, C,E) and two-way ANOVA followed by Tukey's multiple comparisons test (D,F). Data are represented as mean ± SEM; * $p < 0.05$, ** $p < 0.01$, **** $p < 0.0001$.

6. DISCUSSION

6.1 Baseline expression difference of miR-146a/b in neuronal and microglial cells

Despite sequence and target similarities of miR-146a/b, as well as their overlapping neuroinflammatory roles, their cellular distribution in neuronal and non-neuronal cell types were incompletely characterized from the previous studies. In our study, we show that miR-146a was enriched in microglial cells, with lower expression detected in astroglia cells, but it is almost absent in neuronal cells in the adult mice. This is in line with the previously published studies where enrichment of miR-146a in microglial cells have been demonstrated (27). In contrast, miR-146b exhibited a markedly different expression pattern with high expression of in neuronal cells, with lower levels in microglial and astroglial cells. This differential expression of miR-146a/b indicated that there is a need to explore the functions of these miRNAs more as they might have different roles in neuronal and microglial cells.

6.2 Cognitive functions and brain cell alterations upon *Mir146b-/-* and *Mir146a-/-* mice

One of the significant findings of our study is the enhanced memory observed in miR-146b deficient mice. These mice demonstrated enhanced episodic recognition memory, and better memory acquisition and recall in the novel object and fear conditioning tests. These behavioral outcomes suggest that miR-146b plays a critical role in regulating memory and learning processes. Flow cytometry experiments revealed striking abnormalities in the cellular composition of the brains of *Mir146b-/-* mice. Specifically, we found that the loss of miR-146b led to an increased number of neurons, particularly, the population of Vglut2+ glutamatergic neurons was significantly elevated in the HP of *Mir146b-/-* mice. These findings were corroborated by immunohistochemical analysis, which showed an increased neuronal density in FC sections of miR-146b deficient mice. These results are in line with previous studies showing that miR-146b overexpression by lentivirus vector could inhibit the proliferation of primary hippocampal neural stem cells (143). Another study has demonstrated that optogenetic stimulation of prefrontal glutamatergic neurons significantly enhances associative recognition memory in mice. This enhancement was achieved by selectively stimulating these neurons during the maintenance of information, leading to improved performance in memory tasks, indicating that enhancing the activity of glutamatergic neurons can directly improve cognitive functions (192). Similarly, we found increased number of glutamatergic neurons in miR-146b deficient mice, which could be the reason why we observed enhanced cognition in these mice.

Additionally, we observed reduction in astroglial cells in *Mir146b-/-* mice. During early development and adult neurogenesis, cell fate determination in neural and astroglial tissues is influenced by complex interactions between multiple signaling pathways (193). Both neurons and astroglia are produced from the radial glial progenitor cells, and cross talk between JAK-STAT signaling and Wnt signaling is responsible for this switch from neurogenesis to gliogenesis and for differentiation of astrocytes (194). Since miR-146b is downstream of the JAK-STAT pathway and modulates NF-κB signaling, its absence could disrupt the balance of these pathways (195) and other pathways such as Wnt signaling (196) potentially leading to a reduction in astroglial populations during critical developmental windows.

In contrast to miR-146b deficient mice, we found that miR-146a deficient mice had no significant change in cognitive functions (197). This was in line with a previous study reporting that there were no changes in short-term spatial memory and fear conditioning cognitive tests in middle-aged (9-12 months) miR-146a knockout mice (198). This suggests that miR-146a's primary functions may lie outside of cognitive regulation in adult mice. However, a study by Fregeac *et al.* found that miR-146a knockout mice exhibited cognitive impairments at 3 months of age when in NORT test. Importantly, this cognitive decline occurred without any apparent changes in neuronal numbers in the adult brain (10). This suggests that miR-146a may play role in cognitive functions at an earlier stage, in contrast to our findings in 4-month-old mice, where no such impairments were observed. While both studies used the NORT, the subtle age difference (3 months vs. 4 months) may explain the discrepancy in cognitive outcomes. It is possible that miR-146a influence on cognition is more pronounced at younger ages, with cognitive impairments becoming less detectable as the animals mature.

6.3 Changes in neurogenesis and synaptic plasticity in miR-146b deficient mice

To understand the reasons behind the increased neuronal cell numbers, more deep analysis of neurogenesis in the DG of HP was conducted. Interestingly, miR-146b deficient mice had enhanced neurogenesis in DG, as demonstrated by the higher numbers of neuronal precursors, proliferative cells, and their better survival. When assessing the phenotype of newly generated cells, we found that a larger proportion of cells expressed a mature neuronal marker, calbindin, in miR-146b deficient mice, indicating to increased differentiation into neurons. Previous rodent studies have shown that neurogenesis is important for hippocampal-dependent learning as reduced neurogenesis impairs fear conditioning (199) and long-term spatial memory formation (200). Thus, increased neurogenesis can also positively modulate memory acquisition. In line with the neuronal phenotype of *Mir146b-/-* mice, the pathway analysis of conserved miR-146b targets revealed that neurogenesis-related genes are overrepresented among miR-146b target genes, indicating that miR-146b might influence neuronal

development through several different genes. From putative targets, we selected *Gdnf* and explored its expression in miR-146b deficient mouse brain. Indeed, we observed an increased expression of *Gdnf* mRNA in the HP of *Mir146b-/-* mice. *Gdnf* participates in proliferation, migration and differentiation of the neural cells (201), and upregulation of *Gdnf* in *Mir146b-/-* mice might contribute to increased neuronal proliferation and survival in these mice.

6.4 Microglial phagocytosis in miR-146b deficient mice

Even though lower expression of miR-146b is found in microglial cells, we observed significantly increased phagocytosis of Vglut2+ synapses in *Mir146b-/-* mice. This elevated phagocytosis could be linked to the increased neuronal density observed in these mice, suggesting that microglia may be actively engaged in remodeling synaptic circuits as part of an ongoing neurogenesis process. Several studies have indicated that microglia play a central role in the regulation of synaptic plasticity, particularly during periods of neurogenesis, when synaptic connections are being refined to support the development of new networks (184,202). Interestingly, previous studies with miR-146a knockout mice microglia have shown no changes in phagocytic activity at baseline, while LPS stimulation led to decreased phagocytosis (27). In contrast, where we observed baseline phagocytosis of Vglut2+ synapses were increased in *Mir146b-/-* mice. These divergent results suggest that miR-146a/b may have distinct roles in modulating microglial behavior, with miR-146b potentially involved in synaptic remodeling during neurogenesis and thereby neuroplasticity, while miR-146a may be more implicated in inflammatory responses and phagocytic activity.

6.5 Crosstalk between miR-146a/b during neuroinflammation

miR-146a/b are well-established anti-inflammatory miRNAs that are rapidly induced under neuroinflammatory conditions (109,138). They are primarily upregulated in activated microglial cells in response to pro-inflammatory stimuli and act as negative feedback regulators by targeting key upstream molecules IRAK1 and TRAF6 leading to suppression of the overactivation of the NF-κB pathway, thereby dampening the inflammatory response (109,137). Previous study has shown that miR-146a deficiency lead to increased production of pro-inflammatory cytokines and inflammasome component in the brain of miR-146a knockout mice (198). This indicates that miR-146a is critical for maintaining microglial homeostasis and preventing excessive inflammation in the CNS. Although miR-146a/b target similar set of genes, their expression and regulation during neuroinflammation can be distinct, as miR-146b is predominantly expressed in neuronal cells and less in microglia compared to miR-146a. Interes-

tingly, our study revealed that *Mir146b-/-* mice have attenuated neuroinflammatory response upon LPS challenge, as evidenced by less prominent sickness behavior and microglial activation. Although sickness behavior is believed to be associated with neuroinflammation, the impact of peripheral inflammatory reaction cannot be excluded (203,204). In line with behavior studies and microglial status, LPS-mediated stimulation of the expression of pro-inflammatory cytokines, was weaker in HP of *Mir146b-/-* LPS mice compared to *WT* LPS animals.

Although miR-146a/b are expressed in distinct cell types, their regulatory roles can be interconnected. We report here that in miR-146b deficient mice, neuroinflammatory responses were unexpectedly reduced upon LPS challenge, which may be due to upregulation of miR-146a in hippocampal tissues and in microglial cells isolated from the hippocampal tissue. In line with this, in miR-146a/b knockout mice, LPS-induced sickness behavior and expression of pro-inflammatory cytokines were similar than that of in *WT* mice as shown in figure 9 in Publication II (205). These results highlight partial functional redundancy of miR-146a/b. We also observed that miR-146a was upregulated at the baseline in miR-146b deficient mice in microglial cells without any stimulus, while in a study using miR-146a deficient model, no upregulation of miR-146b was found (198). This can be because of the low expression of miR-146b in the microglial cells, or because miR-146b expression does not depend strongly on the NF-κB pathway. Our results also indicate that the reduced activation of NF-κB may be due to the diminished ability of Tlr4 to become upregulated in response to LPS, and this may cause decreased activation of NF-κB and reduced inflammation. Although TLR4 has been shown to be direct target of miR-146a in human (97), this has not proven in mouse. In addition, our results are in line with a previous study showing that miR-146a overexpression reduces microglia mediated neuroinflammatory responses and sickness behavior in mice (206).

To explain possible mechanisms of the observed miR-146a upregulation, we measured the transcription factor *Irf7*, and found its upregulation in HP of miR-146b deficient mice, which is responsible for the overexpression of miR-146a. There is evidence that *Irf7* plays an essential role in the LPS-induced interferon-β gene expression and endotoxic shock (207) and suppression of inflammatory reaction upon LPS challenge (208). We, therefore, propose that upregulation of *Irf7* may lead to the overexpression of miR-146a, which in turn inhibits NF-κB activation leading to the blunted inflammatory response. It should be noted that the mechanism by which miR-146b can regulate the expression of *Irf7* remains to be studied.

6.6 HFD-induced microglial senescence and miR-146a regulation

In the current thesis, we also studied the intricate role of miR-146a in regulating HFD-induced microglial senescence and inflammation, with specific focus on the

hypothalamus. We demonstrate that HFD induces pronounced microglial senescence in the hypothalamus, characterized by elevated levels of *p16*, *p21*, SA-β gal positive microglial cells and SASP cytokines (*Il1b*, *Il18*, *tnf* and *Il6*), alongside an increase in β-gal positive microglial cells, indicating an advanced stage of senescence in this brain region. This aligns with existing literature that highlights the sensitivity of hypothalamic neurons and glia to metabolic insults and their pivotal role in the central regulation of energy balance (209). The increased β-gal positive microglial cells in the hypothalamus underscores the advanced nature of senescence in this region, further suggesting that neuroinflammation and cellular aging in the brain are closely linked to dietary-induced metabolic disturbances. The senescent microglial cells likely adopt a senescence-associated secretory phenotype, releasing pro-inflammatory cytokines, such as *Il1b*, *Il18*, *Tnf*, and *Il6*. This cytokine production in the hypothalamus suggests that SASP is a central contributor to neuroinflammation under HFD conditions, linking cellular senescence with metabolic stress-induced inflammatory signaling. The HFD-induced obesity also induced downregulation of miR-146a in hypothalamus of the mouse brain. Interestingly, although other studies have shown that miR-146a is upregulated in response to obesity and can suppress inflammation in adipose tissue (210), our findings indicate a different pattern of its expression in the hypothalamus. Another study has shown miR-146a downregulation in the brain region of the nucleus accumbens under HFD conditions, further suggesting that miR-146a downregulation in response to HFD may be characteristic to certain brain regions. (121). In the hypothalamus of *Mir146a-/-* mice, we observed an increased expression of senescence markers *p16*, *p21* and SA-β gal positive microglial cells upon HFD treatment, indicating that miR-146a may act as a protective factor against HFD-induced cellular senescence in the hypothalamus.

Our study clearly demonstrated that Elo, a non-hypercalcemic fluorinated analogue of vitamin D, has a protective effect against HFD-induced hypothalamic senescence by inducing miR-146a expression. Concomitant administration of Elo reduced the expression of senescence markers and inflammatory cytokines in *WT* mice. By contrast, in *Mir146a-/-* mice, Elo failed to reduce the expression of senescence markers suggesting that the protective effects of Elo are mediated, at least in part, through miR-146a pathways. Notably, Elo treatment led to upregulation of miR-146a expression in the hypothalamus, which further indicates that HFD-induced changes in the hypothalamus may be due Elo beneficial effects through the restoration of miR-146a levels. Importantly, we are the first to show that Elo can reverse cellular senescence, highlighting its potential as a novel therapeutic agent for combating age-related and metabolic disorders. The reduction in senescence markers, such as *p16* and *p21*, and SASP cytokines further supports the anti-aging properties of Elo. To explore which targets of mir-146a might be involved in the regulation of senescence, we measured the expression of its direct targets *Irak1* (96) and *Smad4* (211) in the hypothalamus of *Mir146a-/-* mice and *WT* mice upon HFD treatment. Our data show that *Smad4* mRNA levels were increased in the hypothalamus of HFD mice and even more so in the

Mir146a-/- HFD group, supporting the hypothesis that miR-146a negatively regulates *Smad4* in the brain. Previously, it has been also shown that miR-146a can target *Smad4*, thereby modulating senescence pathways (212). The heightened levels of *Smad4* in the absence of miR-146a may contribute to the enhanced senescence observed in the hypothalamus of *Mir146a-/-* HFD mice. Interestingly, we found no significant changes in *Irak1* expression in the hypothalamus of either *WT* HFD or *Mir146a-/-* HFD mice, suggesting that *Irak1* has less important role in the brain under HFD conditions.

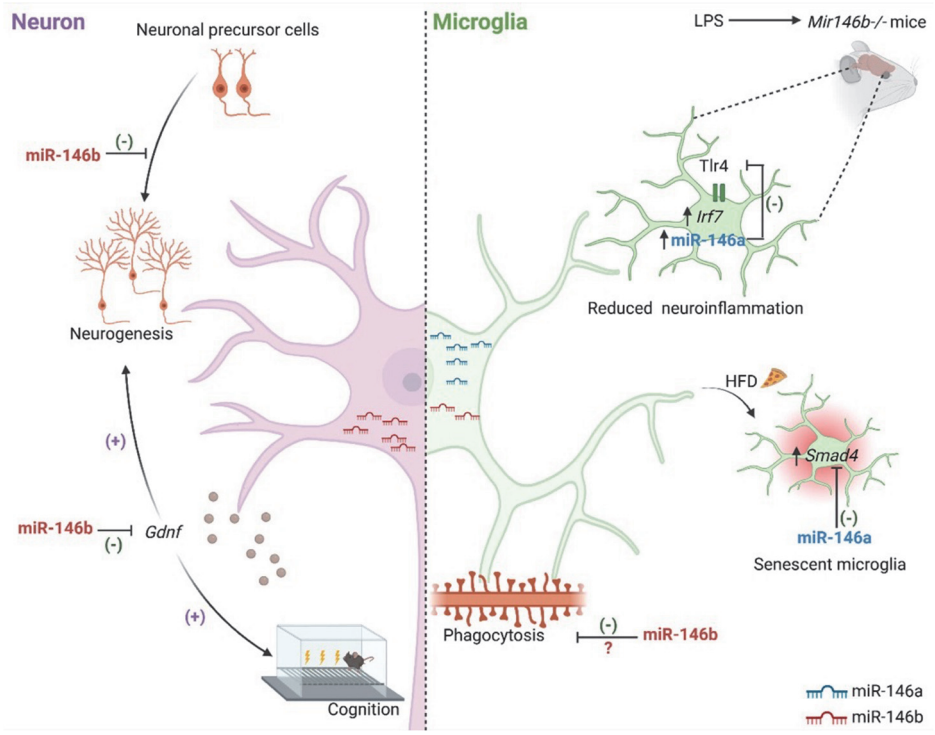

Figure 26: Roles of miR-146b in neurons and miR-146a/b in microglia. miR-146b is a negative regulator of neurogenesis and *Gdnf* in neurons, and may reduce microglial-mediated phagocytic activity. Absence of miR-146b leads to elevation of miR-146a, which may reduce microglia activation upon inflammatory stimulus via suppression of the Tlr4 pathway, leading to reduced neuroinflammation. miR-146a also mitigates hypothalamic microglial senescence through Smad4 under HFD conditions. Arrows indicate positive (+) or negative (-) regulation by miR-146a/b.

7. GENERAL REMARKS AND FUTURE DIRECTIONS

In the context of neurogenesis and cognition, while increased numbers of neurons were observed in miR-146b knockout mice, it remains unclear whether these neurons form functional synapses. Electrophysiological recordings, such as patch-clamp or multi-electrode array analyses, could be performed to assess the ratio of functional to non-functional synapses. Additionally, the intriguing observation of increased phagocytosis in miR-146b knockout mice raises the question of whether this is due to microglial dysfunction or an overabundance of neurons. Conditional knockout models targeting miR-146b in either neurons or microglia specifically could help resolve this. These models would allow us to measure synaptic density and microglial activity independently, providing insights into the cell type-specific contributions of miR-146b. Crossing miR-146b knockout mice with Alzheimer's disease models represents another promising direction to investigate whether enhanced neurogenesis can counteract memory impairments. Behavioral tests, such as the Morris water maze, coupled with analyses of neuronal survival and synaptic density, could provide valuable data on therapeutic potential. To assess the developmental specificity of miR-146b's role, miR-146b expression levels could be measured across different developmental stages using RNA in situ hybridization or single-cell RNA sequencing. These experiments would help determine whether miR-146b is restricted to adult mature neurons or plays roles in earlier stages of neuronal development. Moreover, given the observed imbalance in cell types (fewer astroglia and more neurons), examining potential shifts in the JAK-STAT signaling pathway could uncover underlying mechanisms. In the context of LPS-induced neuroinflammation, future research could investigate how miR-146b negatively regulates IRF7, whether through direct binding or via an intermediary pathway. Techniques such as luciferase reporter assays or RNA immunoprecipitation could clarify the mechanism. For HFD-induced senescence, future experiments should determine whether senescence is restricted to microglia or also affects other cell types, such as astrocytes or neurons. Additionally, single-cell RNA sequencing of HFD-treated brains could identify the specific subpopulations affected by senescence and their unique transcriptomic profiles. Exploring miR-146b's role in senescence could provide novel insights, particularly by evaluating its expression in senescent versus non-senescent cells under HFD. Future studies could further investigate the detailed molecular mechanisms by which miR-146a modulates TGF/Smad4 pathway. Specifically, exploring the interaction between miR-146a and other components of the TGF-β signaling axis, including downstream signaling molecules like Smad3, could provide deeper insights into how miR-146a affects cellular senescence at the molecular level. Another direction is to see the long-term effects of elocalcitol on chronic obesity-induced inflammation and to evaluate if elocalcitol could have sustained benefits on cognitive function, microglial activation, and neurogenesis over extended periods. Since we used only male mice in our studies, investigating whether similar effects are observed in females would be an important future direction, particularly given potential sex-specific differences in immune and neuroinflammatory responses.

8. CONCLUSIONS

1. miR-146b is higher in neuronal cells and miR-146a is enriched in microglial cells of the brain. miR-146b deficient mice showed increased density of neurons, which may be caused by increased adult hippocampal neurogenesis as indicated by increased proliferation, differentiation, survival of neuronal precursors and calbindin+ mature neurons. These changes in neurogenesis may be connected with enhanced cognition and fear memory in these mice. miR-146b probably exerts its actions via regulation of its target *Gdnf* expression, which promotes neuronal survival in *Mir146b-/-* mice. These data together open new avenues for the regulation of neurogenesis via modulation of miR-146b.
2. miR-146a/b are upregulated in the hippocampal tissue and in the microglial cells upon LPS treatment, with higher baseline level of miR-146a in microglial cells. LPS administration induced weaker upregulation of proinflammatory cytokines and NF-κB activation in the HP of *Mir146b-/-* mice compared to *WT* mice. The blunted neuroinflammatory reaction upon LPS challenge observed in *Mir146b-/-* mice may be due to the compensatory upregulation of miR-146a, which may be mediated by Irf7 while miR-146a may attenuate neuroinflammation via impact on TLR4 signaling. These data highlight the crosstalk between miR-146a/b in the regulation of neuroinflammation.
3. HFD inhibits the expression of miR-146a in the hypothalamus while *Mir146a-/-* mice are more vulnerable to HFD-induced cellular senescence, as indicated by elevated senescence markers *p16*, *p21* and enhanced number of SA-β-gal positive microglial cells. *Smad4* mRNA levels were elevated upon HFD, and this increase was more pronounced when miR-146a is absent, suggesting that miR-146a exerts its protective effects by downregulating *Smad4* in the hypothalamus. Notably, this mechanism appears to be independent of Irak1, suggesting that miR-146a's anti-senescence action is linked to Smad4-mediated pathways. These findings underscore miR-146a role in regulation of senescence-driven inflammation.
4. Elo, a vitamin D analogue, exhibits significant anti-senescent properties in HFD-induced obesity models. In *WT* mice, Elo effectively attenuates cellular senescence by reducing markers of inflammation and senescence-associated phenotypes. However, the absence of this protective effect in miR-146a-deficient mice treated with Elo suggests that the anti-senescence actions of Elo are mediated through miR-146a. These findings position Elo as a promising therapeutic compound, acting via miR-146a, with potential applications to treat metabolic and neurodegenerative diseases.

9. SUMMARY IN ESTONIAN

miR-146a ja miR-146b erinevad rollid neuronites ja mikrogliias

Käesoleva uurimistöö keskendub miR-146b ja miR-146a (miR-146a/b) rollile neurogeneesi, neuropõletiku ja mikrogliia vananemise reguleerimisel. MikroRNA-d (miRNA-d) on väikesed, mittekodeerivad RNA-d, mis on tavaliselt umbes 18–22 nukleotiidi pikkused ja reguleerivad geeniekspressiooni, seondudes nende sihtmärk-mRNA-de 3' transleerimata piirkonnaga, mis viib mRNA lagunemiseni ja/või translatsiooni inhibeerimiseni, mõjutades seeläbi mitmesuguseid rakkudes toimuvaid protsesse. Nii miR-146b kui ka miR-146a kuuluvad miR-146 perekonda, ning nende rolli põletikuliste protesesside reguleerimises on varem põhjalikult uuritud erinevates rakkudes ja seoses paljude haigustega, kuid vähem soeses neuropõletikuliste olukordadega.

Uurimistöö eesmärgiks oli selgitada välja miR-146a/b regulatoorsed toimed neurogeneesile ja mikrogliia vananemisele ning neuropõletikule, kasutades transgeenseid miR-146a/b puudulikke (*Mir146a-/-*, *Mir146b-/-)* hiiri.

Saadud tulemused näitasid, et miR-146b, kuigi vähem uuritud kui miR-146a, omab olulist immunomoduleerivat ja neuroprotektiivset rolli. Tuvastasime ka, et miR-146b avaldus peamiselt neuronite ja vähem mikrogliia- ja astrogliaalsetes rakkudes. Kasutades *Mir146b-/-* hiiri, selgitasime välja miR-146b rolli täiskasvanud hiirte hipokampuses neurogeneesi reguleerimisel. *Mir146b-/-* puudulikel hiirtel tuvastati neuronite prekursorite suurenenud proliferatsioon ja diferentseerumine ning suurenenud kalbindiin-positiivsete küpsete neuronite arv. Käitumusliku fenotüübi iseloomustamisel ilmnes *Mir146b-/-* puudulikel hiirte parem assotsiatiivne ja kontekstuaalne mälu. Samuti leidsime, et nendes hiirtes on kõrgem Gdnf mRNA tase, mis omakorda võib soodustada neuronite elulemust ja neurogeneesi.

Kuigi miR-146b oli avaldunud mikrogliias madalamal tasemel kui miR-146a, uurisime *Mir146b-/-* hiiri LPS-indutseeritud neuropõletiku mudelis. Selleks manustasime *Mir146b-/-* hiirtele LPS-i, mille järgselt täheldasime miR-146a ekspressiooni tõusu hipokampuse koes ja samuti hipokampuse koest eraldatud mikrogliia rakkudes. Tuvastasime, et miR-146b puudulikel hiirtel oli madalam LPS-indutseeritud neuropõletik, mida kinnitas haigusnähtude vähenemine ja mikrogliia vähenenud aktivatsioon. Geeni- ja valguekspressioonianalüüs näitas, et LPS-i manustamine kutsus *Mir146b-/-* hiirte ajus esile põletikueelsete tsütokiinide väiksema tõusu. Meie edasised katsed näitavad, et LPS-indutseeritud vähenenud neuropõletikuline reaktsioon *Mir146b-/-* hiirtel on tõenäoliselt tingitud miR-146a üleekspressioonist nendes hiirtes, mida võib vahendada transkriptsiooniregulaator Irf7. Käesolev uuring näitab, et miR-146a/b omavad keerukat ja omavahel seotud rolli neuropõletikuliste protsesside regulatsioonis.

Varasemad publikatsioonid on näidanud, et miR-146a osaleb neuropõletikus oksüdatiivse stressi ja mikrogliia polariseerumise regulaatorina. Seetõttu uurisime ka miR-146a rolli kõrge rasvasisaldusega dieedi (KRD) poolt põhjustatud

hüpotaalamuse vananemises. Kõigepealt leidsime, et miR-146a ekspressioon on KRD-ga mõjutatud loomade hüpotaalamuses märkimisväärselt vähenenud, samas kui *Mir146a-/-* hiirtel tingis KRD suurema vastuvõtlikkuse rakulisele vananemisele. Sellele viitasid vananemise markerite p16 ja p21 ekspressiooni tõus ning mikrogliia vananemise tugevam fenotüüp. Meie järgnevates katsetes tuvastasime, et *Mir146a-/-* hiirtes on *Smad4* ekspressioon, viidates võimalusele, et miR-146a toimib Smad4 pärssijana ja kaitseb seeläbi rakke vananemise eest hüpotaalamuses. Edasi proovisime oma katsetes, kas D-vitamiini analoog, elokaltsitool võib omada ravitoimet KRD-st põhjustatud metaboolse stressi mõju leevendamisel. Leidsime, et elokaltsitooli manustamine kutsus esile miR-146a ekspressiooni tõusu hüpotaalamuses, viidates võimalusele, et see võiks olla tõhus ühend taastamaks KRD toimel vähenenud miR-146a ekspressiooni ajus. Katsed, milles kasutati nii metsiktüüpi kui ka *Mir146a-/-* hiiri, näitasid, et elokaltsitool vähendas dieedist indutseeritud vananemise markereid hüpotaalamuses. Ühtlasi leidsime, et kui metsiktüüpi loomadel avaldus KRD-st põhjustatud rasvumise mudelis elokaltsitooli vananemisvastane toime, siis *Mir146a-/-* hiirtel mitte. Need tulemused viitavad võimlusele, et elokaltsitool avaldab oma vananemisvastast toimet miR-146a kaudu.

Kokkuvõttes iseloomustavad käesoleva uuringu tulemused üksikasjalikult miR-146a/b rolle nii neuronaalsetes kui mikrogliaalsetes rakkudes, tuues esile miR-146a/b keerukad ja omavahel seotud rollid neuropõletikuliste protsesside regulatsioonides, muutes nad võimalikeks terapeutilisteks sihtmärkideks neuronaalsete põletike ja metaboolsete häiretega seotud ajupatoloogiate korral.

10. REFERENCES

1. Bartel DP. Metazoan MicroRNAs. Cell. 2018 Mar 22;173(1):20–51.
2. Anglicheau D, Muthukumar T, Suthanthiran M. MicroRNAs: small RNAs with big effects. Transplantation. 2010 Jul 27;90(2):105–12.
3. Stappert L, Roese-Koerner B, Brüstle O. The role of microRNAs in human neural stem cells, neuronal differentiation and subtype specification. Cell Tissue Res. 2015 Jan;359(1):47–64.
4. Bian S, Xu T le, Sun T. Tuning the cell fate of neurons and glia by microRNAs. Curr Opin Neurobiol. 2013 Dec;23(6):928–34.
5. Tsai YC, Chang CH, Chong YB, Wu CH, Tsai HP, Cheng TL, et al. MicroRNA-195-5p Inhibits Intracerebral Hemorrhage-Induced Inflammatory Response and Neuron Cell Apoptosis. Int J Mol Sci. 2024 Sep 25;25(19):10321.
6. Parisi C, Arisi I, D'Ambrosi N, Storti AE, Brandi R, D'Onofrio M, et al. Dysregulated microRNAs in amyotrophic lateral sclerosis microglia modulate genes linked to neuroinflammation. Cell Death Dis. 2013 Dec 12;4(12):e959.
7. Schratt GM, Tuebing F, Nigh EA, Kane CG, Sabatini ME, Kiebler M, et al. A brain-specific microRNA regulates dendritic spine development. Nature. 2006 Jan 19; 439(7074):283–9.
8. Aten S, Hansen KF, Hoyt KR, Obrietan K. The miR-132/212 locus: a complex regulator of neuronal plasticity, gene expression and cognition. RNA Dis. 2016;3(2): e1375.
9. Yan HL, Sun XW, Wang ZM, Liu PP, Mi TW, Liu C, et al. MiR-137 Deficiency Causes Anxiety-Like Behaviors in Mice. Front Mol Neurosci. 2019;12:260.
10. Fregeac J, Moriceau S, Poli A, Nguyen LS, Oury F, Colleaux L. Loss of the neurodevelopmental disease-associated gene miR-146a impairs neural progenitor differentiation and causes learning and memory deficits. Molecular autism. 2020; 11(1):1–14.
11. Jauhari A, Singh T, Mishra S, Shankar J, Yadav S. Coordinated action of miR-146a and parkin gene regulate rotenone-induced neurodegeneration. Toxicological Sciences. 2020;176(2):433–45.
12. Jayadev S, Case A, Alajajian B, Eastman AJ, Möller T, Garden GA. Presenilin 2 influences miR146 level and activity in microglia. J Neurochem. 2013 Dec; 127(5):592–9.
13. Bai M, Zhu X, Zhang Y, Zhang S, Zhang L, Xue L, et al. Abnormal hippocampal BDNF and miR-16 expression is associated with depression-like behaviors induced by stress during early life. PLoS One. 2012;7(10):e46921.
14. Lopez JP, Fiori LM, Cruceanu C, Lin R, Labonte B, Cates HM, et al. MicroRNAs 146a/b-5 and 425-3p and 24-3p are markers of antidepressant response and regulate MAPK/Wnt-system genes. Nat Commun. 2017 May 22;8:15497.
15. Laanesoo A, Urgard E, Periyasamy K, Laan M, Bochkov YA, Aab A, et al. Dual role of the miR-146 family in rhinovirus-induced airway inflammation and allergic asthma exacerbation. Clin Transl Med. 2021 Jun;11(6):e427.
16. Rebane A, Runnel T, Aab A, Maslovskaja J, Rückert B, Zimmermann M, et al. MicroRNA-146a alleviates chronic skin inflammation in atopic dermatitis through suppression of innate immune responses in keratinocytes. J Allergy Clin Immunol. 2014 Oct;134(4):836-847.e11.
17. Hermann H, Runnel T, Aab A, Baurecht H, Rodriguez E, Magilnick N, et al. miR-146b probably assists miRNA-146a in the suppression of keratinocyte proliferation

and inflammatory responses in psoriasis. Journal of Investigative Dermatology. 2017;137(9):1945–54.
18. Paterson MR, Kriegel AJ. MiR-146a/b: a family with shared seeds and different roots. Physiological genomics. 2017;49(4):243–52.
19. So AY, Zhao JL, Baltimore D. The Y in and Y ang of micro RNA s: leukemia and immunity. Immunological reviews. 2013;253(1):129–45.
20. Curtale G, Mirolo M, Renzi TA, Rossato M, Bazzoni F, Locati M. Negative regulation of Toll-like receptor 4 signaling by IL-10–dependent microRNA-146b. Proceedings of the National Academy of Sciences. 2013;110(28):11499–504.
21. Xiang M, Birkbak NJ, Vafaizadeh V, Walker SR, Yeh JE, Liu S, et al. STAT3 induction of miR-146b forms a feedback loop to inhibit the NF-κB to IL-6 signaling axis and STAT3-driven cancer phenotypes. Science signaling. 2014;7(310):ra11–ra11.
22. Zhao JL, Starczynowski DT. Role of microRNA-146a in normal and malignant hematopoietic stem cell function. Front Genet. 2014;5:219.
23. Aslani M, Mortazavi-Jahromi SS, Mirshafiey A. Efficient roles of miR-146a in cellular and molecular mechanisms of neuroinflammatory disorders: An effectual review in neuroimmunology. Immunol Lett. 2021 Oct;238:1–20.
24. Müller M, Kuiperij HB, Versleijen AAM, Chiasserini D, Farotti L, Baschieri F, et al. Validation of microRNAs in Cerebrospinal Fluid as Biomarkers for Different Forms of Dementia in a Multicenter Study. J Alzheimers Dis. 2016 Apr 16; 52(4):1321–33.
25. Wang J, Yu JT, Tan L, Tian Y, Ma J, Tan CC, et al. Genome-wide circulating microRNA expression profiling indicates biomarkers for epilepsy. Sci Rep. 2015 Mar 31;5:9522.
26. Beylerli O, Gareev I, Sufianov A, Ilyasova T, Zhang F. The role of microRNA in the pathogenesis of glial brain tumors. Noncoding RNA Res. 2022 Jun;7(2):71–6.
27. Martin NA, Hyrlov KH, Elkjaer ML, Thygesen EK, Wlodarczyk A, Elbaek KJ, et al. Absence of miRNA-146a differentially alters microglia function and proteome. Frontiers in immunology. 2020;11:1110.
28. Liu GJ, Zhang QR, Gao X, Wang H, Tao T, Gao YY, et al. MiR-146a ameliorates hemoglobin-induced microglial inflammatory response via TLR4/IRAK1/TRAF6 associated pathways. Frontiers in Neuroscience. 2020;14:311.
29. Zhan-Qiang H, Hai-Hua Q, Chi Z, Miao W, Cui Z, Zi-Yin L, et al. miR-146a aggravates cognitive impairment and Alzheimer disease-like pathology by triggering oxidative stress through MAPK signaling. Neurología. 2021;
30. Gunasekaran S, Omkumar RV. miR-146a and miR-200b alter cognition by targeting NMDA receptor subunits. iScience. 2022 Dec 22;25(12):105515.
31. Yang G, Zhao Y. Overexpression of miR-146b-5p ameliorates neonatal hypoxic ischemic encephalopathy by inhibiting IRAK1/TRAF6/TAK1/NF-αB signaling. Yonsei Medical Journal. 2020;61(8):660.
32. Vaughan S, Jat PS. Deciphering the role of nuclear factor-κB in cellular senescence. Aging (Albany NY). 2011 Oct;3(10):913–9.
33. Songkiatisak P, Rahman SMT, Aqdas M, Sung MH. NF-κB, a culprit of both inflamm-ageing and declining immunity? Immun Ageing. 2022 May 17;19(1):20.
34. Shang R, Lee S, Senavirathne G, Lai EC. microRNAs in action: biogenesis, function and regulation. Nat Rev Genet. 2023 Dec;24(12):816–33.

35. Ørom UA, Nielsen FC, Lund AH. MicroRNA-10a binds the 5'UTR of ribosomal protein mRNAs and enhances their translation. Mol Cell. 2008 May 23;30(4):460–71.
36. Broughton JP, Lovci MT, Huang JL, Yeo GW, Pasquinelli AE. Pairing beyond the Seed Supports MicroRNA Targeting Specificity. Mol Cell. 2016 Oct 20;64(2):320–33.
37. Melton C, Judson RL, Blelloch R. Opposing microRNA families regulate self-renewal in mouse embryonic stem cells. Nature. 2010 Feb 4;463(7281):621–6.
38. Mayya VK, Duchaine TF. Ciphers and Executioners: How 3'-Untranslated Regions Determine the Fate of Messenger RNAs. Front Genet. 2019;10:6.
39. Miettinen TP, Björklund M. Modified ribosome profiling reveals high abundance of ribosome protected mRNA fragments derived from 3' untranslated regions. Nucleic Acids Res. 2015 Jan;43(2):1019–34.
40. Friedman RC, Farh KKH, Burge CB, Bartel DP. Most mammalian mRNAs are conserved targets of microRNAs. Genome Res. 2009 Jan;19(1):92–105.
41. Riolo G, Cantara S, Marzocchi C, Ricci C. miRNA Targets: From Prediction Tools to Experimental Validation. Methods Protoc. 2020 Dec 24;4(1):1.
42. Lee RC, Feinbaum RL, Ambros V. The C. elegans heterochronic gene lin-4 encodes small RNAs with antisense complementarity to lin-14. Cell. 1993 Dec 3;75(5):843–54.
43. Olsen PH, Ambros V. The lin-4 regulatory RNA controls developmental timing in Caenorhabditis elegans by blocking LIN-14 protein synthesis after the initiation of translation. Dev Biol. 1999 Dec 15;216(2):671–80.
44. Slack FJ, Basson M, Liu Z, Ambros V, Horvitz HR, Ruvkun G. The lin-41 RBCC gene acts in the C. elegans heterochronic pathway between the let-7 regulatory RNA and the LIN-29 transcription factor. Mol Cell. 2000 Apr;5(4):659–69.
45. Abrahante JE, Daul AL, Li M, Volk ML, Tennessen JM, Miller EA, et al. The Caenorhabditis elegans hunchback-like gene lin-57/hbl-1 controls developmental time and is regulated by microRNAs. Dev Cell. 2003 May;4(5):625–37.
46. Lee RC, Ambros V. An extensive class of small RNAs in Caenorhabditis elegans. Science. 2001 Oct 26;294(5543):862–4.
47. Kozomara A, Birgaoanu M, Griffiths-Jones S. miRBase: from microRNA sequences to function. Nucleic Acids Res. 2019 Jan 8;47(D1):D155–62.
48. Karp X, Ambros V. Developmental biology. Encountering microRNAs in cell fate signaling. Science. 2005 Nov 25;310(5752):1288–9.
49. Smith-Vikos T, Slack FJ. MicroRNAs and their roles in aging. J Cell Sci. 2012 Jan 1;125(Pt 1):7–17.
50. Raisch J, Darfeuille-Michaud A, Nguyen HTT. Role of microRNAs in the immune system, inflammation and cancer. World J Gastroenterol. 2013 May 28;19(20): 2985–96.
51. Kapplingattu SV, Bhattacharya S, Adlakha YK. MiRNAs as major players in brain health and disease: current knowledge and future perspectives. Cell Death Discov. 2025 Jan 13;11(1):7.
52. Tüfekci KU, Meuwissen RLJ, Genç S. The role of microRNAs in biological processes. Methods Mol Biol. 2014;1107:15–31.
53. Ying SY, Chang DC, Lin SL. The microRNA (miRNA): overview of the RNA genes that modulate gene function. Mol Biotechnol. 2008 Mar;38(3):257–68.

54. Wang Y, Luo J, Zhang H, Lu J. microRNAs in the Same Clusters Evolve to Coordinately Regulate Functionally Related Genes. Mol Biol Evol. 2016 Sep; 33(9):2232–47.
55. O'Brien J, Hayder H, Zayed Y, Peng C. Overview of MicroRNA Biogenesis, Mechanisms of Actions, and Circulation. Front Endocrinol (Lausanne). 2018;9:402.
56. Gregory RI, Yan KP, Amuthan G, Chendrimada T, Doratotaj B, Cooch N, et al. The Microprocessor complex mediates the genesis of microRNAs. Nature. 2004 Nov 11;432(7014):235–40.
57. Bofill-De Ros X, Vang Ørom UA. Recent progress in miRNA biogenesis and decay. RNA Biol. 2024 Jan;21(1):1–8.
58. Yi R, Qin Y, Macara IG, Cullen BR. Exportin-5 mediates the nuclear export of pre-microRNAs and short hairpin RNAs. Genes Dev. 2003 Dec 15;17(24):3011–6.
59. Medley JC, Panzade G, Zinovyeva AY. microRNA strand selection: Unwinding the rules. Wiley Interdiscip Rev RNA. 2021 May;12(3):e1627.
60. Kim H, Lee YY, Kim VN. The biogenesis and regulation of animal microRNAs. Nat Rev Mol Cell Biol. 2024 Dec 19;
61. Eichhorn SW, Guo H, McGeary SE, Rodriguez-Mias RA, Shin C, Baek D, et al. mRNA destabilization is the dominant effect of mammalian microRNAs by the time substantial repression ensues. Mol Cell. 2014 Oct 2;56(1):104–15.
62. Guo H, Ingolia NT, Weissman JS, Bartel DP. Mammalian microRNAs predominantly act to decrease target mRNA levels. Nature. 2010 Aug 12;466(7308):835–40.
63. Bartel DP. MicroRNAs: genomics, biogenesis, mechanism, and function. Cell. 2004 Jan 23;116(2):281–97.
64. Havens MA, Reich AA, Duelli DM, Hastings ML. Biogenesis of mammalian microRNAs by a non-canonical processing pathway. Nucleic Acids Res. 2012 May;40(10):4626–40.
65. Yang JS, Lai EC. Dicer-independent, Ago2-mediated microRNA biogenesis in vertebrates. Cell Cycle. 2010 Nov 15;9(22):4455–60.
66. Abdelfattah AM, Park C, Choi MY. Update on non-canonical microRNAs. Biomolecular concepts. 2014 Aug;5(4):275.
67. De Pietri Tonelli D, Clovis YM, Huttner WB. Detection and monitoring of microRNA expression in developing mouse brain and fixed brain cryosections. Methods Mol Biol. 2014;1092:31–42.
68. Smirnova L, Gräfe A, Seiler A, Schumacher S, Nitsch R, Wulczyn FG. Regulation of miRNA expression during neural cell specification. Eur J Neurosci. 2005 Mar; 21(6):1469–77.
69. Cardoso AL, Guedes JR, Pereira de Almeida L, Pedroso de Lima MC. miR-155 modulates microglia-mediated immune response by down-regulating SOCS-1 and promoting cytokine and nitric oxide production. Immunology. 2012 Jan;135(1):73–88.
70. Martin NA, Hyrlov KH, Elkjaer ML, Thygesen EK, Wlodarczyk A, Elbaek KJ, et al. Absence of miRNA-146a Differentially Alters Microglia Function and Proteome. Front Immunol. 2020;11:1110.
71. Mu C, Gao M, Xu W, Sun X, Chen T, Xu H, et al. Mechanisms of microRNA-132 in central neurodegenerative diseases: A comprehensive review. Biomed Pharmacother. 2024 Jan;170:116029.
72. Pomper N, Liu Y, Hoye ML, Dougherty JD, Miller TM. CNS microRNA profiles: a database for cell type enriched microRNA expression across the mouse central nervous system. Sci Rep. 2020 Mar 18;10:4921.

73. Edbauer D, Neilson JR, Foster KA, Wang CF, Seeburg DP, Batterton MN, et al. Regulation of synaptic structure and function by FMRP-associated microRNAs miR-125b and miR-132. Neuron. 2010 Feb 11;65(3):373–84.
74. Todorov H, Weißbach S, Schlichtholz L, Mueller H, Hartwich D, Gerber S, et al. Stage-specific expression patterns and co-targeting relationships among miRNAs in the developing mouse cerebral cortex. Commun Biol. 2024 Oct 22;7(1):1366.
75. Jovičić A, Roshan R, Moisoi N, Pradervand S, Moser R, Pillai B, et al. Comprehensive expression analyses of neural cell-type-specific miRNAs identify new determinants of the specification and maintenance of neuronal phenotypes. J Neurosci. 2013 Mar 20;33(12):5127–37.
76. Sim SE, Bakes J, Kaang BK. Neuronal activity-dependent regulation of MicroRNAs. Mol Cells. 2014 Jul;37(7):511–7.
77. Walsh AD, Stone S, Freytag S, Aprico A, Kilpatrick TJ, Ansell BRE, et al. Mouse microglia express unique miRNA-mRNA networks to facilitate age-specific functions in the developing central nervous system. Commun Biol. 2023 May 22; 6(1):555.
78. Cardoso AL, Guedes JR, Pereira de Almeida L, Pedroso de Lima MC. miR-155 modulates microglia-mediated immune response by down-regulating SOCS-1 and promoting cytokine and nitric oxide production. Immunology. 2012 Jan;135(1):73–88.
79. Louafi F, Martinez-Nunez RT, Sanchez-Elsner T. MicroRNA-155 targets SMAD2 and modulates the response of macrophages to transforming growth factor-{beta}. J Biol Chem. 2010 Dec 31;285(53):41328–36.
80. Ponomarev ED, Veremeyko T, Barteneva N, Krichevsky AM, Weiner HL. MicroRNA-124 promotes microglia quiescence and suppresses EAE by deactivating macrophages via the C/EBP-α-PU.1 pathway. Nat Med. 2011 Jan;17(1):64–70.
81. Liu X, Ma J, Ding G, Gong Q, Wang Y, Yu H, et al. Microglia Polarization from M1 toward M2 Phenotype Is Promoted by Astragalus Polysaccharides Mediated through Inhibition of miR-155 in Experimental Autoimmune Encephalomyelitis. Oxid Med Cell Longev. 2021 Dec 24;2021:5753452.
82. Huang Y, Liao Z, Lin X, Wu X, Chen X, Bai X, et al. Overexpression of miR-146a Might Regulate Polarization Transitions of BV-2 Cells Induced by High Glucose and Glucose Fluctuations. Front Endocrinol (Lausanne). 2019;10:719.
83. Guo Y, Hong W, Wang X, Zhang P, Körner H, Tu J, et al. MicroRNAs in Microglia: How do MicroRNAs Affect Activation, Inflammation, Polarization of Microglia and Mediate the Interaction Between Microglia and Glioma? Front Mol Neurosci [Internet]. 2019 May 10 [cited 2025 Jan 20];12. Available from: https://www.frontiersin.org/journals/molecular-neuroscience/articles/10.3389/fnmol.2019.00125/full
84. An F, Gong G, Wang Y, Bian M, Yu L, Wei C. MiR-124 acts as a target for Alzheimer's disease by regulating BACE1. Oncotarget. 2017 Dec 26;8(69):114065–71.
85. Liang C, Zou T, Zhang M, Fan W, Zhang T, Jiang Y, et al. MicroRNA-146a switches microglial phenotypes to resist the pathological processes and cognitive degradation of Alzheimer's disease. Theranostics. 2021;11(9):4103–21.
86. Aloi MS, Prater KE, Sánchez REA, Beck A, Pathan JL, Davidson S, et al. Microglia specific deletion of miR-155 in Alzheimer's disease mouse models reduces amyloid-β pathology but causes hyperexcitability and seizures. J Neuroinflammation. 2023 Mar 7;20(1):60.

87. Song C, Li S, Mai Y, Li L, Dai G, Zhou Y, et al. Dysregulated expression of miR-140 and miR-122 compromised microglial chemotaxis and led to reduced restriction of AD pathology. J Neuroinflammation. 2024 Jul 2;21(1):167.
88. Kim W, Noh H, Lee Y, Jeon J, Shanmugavadivu A, McPhie DL, et al. MiR-126 Regulates Growth Factor Activities and Vulnerability to Toxic Insult in Neurons. Mol Neurobiol. 2016 Jan;53(1):95–108.
89. Jauhari A, Singh T, Mishra S, Shankar J, Yadav S. Coordinated Action of miR-146a and Parkin Gene Regulate Rotenone-induced Neurodegeneration. Toxicol Sci. 2020 Aug 1;176(2):433–45.
90. Barnett MM, Reay WR, Geaghan MP, Kiltschewskij DJ, Green MJ, Weidenhofer J, et al. miRNA cargo in circulating vesicles from neurons is altered in individuals with schizophrenia and associated with severe disease. Sci Adv. 2023 Dec;9(48): eadi4386.
91. Zhang Y, Chen M, Qiu Z, Hu K, McGee W, Chen X, et al. MiR-130a regulates neurite outgrowth and dendritic spine density by targeting MeCP2. Protein Cell. 2016 Jul;7(7):489–500.
92. Nguyen LS, Fregeac J, Bole-Feysot C, Cagnard N, Iyer A, Anink J, et al. Role of miR-146a in neural stem cell differentiation and neural lineage determination: relevance for neurodevelopmental disorders. Mol Autism. 2018;9:38.
93. Roy B, Dunbar M, Shelton RC, Dwivedi Y. Identification of MicroRNA-124-3p as a Putative Epigenetic Signature of Major Depressive Disorder. Neuropsychopharmacology. 2017 Mar;42(4):864–75.
94. Lagos-Quintana M, Rauhut R, Yalcin A, Meyer J, Lendeckel W, Tuschl T. Identification of tissue-specific microRNAs from mouse. Curr Biol. 2002 Apr 30;12(9): 735–9.
95. Cai X, Lu S, Zhang Z, Gonzalez CM, Damania B, Cullen BR. Kaposi's sarcoma-associated herpesvirus expresses an array of viral microRNAs in latently infected cells. Proc Natl Acad Sci U S A. 2005 Apr 12;102(15):5570–5.
96. Taganov KD, Boldin MP, Chang KJ, Baltimore D. NF-kappaB-dependent induction of microRNA miR-146, an inhibitor targeted to signaling proteins of innate immune responses. Proc Natl Acad Sci U S A. 2006 Aug 15;103(33):12481–6.
97. Yang K, He YS, Wang XQ, Lu L, Chen QJ, Liu J, et al. MiR-146a inhibits oxidized low-density lipoprotein-induced lipid accumulation and inflammatory response via targeting toll-like receptor 4. FEBS Lett. 2011 Mar 23;585(6):854–60.
98. Curtale G, Mirolo M, Renzi TA, Rossato M, Bazzoni F, Locati M. Negative regulation of Toll-like receptor 4 signaling by IL-10-dependent microRNA-146b. Proc Natl Acad Sci U S A. 2013 Jul 9;110(28):11499–504.
99. Paterson MR, Kriegel AJ. MiR-146a/b: a family with shared seeds and different roots. Physiological genomics. 2017;49(4):243–52.
100. Liu R, Liu C, Chen D, Yang WH, Liu X, Liu CG, et al. FOXP3 Controls an miR-146/NF-κB Negative Feedback Loop That Inhibits Apoptosis in Breast Cancer Cells. Cancer Res. 2015 Apr 15;75(8):1703–13.
101. Luo X, Yang W, Ye DQ, Cui H, Zhang Y, Hirankarn N, et al. A functional variant in microRNA-146a promoter modulates its expression and confers disease risk for systemic lupus erythematosus. PLoS Genet. 2011 Jun;7(6):e1002128.
102. Forloni M, Dogra SK, Dong Y, Conte D, Ou J, Zhu LJ, et al. miR-146a promotes the initiation and progression of melanoma by activating Notch signaling. eLife. 2014 Feb 18;3:e01460.

103. Curtale G, Mirolo M, Renzi TA, Rossato M, Bazzoni F, Locati M. Negative regulation of Toll-like receptor 4 signaling by IL-10-dependent microRNA-146b. Proc Natl Acad Sci U S A. 2013 Jul 9;110(28):11499–504.
104. Li J, Shan F, Xiong G, Wang JM, Wang WL, Xu X, et al. Transcriptional regulation of miR-146b by C/EBPβ LAP2 in esophageal cancer cells. Biochem Biophys Res Commun. 2014 Mar 28;446(1):267–71.
105. Wang D, Feng M, Ma X, Tao K, Wang G. Transcription factor SP1-induced microRNA-146b-3p facilitates the progression and metastasis of colorectal cancer via regulating FAM107A. Life Sci. 2021 Jul 15;277:119398.
106. Wei J, Wang J, Zhou Y, Yan S, Li K, Lin H. MicroRNA-146a Contributes to SCI Recovery via Regulating TRAF6 and IRAK1 Expression. Biomed Res Int. 2016; 2016:4013487.
107. Liu GJ, Zhang QR, Gao X, Wang H, Tao T, Gao YY, et al. MiR-146a Ameliorates Hemoglobin-Induced Microglial Inflammatory Response via TLR4/IRAK1/TRAF6 Associated Pathways. Front Neurosci. 2020;14:311.
108. Fan W, Liang C, Ou M, Zou T, Sun F, Zhou H, et al. MicroRNA-146a Is a Wide-Reaching Neuroinflammatory Regulator and Potential Treatment Target in Neurological Diseases. Front Mol Neurosci. 2020;13:90.
109. Ge YT, Zhong AQ, Xu GF, Lu Y. Resveratrol protects BV2 mouse microglial cells against LPS-induced inflammatory injury by altering the miR-146a-5p/TRAF6/NF-κB axis. Immunopharmacol Immunotoxicol. 2019 Oct;41(5):549–57.
110. Saba R, Gushue S, Huzarewich RLCH, Manguiat K, Medina S, Robertson C, et al. MicroRNA 146a (miR-146a) is over-expressed during prion disease and modulates the innate immune response and the microglial activation state. PLoS One. 2012; 7(2):e30832.
111. Liang C, Zou T, Zhang M, Fan W, Zhang T, Jiang Y, et al. MicroRNA-146a switches microglial phenotypes to resist the pathological processes and cognitive degradation of Alzheimer's disease. Theranostics. 2021;11(9):4103–21.
112. Fan C, Li Y, Lan T, Wang W, Long Y, Yu SY. Microglia secrete miR-146a-5p-containing exosomes to regulate neurogenesis in depression. Molecular Therapy. 2022;30(3):1300–14.
113. Zhao W, Spiers JG, Vassileff N, Khadka A, Jaehne EJ, van den Buuse M, et al. microRNA-146a modulates behavioural activity, neuroinflammation, and oxidative stress in adult mice. Mol Cell Neurosci. 2023 Mar;124:103820.
114. Karthikeyan A, Gupta N, Tang C, Mallilankaraman K, Silambarasan M, Shi M, et al. Microglial SMAD4 regulated by microRNA-146a promotes migration of microglia which support tumor progression in a glioma environment. Oncotarget. 2018 May 18;9(38):24950–69.
115. Battineni G, Sagaro GG, Chintalapudi N, Amenta F, Tomassoni D, Tayebati SK. Impact of Obesity-Induced Inflammation on Cardiovascular Diseases (CVD). Int J Mol Sci. 2021 Apr 30;22(9):4798.
116. Palavra F, Almeida L, Ambrósio AF, Reis F. Obesity and brain inflammation: a focus on multiple sclerosis. Obes Rev. 2016 Mar;17(3):211–24.
117. Monteiro R, Azevedo I. Chronic inflammation in obesity and the metabolic syndrome. Mediators Inflamm. 2010;2010:289645.
118. Rohm TV, Meier DT, Olefsky JM, Donath MY. Inflammation in obesity, diabetes, and related disorders. Immunity. 2022 Jan 11;55(1):31–55.

119. Li K, Zhao B, Wei D, Wang W, Cui Y, Qian L, et al. miR-146a improves hepatic lipid and glucose metabolism by targeting MED1. Int J Mol Med. 2020 Feb; 45(2):543–55.
120. Du J, Niu X, Wang Y, Kong L, Wang R, Zhang Y, et al. MiR-146a-5p suppresses activation and proliferation of hepatic stellate cells in nonalcoholic fibrosing steatohepatitis through directly targeting Wnt1 and Wnt5a. Sci Rep. 2015 Nov 5;5: 16163.
121. Maldonado-Avilés JG, Guarnieri DJ, Zhu X, DiLeone RJ. Down-regulation of miRNAs in the brain and development of diet-induced obesity. Int J Dev Neurosci. 2018 Feb;64:2–7.
122. Xie Y, Chu A, Feng Y, Chen L, Shao Y, Luo Q, et al. MicroRNA-146a: A Comprehensive Indicator of Inflammation and Oxidative Stress Status Induced in the Brain of Chronic T2DM Rats. Front Pharmacol. 2018;9:478.
123. Ogrodnik M, Zhu Y, Langhi LGP, Tchkonia T, Krüger P, Fielder E, et al. Obesity-Induced Cellular Senescence Drives Anxiety and Impairs Neurogenesis. Cell Metab. 2019 May 7;29(5):1061-1077.e8.
124. Hewitt G, Jurk D, Marques FDM, Correia-Melo C, Hardy T, Gackowska A, et al. Telomeres are favoured targets of a persistent DNA damage response in ageing and stress-induced senescence. Nat Commun. 2012 Feb 28;3:708.
125. Dimri GP, Lee X, Basile G, Acosta M, Scott G, Roskelley C, et al. A biomarker that identifies senescent human cells in culture and in aging skin in vivo. Proc Natl Acad Sci U S A. 1995 Sep 26;92(20):9363–7.
126. Wagner KD, Wagner N. The Senescence Markers p16INK4A, p14ARF/p19ARF, and p21 in Organ Development and Homeostasis. Cells. 2022 Jun 19;11(12):1966.
127. Coppé JP, Patil CK, Rodier F, Sun Y, Muñoz DP, Goldstein J, et al. Senescence-associated secretory phenotypes reveal cell-nonautonomous functions of oncogenic RAS and the p53 tumor suppressor. PLoS Biol. 2008 Dec 2;6(12):2853–68.
128. Cuollo L, Antonangeli F, Santoni A, Soriani A. The Senescence-Associated Secretory Phenotype (SASP) in the Challenging Future of Cancer Therapy and Age-Related Diseases. Biology (Basel). 2020 Dec 21;9(12):485.
129. Spencer SJ, Basri B, Sominsky L, Soch A, Ayala MT, Reineck P, et al. High-fat diet worsens the impact of aging on microglial function and morphology in a region-specific manner. Neurobiol Aging. 2019 Feb;74:121–34.
130. Gong H, Chen H, Xiao P, Huang N, Han X, Zhang J, et al. miR-146a impedes the anti-aging effect of AMPK via NAMPT suppression and NAD+/SIRT inactivation. Signal Transduct Target Ther. 2022 Mar 4;7(1):66.
131. Zhao W, Spiers JG, Vassileff N, Khadka A, Jaehne EJ, van den Buuse M, et al. microRNA-146a modulates behavioural activity, neuroinflammation, and oxidative stress in adult mice. Mol Cell Neurosci. 2023 Mar;124:103820.
132. Nguyen LS, Lepleux M, Makhlouf M, Martin C, Fregeac J, Siquier-Pernet K, et al. Profiling olfactory stem cells from living patients identifies miRNAs relevant for autism pathophysiology. Mol Autism. 2016;7:1.
133. Nguyen LS, Fregeac J, Bole-Feysot C, Cagnard N, Iyer A, Anink J, et al. Role of miR-146a in neural stem cell differentiation and neural lineage determination: relevance for neurodevelopmental disorders. Mol Autism. 2018;9:38.
134. Deng LJ, Wu D, Yang XF, Li T. miR-146a-5p Modulates Adult Hippocampal Neurogenesis Deficits Through Klf4/p-Stat3 Signaling in APP/PS1 Mice. Neuroscience. 2023 Aug 21;526:314–25.

135. Kumar A, Kopra J, Varendi K, Porokuokka LL, Panhelainen A, Kuure S, et al. GDNF Overexpression from the Native Locus Reveals its Role in the Nigrostriatal Dopaminergic System Function. PLoS Genet. 2015 Dec;11(12):e1005710.
136. Aron L, Klein R. Repairing the parkinsonian brain with neurotrophic factors. Trends Neurosci. 2011 Feb;34(2):88–100.
137. Bokobza C, Joshi P, Schang A, Csaba Z, Faivre V, Montané A, et al. miR-146b Protects the Perinatal Brain against Microglia-Induced Hypomyelination. Annals of neurology. 2022;91(1):48–65.
138. Ma X, Zhou J, Zhong Y, Jiang L, Mu P, Li Y, et al. Expression, regulation and function of microRNAs in multiple sclerosis. Int J Med Sci. 2014;11(8):810–8.
139. He X, Zhang Q, Liu Y, Pan X. Cloning and identification of novel microRNAs from rat hippocampus. Acta Biochim Biophys Sin (Shanghai). 2007 Sep;39(9):708–14.
140. Liu DZ, Ander BP, Tian Y, Stamova B, Jickling GC, Davis RR, et al. Integrated analysis of mRNA and microRNA expression in mature neurons, neural progenitor cells and neuroblastoma cells. Gene. 2012 Mar 10;495(2):120–7.
141. Hsu PK, Xu B, Mukai J, Karayiorgou M, Gogos JA. The BDNF Val66Met variant affects gene expression through miR-146b. Neurobiol Dis. 2015 May;77:228–37.
142. Gao L, Zhang Y, Sterling K, Song W. Brain-derived neurotrophic factor in Alzheimer's disease and its pharmaceutical potential. Transl Neurodegener. 2022 Jan 28;11(1):4.
143. Dai Yaling CL, He X, Lin H, Jia W, Chen L, Tao J, et al. Construction of miR-146b overexpression lentiviral vector and the effect on the proliferation of hippocampal neural stem cells. Chinese Journal of Tissue Engineering Research. 2021;25(19): 3024.
144. Sandau US, McFarland TJ, Smith SJ, Galasko DR, Quinn JF, Saugstad JA. Differential Effects of APOE Genotype on MicroRNA Cargo of Cerebrospinal Fluid Extracellular Vesicles in Females With Alzheimer's Disease Compared to Males. Front Cell Dev Biol. 2022;10:864022.
145. Dong H, Wang C, Lu S, Yu C, Huang L, Feng W, et al. A panel of four decreased serum microRNAs as a novel biomarker for early Parkinson's disease. Biomarkers. 2016;21(2):129–37.
146. Yan JH, Hua P, Chen Y, Li LT, Yu CY, Yan L, et al. Identification of microRNAs for the early diagnosis of Parkinson's disease and multiple system atrophy. J Integr Neurosci. 2020 Sep 30;19(3):429–36.
147. Li WY, Zhang WT, Cheng YX, Liu YC, Zhai FG, Sun P, et al. Inhibition of KLF7-Targeting MicroRNA 146b Promotes Sciatic Nerve Regeneration. Neurosci Bull. 2018 Jun;34(3):419–37.
148. Chen Z, Wang K, Huang J, Zheng G, Lv Y, Luo N, et al. Upregulated Serum MiR-146b Serves as a Biomarker for Acute Ischemic Stroke. Cell Physiol Biochem. 2018;45(1):397–405.
149. Su ZF, Sun ZW, Zhang Y, Wang S, Yu QG, Wu ZB. Regulatory effects of miR-146a/b on the function of endothelial progenitor cells in acute ischemic stroke in mice. Kaohsiung J Med Sci. 2017 Aug;33(8):369–78.
150. Yang R, Zeng C. Protective effects of MiR-146b in cerebral infarction via targeting SIRT1/FOXO1 signaling pathway. Cell Mol Biol (Noisy-le-grand). 2023 Nov 30;69(12):156–62.
151. Liu J, Xu J, Li H, Sun C, Yu L, Li Y, et al. miR-146b-5p functions as a tumor suppressor by targeting TRAF6 and predicts the prognosis of human gliomas. Oncotarget. 2015 Oct 6;6(30):29129–42.

152. Xia H, Qi Y, Ng SS, Chen X, Li D, Chen S, et al. microRNA-146b inhibits glioma cell migration and invasion by targeting MMPs. Brain Res. 2009 May 7;1269:158–65.
153. Qian Z, Zhou S, Zhou Z, Yang X, Que S, Lan J, et al. miR-146b-5p suppresses glioblastoma cell resistance to temozolomide through targeting TRAF6. Oncol Rep. 2017 Nov;38(5):2941–50.
154. Khwaja SS, Cai C, Badiyan SN, Wang X, Huang J. The immune-related microRNA miR-146b is upregulated in glioblastoma recurrence. Oncotarget. 2018 Jun 26;9(49): 29036–46.
155. Holick MF. Vitamin D deficiency. N Engl J Med. 2007 Jul 19;357(3):266–81.
156. Bikle DD. Vitamin D metabolism, mechanism of action, and clinical applications. Chem Biol. 2014 Mar 20;21(3):319–29.
157. Hii CS, Ferrante A. The Non-Genomic Actions of Vitamin D. Nutrients. 2016 Mar 2;8(3):135.
158. Tebben PJ, Singh RJ, Kumar R. Vitamin D-Mediated Hypercalcemia: Mechanisms, Diagnosis, and Treatment. Endocr Rev. 2016 Oct;37(5):521–47.
159. Al-Rawaf HA, Gabr SA, Alghadir AH. Molecular Changes in Diabetic Wound Healing following Administration of Vitamin D and Ginger Supplements: Biochemical and Molecular Experimental Study. Evid Based Complement Alternat Med. 2019;2019:4352470.
160. Karkeni E, Bonnet L, Marcotorchino J, Tourniaire F, Astier J, Ye J, et al. Vitamin D limits inflammation-linked microRNA expression in adipocytes in vitro and in vivo: A new mechanism for the regulation of inflammation by vitamin D. Epigenetics. 2018;13(2):156–62.
161. Kalueff AV, Tuohimaa P. Neurosteroid hormone vitamin D and its utility in clinical nutrition. Curr Opin Clin Nutr Metab Care. 2007 Jan;10(1):12–9.
162. Mayne PE, Burne THJ. Vitamin D in Synaptic Plasticity, Cognitive Function, and Neuropsychiatric Illness. Trends Neurosci. 2019 Apr;42(4):293–306.
163. Mokhtari-Zaer A, Hosseini M, Salmani H, Arab Z, Zareian P. Vitamin D3 attenuates lipopolysaccharide-induced cognitive impairment in rats by inhibiting inflammation and oxidative stress. Life Sci. 2020 Jul 15;253:117703.
164. Calvello R, Cianciulli A, Nicolardi G, De Nuccio F, Giannotti L, Salvatore R, et al. Vitamin D Treatment Attenuates Neuroinflammation and Dopaminergic Neurodegeneration in an Animal Model of Parkinson's Disease, Shifting M1 to M2 Microglia Responses. J Neuroimmune Pharmacol. 2017 Jun;12(2):327–39.
165. Maestro MA, Molnár F, Carlberg C. Vitamin D and Its Synthetic Analogs. J Med Chem. 2019 Aug 8;62(15):6854–75.
166. Peleg S, Uskokovic M, Ahene A, Vickery B, Avnur Z. Cellular and molecular events associated with the bone-protecting activity of the noncalcemic vitamin D analog Ro-26-9228 in osteopenic rats. Endocrinology. 2002 May;143(5):1625–36.
167. Nagpal S, Na S, Rathnachalam R. Noncalcemic actions of vitamin D receptor ligands. Endocr Rev. 2005 Aug;26(5):662–87.
168. Peleg S, Uskokovic M, Ahene A, Vickery B, Avnur Z. Cellular and molecular events associated with the bone-protecting activity of the noncalcemic vitamin D analog Ro-26-9228 in osteopenic rats. Endocrinology. 2002 May;143(5):1625–36.
169. Adorini L, Penna G, Amuchastegui S, Cossetti C, Aquilano F, Mariani R, et al. Inhibition of prostate growth and inflammation by the vitamin D receptor agonist BXL-628 (elocalcitol). J Steroid Biochem Mol Biol. 2007 Mar;103(3–5):689–93.

170. Hermann H, Runnel T, Aab A, Baurecht H, Rodriguez E, Magilnick N, et al. miR-146b probably assists miRNA-146a in the suppression of keratinocyte proliferation and inflammatory responses in psoriasis. Journal of Investigative Dermatology. 2017;137(9):1945–54.
171. Jürgenson M, Aonurm-Helm A, Zharkovsky A. Behavioral profile of mice with impaired cognition in the elevated plus-maze due to a deficiency in neural cell adhesion molecule. Pharmacol Biochem Behav. 2010 Oct;96(4):461–8.
172. Fregeac J, Moriceau S, Poli A, Nguyen LS, Oury F, Colleaux L. Loss of the neurodevelopmental disease-associated gene miR-146a impairs neural progenitor differentiation and causes learning and memory deficits. Mol Autism. 2020 Mar 30;11(1):22.
173. Tronson NC, Schrick C, Fischer A, Sananbenesi F, Pagès G, Pouysségur J, et al. Regulatory mechanisms of fear extinction and depression-like behavior. Neuropsychopharmacology. 2008 Jun;33(7):1570–83.
174. Jürgenson M, Aonurm-Helm A, Zharkovsky A. Partial reduction in neural cell adhesion molecule (NCAM) in heterozygous mice induces depression-related behaviour without cognitive impairment. Brain Res. 2012 Apr 4;1447:106–18.
175. Jürgenson M, Zharkovskaja T, Noortoots A, Morozova M, Beniashvili A, Zapolski M, et al. Effects of the drug combination memantine and melatonin on impaired memory and brain neuronal deficits in an amyloid-predominant mouse model of Alzheimer's disease. J Pharm Pharmacol. 2019 Nov;71(11):1695–705.
176. Hovens I, Nyakas C, Schoemaker R. A novel method for evaluating microglial activation using ionized calcium-binding adaptor protein-1 staining: cell body to cell size ratio. Neuroimmunology and Neuroinflammation. 2014;82–8.
177. Somelar K, Jürgenson M, Jaako K, Anier K, Aonurm-Helm A, Zvejniece L, et al. Development of depression-like behavior and altered hippocampal neurogenesis in a mouse model of chronic neuropathic pain. Brain Res. 2021 May 1;1758:147329.
178. Chithanathan K, Somelar K, Jürgenson M, Žarkovskaja T, Periyasamy K, Yan L, et al. Enhanced Cognition and Neurogenesis in miR-146b Deficient Mice. Cells. 2022;11(13):2002.
179. Agarwal V, Bell GW, Nam JW, Bartel DP. Predicting effective microRNA target sites in mammalian mRNAs. Elife. 2015 Aug 12;4:e05005.
180. Reimand J, Kull M, Peterson H, Hansen J, Vilo J. g:Profiler--a web-based toolset for functional profiling of gene lists from large-scale experiments. Nucleic Acids Res. 2007 Jul;35(Web Server issue):W193-200.
181. Zhang Y, Chen K, Sloan SA, Bennett ML, Scholze AR, O'Keeffe S, et al. An RNA-sequencing transcriptome and splicing database of glia, neurons, and vascular cells of the cerebral cortex. J Neurosci. 2014 Sep 3;34(36):11929–47.
182. Zhang Y, Chen K, Sloan SA, Bennett ML, Scholze AR, O'Keeffe S, et al. An RNA-sequencing transcriptome and splicing database of glia, neurons, and vascular cells of the cerebral cortex. J Neurosci. 2014 Sep 3;34(36):11929–47.
183. Hsu PK, Xu B, Mukai J, Karayiorgou M, Gogos JA. The BDNF Val66Met variant affects gene expression through miR-146b. Neurobiol Dis. 2015 May;77:228–37.
184. Mordelt A, de Witte LD. Microglia-mediated synaptic pruning as a key deficit in neurodevelopmental disorders: Hype or hope? Curr Opin Neurobiol. 2023 Apr;79: 102674.
185. Biesmans S, Meert TF, Bouwknecht JA, Acton PD, Davoodi N, De Haes P, et al. Systemic immune activation leads to neuroinflammation and sickness behavior in mice. Mediators of inflammation. 2013;2013.

186. Ibrahim AS, El-Remessy AB, Matragoon S, Zhang W, Patel Y, Khan S, et al. Retinal microglial activation and inflammation induced by amadori-glycated albumin in a rat model of diabetes. Diabetes. 2011 Apr;60(4):1122–33.
187. Green TRF, Rowe RK. Quantifying microglial morphology: an insight into function. Clin Exp Immunol. 2024 May 16;216(3):221–9.
188. Kim JD, Yoon NA, Jin S, Diano S. Microglial UCP2 Mediates Inflammation and Obesity Induced by High-Fat Feeding. Cell Metabolism. 2019 Nov 5;30(5):952-962.e5.
189. Hou J, Jeon B, Baek J, Yun Y, Kim D, Chang B, et al. High fat diet-induced brain damaging effects through autophagy-mediated senescence, inflammation and apoptosis mitigated by ginsenoside F1-enhanced mixture. J Ginseng Res. 2022 Jan; 46(1):79–90.
190. Bhaumik D, Scott GK, Schokrpur S, Patil CK, Orjalo AV, Rodier F, et al. MicroRNAs miR-146a/b negatively modulate the senescence-associated inflammatory mediators IL-6 and IL-8. Aging (Albany NY). 2009 Apr 21;1(4):402–11.
191. Zhong H, Wang H rong, Yang S, Zhong J hua, Wang T, Wang C, et al. Targeting Smad4 links microRNA-146a to the TGF-beta pathway during retinoid acid induction in acute promyelocytic leukemia cell line. Int J Hematol. 2010 Jul;92(1):129–35.
192. Benn A, Barker GRI, Stuart SA, Roloff EVL, Teschemacher AG, Warburton EC, et al. Optogenetic Stimulation of Prefrontal Glutamatergic Neurons Enhances Recognition Memory. J Neurosci. 2016 May 4;36(18):4930–9.
193. Bejoy J, Bijonowski B, Marzano M, Jeske R, Ma T, Li Y. Wnt-Notch Signaling Interactions During Neural and Astroglial Patterning of Human Stem Cells. Tissue Eng Part A. 2020 Apr;26(7–8):419–31.
194. Lee HC, Tan KL, Cheah PS, Ling KH. Potential Role of JAK-STAT Signaling Pathway in the Neurogenic-to-Gliogenic Shift in Down Syndrome Brain. Neural Plast. 2016;2016:7434191.
195. Xiang M, Birkbak NJ, Vafaizadeh V, Walker SR, Yeh JE, Liu S, et al. STAT3 induction of miR-146b forms a feedback loop to inhibit the NF-κB to IL-6 signaling axis and STAT3-driven cancer phenotypes. Sci Signal. 2014 Jan 28;7(310):ra11.
196. Deng X, Wu B, Xiao K, Kang J, Xie J, Zhang X, et al. MiR-146b-5p promotes metastasis and induces epithelial-mesenchymal transition in thyroid cancer by targeting ZNRF3. Cell Physiol Biochem. 2015;35(1):71–82.
197. Chithanathan K, Jürgenson M, Ducena K, Remm A, Kask K, Rebane A, et al. Elocalcitol mitigates high-fat diet-induced microglial senescence via miR-146a modulation. Immun Ageing. 2024 Nov 22;21(1):82.
198. Zhao W, Spiers JG, Vassileff N, Khadka A, Jaehne EJ, van den Buuse M, et al. microRNA-146a modulates behavioural activity, neuroinflammation, and oxidative stress in adult mice. Mol Cell Neurosci. 2023 Mar;124:103820.
199. Saxe MD, Battaglia F, Wang JW, Malleret G, David DJ, Monckton JE, et al. Ablation of hippocampal neurogenesis impairs contextual fear conditioning and synaptic plasticity in the dentate gyrus. Proc Natl Acad Sci U S A. 2006 Nov 14;103(46): 17501–6.
200. Snyder JS, Hong NS, McDonald RJ, Wojtowicz JM. A role for adult neurogenesis in spatial long-term memory. Neuroscience. 2005;130(4):843–52.
201. Gianino S, Grider JR, Cresswell J, Enomoto H, Heuckeroth RO. GDNF availability determines enteric neuron number by controlling precursor proliferation. Development. 2003 May;130(10):2187–98.

202. Ekdahl CT. Microglial activation–tuning and pruning adult neurogenesis. Frontiers in pharmacology. 2012;3:41.
203. Dantzer R. Cytokine-induced sickness behavior: mechanisms and implications. Annals of the New York academy of sciences. 2001;933(1):222–34.
204. Dantzer R, O'connor JC, Freund GG, Johnson RW, Kelley KW. From inflammation to sickness and depression: when the immune system subjugates the brain. Nature reviews neuroscience. 2008;9(1):46–56.
205. Chithanathan K, Jürgenson M, Guha M, Yan L, Žarkovskaja T, Pook M, et al. Paradoxical attenuation of neuroinflammatory response upon LPS challenge in miR-146b deficient mice. Front Immunol. 2022 Oct 31;13:996415.
206. Liu CP, Zhong M, Sun JX, He J, Gao Y, Qin FX. miR-146a reduces depressive behavior by inhibiting microglial activation. Mol Med Rep. 2021 Jun;23(6):463.
207. Sakaguchi S, Negishi H, Asagiri M, Nakajima C, Mizutani T, Takaoka A, et al. Essential role of IRF-3 in lipopolysaccharide-induced interferon-beta gene expression and endotoxin shock. Biochem Biophys Res Commun. 2003 Jul 11;306(4):860–6.
208. Chen PG, Guan YJ, Zha GM, Jiao XQ, Zhu HS, Zhang CY, et al. Swine IRF3/IRF7 attenuates inflammatory responses through TLR4 signaling pathway. Oncotarget. 2017 Sep 22;8(37):61958–68.
209. Rahman MH, Kim MS, Lee IK, Yu R, Suk K. Interglial Crosstalk in Obesity-Induced Hypothalamic Inflammation. Front Neurosci. 2018;12:939.
210. Roos J, Enlund E, Funcke JB, Tews D, Holzmann K, Debatin KM, et al. miR-146a-mediated suppression of the inflammatory response in human adipocytes. Sci Rep. 2016 Dec 6;6(1):38339.
211. Xiao B, Zhu ED, Li N, Lu DS, Li W, Li BS, et al. Increased miR-146a in gastric cancer directly targets SMAD4 and is involved in modulating cell proliferation and apoptosis. Oncology reports. 2012;27(2):559–66.
212. Min SK, Jung SY, Kang HK, Jo SB, Kim MJ, Min BM. MicroRNA-146a-5p Limits Elevated TGF-β Signal during Cell Senescence. Mol Ther Nucleic Acids. 2017 Jun 16;7:335–8.

11. ACKNOWLEDGEMENTS

Just like a brain function with different cells working together, this thesis would not have possible without the support of my four supervisors.

- First and foremost, I would like to express my sincere gratitude to Aleksandr Žarkovski, he is like a neuron, always firing ideas non-stop and making sure my brain never got a moment of peace! His training to work with deadlines, ensured that progress never delayed. I truly appreciate his guidance even on weekends because true neurons never rest! and for our engaging discussions, whether about research or about India.
- My sincere thanks goes to Monika, is like an astrocyte, the backbone keeping everything together. Her energy and dedication to experiments were inspiring. Spending countless hours together in the animal house made us both experts in managing stress, though sometimes it felt like the animals had a calmer life than us!
- I am also deeply thankful to Ana Rebane - cool, ambitious oligodendrocyte always ensuring that things ran smoothly. I appreciate her for taking time to teach me scientific writing and her inputs in improving the quality of the manuscript and thesis. Of course, there were moments when we applied some (gentle) pressure during paper deadlines, but her positive outlook always kept the things going.
- I would like to thank Li Tian, the microglia, who always critically analyzing my work, thinking ahead like a reviewer, and preparing me to address challenges even before they arose. Thank you for providing the opportunity to start the PhD journey and made me fascinated with glial biology.
- I am grateful to Kersti Lilleväli for her warm and friendly approach and for the support she provided at the beginning of this journey.
- I thank all my co-authors and colleagues, especially Kelli, Katrina, Maria, Fangling and Ling – it was truly fun working with you all.
- I would also like to express my gratitude to the internal reviewers Indrek Koppel and Aili tagoma for dedicating time to evaluate my thesis and for offering suggestions for its improvement.
- Furthermore, thanks to my friends who made Tartu feel like home – Sudhi, Arun, Ruby, Qurat, Gracy, Rathi, Vivi, Punya, Sharvari and Sandeep.
- I would also like to thank to my mother, Chandrika, and my sister, Selva, for their love and encouragement from afar.
- A very special thanks to my husband, Kapil, has simple but effective strategy just telling me to “go on” which somehow always worked. And my daughter, Ela, for spending so much time with me at university that she might as well receive an honorary degree! Their love and support have been my greatest strength.
- Finally, I dedicate this thesis to my father, Chithanathan. His battle with glioma led me to explore neuroscience and that journey into a passion.

This study was supported by the Estonian Research Council personal research funding team grants PRG878 and PRG1259, European Regional Development Fund (Project No. 2014-2020.4.01.15-0012) and Estonian Research Council-European Union Regional Developmental Fund Mobilitas Pluss Program No. MOBTT77.

12. PUBLICATIONS

CURRICULUM VITAE

Name: Keerthana Chithanathan
Date of birth: September 27th, 1994
E-mail: keerthana.chithanathan@ut.ee,
keerthanachithanathan@gmail.com
Telephone: +37258822089, +919688237868

Education and employment

2025	Specialist, RNA Biology Research Group, University of Tartu
2023–2024	Specialist of Pharmacology, University of Tartu
2019–....	Doctoral studies in neuroscience, University of Tartu
2017–2019	Indian Institute of Science, India – Research Assistant
2018	University of Valencia, Spain – Visiting student
2016–2017	National Brain research Centre, India – Master student
2012–2017	Integrated master of Science (Int. M.Sc), Department of Biomedical sciences, University of Bharathidasan University, Tamilnadu, India

Awards & stipends

2024	Valda and Bernard Õun scholarship
2019	DORA+ stipend to visit Claudio Rivera's group at the HiLife-Neuroscience Center, University of Helsinki, Finland
2016	IASc-INSA-NASI summer research fellowship

Professional training

2023	Hands-on training course for beginners in confocal microscopy, University of Tartu
2019	Laboratory animal science course, Estonian University of Life sciences
2016	Centre for DNA Fingerprinting and Diagnostics, India

Main research fields – Neuroscience, Neuroimmunology

List of publications

1. Jürgenson Monika, **Keerthana Chithanathan**, Aivar Orav, Külli Jaako, Janeli Viil, Mithu Guha, Kalev Kask, and Alexander Zharkovsky. "Elocalcitol, a fluorinated vitamin D derivative, prevents high-fat diet-induced obesity via SCAP downregulation and miR-146a-associated mechanisms." Frontiers in Pharmacology 15 (2025): 1505729
2. **Chithanathan Keerthana**, Monika Jürgenson, Katrina Ducena, Anu Remm, Kalev Kask, Ana Rebane, Li Tian, and Alexander Zharkovsky. Elocalcitol mitigates high-fat diet-induced microglial senescence via miR-146a modulation. *Immunity & Ageing* 21, no. 1 (2024): 82. DOI: 10.1186/s12979-024-00485-6

3. Ling Yan, Yanli Li, Fengmei Fan, Mengzhuang Gou, Fangling Xuan, Wei Feng, **Keerthana Chithanathan**, Wei Li, Junchao Huang, Hongna Li, Wenjin Chen, Baopeng Tian, Zhiren Wang, Shuping Tan, Alexander Zharkovsky, L Elliot Hong, Yunlong Tan, Li Tian (2023). CSF1R regulates schizophrenia-related stress response and vascular association of microglia/ macrophages. *BMC medicine.* https://doi.org/10.1186/s12916-023-02959-8.
4. Reddy Peera Kommaddi, Aditi Verma, Graciela Muniz-Terrera, Vivek Tiwari, **Keerthana Chithanathan**, Latha Diwakar, Ruturaj Gowaikar, Smitha Karunakaran, Palash Kumar Malo, Neill R Graff-Radford, Gregory S Day, Christoph Laske, Jonathan Vöglein, Georg Nübling, Takeshi Ikeuchi, Kensaku Kasuga, Dominantly Inherited Alzheimer Network (DIAN), Vijayalakshmi Ravindranath (2023). Sex difference in evolution of cognitive decline: studies on mouse model and the Dominantly Inherited Alzheimer Network cohort. *Translational psychiatry*. https://doi.org/10.1038/s41398-023-02411-8.
5. **Keerthana Chithanathan**, Monika Jürgenson, Mithu Guha, Ling Yan, Tamara Žarkovskaja, Martin Pook, Nathaniel Magilnick, Mark P Boldin, Ana Rebane, Li Tian, Alexander Zharkovsky (2022). Paradoxical attenuation of neuroinflammatory response upon LPS challenge in miR-146b deficient mice. *Frontiers in Immunology*. https://doi.org/10.3389/fimmu.2022.996415.
6. Fang-Ling Xuan, Ling Yan, Yanli Li, Fengmei Fan, Hu Deng, Mengzhuang Gou, **Keerthana Chithanathan**, Indrek Heinla, Liang Yuan, Kadri Seppa, Alexander Zharkovsky, Anti Kalda, L Elliot Hong, Guo-Fu Hu, Yunlong Tan, Li Tian (2022). Glial receptor PLXNB2 regulates schizophrenia-related stress perception via the amygdala. *Frontiers in immunology*. https://doi.org/10.3389/fimmu.2022.1005067.
7. **Keerthana Chithanathan**, Kelli Somelar, Monika Jürgenson, Tamara Žarkovskaja, Kapilraj Periyasamy, Ling Yan, Nathaniel Magilnick, Mark P Boldin, Ana Rebane, Li Tian, Alexander Zharkovsky (2022). Enhanced cognition and neurogenesis in miR-146b deficient mice. *Cells*. https://doi.org/10.3390/cells11132002.
8. **Keerthana Chithanathan**, Fang-Ling Xuan, Miriam Ann Hickey, Li Tian (2022). Enhanced anxiety and olfactory microglial activation in early-stage familial alzheimer's disease mouse model. *Biology*.https://doi.org/10.3390/biology11060938.
9. Maria Piirsalu, **Keerthana Chithanathan**, Mohan Jayaram, Tanel Visnapuu, Kersti Lilleväli, Mihkel Zilmer, Eero Vasar (2022). Lipopolysaccharide-induced strain-specific differences in neuroinflammation and MHC-I pathway regulation in the brains of Bl6 and 129Sv mice. *Cells*. https://doi.org/10.3390/cells11061032.
10. Reddy Peera Kommaddi, Latha Diwakar, Ruturaj Gowaikar, **Keerthana Chithanathan**, Smitha Karunakaran, Vijayalakshmi Ravindranath (2021). Sex-specific differences in cognitive functions and synaptic dysfunction in an Alzheimer's disease mouse model. *Alzheimer's & Dementia.* https://doi.org/10.1002/alz.052825.

11. Ling Yan, Mohan Jayaram, **Keerthana Chithanathan**, Alexander Zharkovsky, Li Tian (2021). Sex-specific microglial activation and SARS-CoV-2 receptor expression induced by chronic unpredictable stress. *Frontiers in Cellular Neuroscience*. https://doi.org/10.3389/fncel.2021.750373.
12. Sami Piirainen, **Keerthana Chithanathan**, Kanchan Bisht, Maria Piirsalu, Julie Conner Savage, Marie-Eve Tremblay, Li Tian (2021). Microglia contribute to social behavioral adaptation to chronic stress. *Glia*. https://doi.org/10.1002/glia.24053.
13. Latha Diwakar, Ruturaj Gowaikar, **Keerthana Chithanathan**, Barathan Gnanabharathi, Deepika Singh Tomar, Vijayalakshmi Ravindranath (2021). Endothelin-1 mediated vasoconstriction leads to memory impairment and synaptic dysfunction. *Scientific reports*. https://doi.org/10.1038/s41598-021-84258-x.
14. Fang-Ling Xuan, **Keerthana Chithanathan**, Kersti Lilleväli, Xiaodong Yuan, Li Tian (2019). Differences of microglia in the brain and the spinal cord. *Frontiers in cellular neuroscience.* https://doi.org/10.3389/fncel.2019.00504

ELUOOKIRJELDUS

Nimi: Keerthana Chithanathan
Sünniaeg: 27. September 1994
E-mail: keerthana.chithanathan@ut.ee, keerthanachithanathan@gmail.com
Telefon: +37258822089, +91968827868

Haridustee ja teenistuskäik

2025 Spetsialist, RNA bioloogia uurimisgrupp, Bio- ja siirdemeditsiini instituut, Tartu Ülikool
2022–2024 Spetsialist, Farmakoloogia osakond, Bio- ja siirdemeditsiini instituut, Tartu Ülikool
2019–... Doktorantuur, Neuroteaduste doktorikool, Arstiteaduskond, Tartu Ülikool
2017–2019 Teadusassistent, India teadusinstituut, India
2018 Külalisüliõpilane, Valencia Ülikool, Hispaania
2016–2017 Magistrant, Riiklik Ajuuuringute keskus, India
2012–2017 Integreeritud teadusmagister (Int. M.Sc), Biomeditsiiniteaduste osakond, Bharathidasani Ülikool

Tunnustused ja stipendiumid

2024 Valda and Bernard Õun mälestusfondi stipendium
2019 DORA+ stipendium Claudio Rivera uurimisrühma külastamiseks HiLife Neuroteaduste Keskuses, Helsingi Ülikool, Soome
2016 IASc-INSA-NASI suvine teadusuuringute stipendium

Erialakoolitused

2023 Praktiline koolituskursus algajatele konfokaalmikroskoopias, Tartu Ülikool
2019 Katseloomateaduste kursus, Eesti Maaülikool
2016 DNA sõrmejäljestamise ja diagnostika keskus, India

Peamised uurimisvaldkonnad – Neuroteadus, neuroimmunoloogia

Publikatsioonid

1. Jürgenson Monika, **Keerthana Chithanathan**, Aivar Orav, Külli Jaako, Janeli Viil, Mithu Guha, Kalev Kask, and Aleksandr Zarkovski. “Elocalcitol, a fluorinated vitamin D derivative, prevents high-fat dietinduced obesity via SCAP downregulation and miR-146a-associated mechanisms.” Frontiers in Pharmacology 15: 1505729. https://doi.org/10.3389/fphar.2024.1505729
2. **Chithanathan Keerthana**, Monika Jürgenson, Katrina Ducena, Anu Remm, Kalev Kask, Ana Rebane, Li Tian, and Alexander Zharkovsky. Elocalcitol

mitigates high-fat diet-induced microglial senescence via miR-146a modulation. *Immunity & Ageing* 21, no. 1 (2024): 82. DOI: 10.1186/s12979-024-00485-6

3. Ling Yan, Yanli Li, Fengmei Fan, Mengzhuang Gou, Fangling Xuan, Wei Feng, **Keerthana Chithanathan**, Wei Li, Junchao Huang, Hongna Li, Wenjin Chen, Baopeng Tian, Zhiren Wang, Shuping Tan, Alexander Zharkovsky, L Elliot Hong, Yunlong Tan, Li Tian (2023). CSF1R regulates schizophrenia-related stress response and vascular association of microglia/macrophages. *BMC medicine.* https://doi.org/10.1186/s12916-023-02959-8.
4. Reddy Peera Kommaddi, Aditi Verma, Graciela Muniz-Terrera, Vivek Tiwari, **Keerthana Chithanathan**, Latha Diwakar, Ruturaj Gowaikar, Smitha Karunakaran, Palash Kumar Malo, Neill R Graff-Radford, Gregory S Day, Christoph Laske, Jonathan Vöglein, Georg Nübling, Takeshi Ikeuchi, Kensaku Kasuga, Dominantly Inherited Alzheimer Network (DIAN), Vijayalakshmi Ravindranath (2023). Sex difference in evolution of cognitive decline: studies on mouse model and the Dominantly Inherited Alzheimer Network cohort. *Translational psychiatry*. https://doi.org/10.1038/s41398-023-02411-8.
5. **Keerthana Chithanathan**, Monika Jürgenson, Mithu Guha, Ling Yan, Tamara Žarkovskaja, Martin Pook, Nathaniel Magilnick, Mark P Boldin, Ana Rebane, Li Tian, Alexander Zharkovsky (2022). Paradoxical attenuation of neuroinflammatory response upon LPS challenge in miR-146b deficient mice. *Frontiers in Immunology*. https://doi.org/10.3389/fimmu.2022.996415.
6. Fang-Ling Xuan, Ling Yan, Yanli Li, Fengmei Fan, Hu Deng, Mengzhuang Gou, **Keerthana Chithanathan**, Indrek Heinla, Liang Yuan, Kadri Seppa, Alexander Zharkovsky, Anti Kalda, L Elliot Hong, Guo-Fu Hu, Yunlong Tan, Li Tian (2022). Glial receptor PLXNB2 regulates schizophrenia-related stress perception via the amygdala. *Frontiers in immunology*. https://doi.org/10.3389/fimmu.2022.1005067.
7. **Keerthana Chithanathan**, Kelli Somelar, Monika Jürgenson, Tamara Žarkovskaja, Kapilraj Periyasamy, Ling Yan, Nathaniel Magilnick, Mark P Boldin, Ana Rebane, Li Tian, Alexander Zharkovsky (2022). Enhanced cognition and neurogenesis in miR-146b deficient mice. *Cells*. https://doi.org/10.3390/cells11132002.
8. **Keerthana Chithanathan**, Fang-Ling Xuan, Miriam Ann Hickey, Li Tian (2022). Enhanced anxiety and olfactory microglial activation in early-stage familial alzheimer's disease mouse model. *Biology*.https://doi.org/10.3390/biology11060938.
9. Maria Piirsalu, **Keerthana Chithanathan**, Mohan Jayaram, Tanel Visnapuu, Kersti Lilleväli, Mihkel Zilmer, Eero Vasar (2022). Lipopolysaccharide-induced strain-specific differences in neuroinflammation and MHC-I pathway regulation in the brains of Bl6 and 129Sv mice. *Cells*. https://doi.org/10.3390/cells11061032.
10. Reddy Peera Kommaddi, Latha Diwakar, Ruturaj Gowaikar, **Keerthana Chithanathan**, Smitha Karunakaran, Vijayalakshmi Ravindranath (2021).

Sex-specific differences in cognitive functions and synaptic dysfunction in an Alzheimer's disease mouse model. *Alzheimer's & Dementia.* https://doi.org/10.1002/alz.052825.

11. Ling Yan, Mohan Jayaram, **Keerthana Chithanathan**, Alexander Zharkovsky, Li Tian (2021). Sex-specific microglial activation and SARS-CoV-2 receptor expression induced by chronic unpredictable stress. *Frontiers in Cellular Neuroscience*. https://doi.org/10.3389/fncel.2021.750373.
12. Sami Piirainen, **Keerthana Chithanathan**, Kanchan Bisht, Maria Piirsalu, Julie Conner Savage, Marie-Eve Tremblay, Li Tian (2021). Microglia contribute to social behavioral adaptation to chronic stress. *Glia*. https://doi.org/10.1002/glia.24053.
13. Latha Diwakar, Ruturaj Gowaikar, **Keerthana Chithanathan**, Barathan Gnanabharathi, Deepika Singh Tomar, Vijayalakshmi Ravindranath (2021). Endothelin-1 mediated vasoconstriction leads to memory impairment and synaptic dysfunction. *Scientific reports*. https://doi.org/10.1038/s41598-021-84258-x.
14. Fang-Ling Xuan, **Keerthana Chithanathan**, Kersti Lilleväli, Xiaodong Yuan, Li Tian (2019). Differences of microglia in the brain and the spinal cord. *Frontiers in cellular neuroscience.* https://doi.org/10.3389/fncel.2019.00504

DISSERTATIONES NEUROSCIENTIAE UNIVERSITATIS TARTUENSIS

1. **Sirli Raud.** Cholecystokinin$_2$ receptor deficient mice: changes in function of GABA-ergic system. Tartu, 2005.
2. **Kati Koido.** Single-nucleotide polymorphism profiling of 22 candidate genes in mood and anxiety disorders. Tartu, 2005.
3. **Dzhamilja Safiulina.** The studies of mitochondria in cultured cerebellar granule neurons: characterization of mitochondrial function, volume homeostasis and interaction with neurosteroids. Tartu, 2006.
4. **Tarmo Areda.** Behavioural and neurogenetic study of mechanisms related to cat odour induced anxiety in rodents. Tartu, 2006.
5. **Aleksei Nelovkov.** Behavioural and neurogenetic study of molecular mechanisms involved in regulation of exploratory behaviour in rodents. Tartu, 2006.
6. **Annika Vaarmann**. The studies on cystatin B deficient mice: neurochemical and behavioural alterations in animal model of progressive myoclonus epilepsy of Unverricht-Lundborg type. Tartu, 2007.
7. **Urho Abramov.** Sex and environmental factors determine the behavioural phenotype of mice lacking CCK_2 receptors: implications for the behavioural studies in transgenic lines. Tartu, 2008.
8. **Hendrik Luuk.** Distribution and behavioral effects of WFS1 protein in the central nervous system. Tartu, 2009.
9. **Anne Must.** Studies on molecular genetics of male completed suicide in Estonian population. Tartu, 2009.
10. **Kaido Kurrikoff**. Involvement of cholecystokinin in chronic pain mechanisms and endogenous antinociception. Tartu, 2009.
11. **Anu Aonurm-Helm.** Depression-like phenotype and altered intracellular signalling in neural cell adhesion molecule (NCAM)-deficient mice. Tartu, 2010.
12. **Silva Sütt.** Role of endocannabinoid system and *Wfs1* in regulation of emotional behaviour: behavioural, pharmacological and genetic studies. Tartu, 2010.
13. **Mari-Anne Philips.** Characterization of *Myg1* gene and protein: expression patterns, subcellular localization, gene deficient mouse and functional polymorphisms in human. Tartu, 2010.
14. **Ranno Rätsep.** Genetics of psoriasis and vitiligo, focus on IL10 family cytokines. Tartu, 2010.
15. **Kairit Joost.** Selective screening of metabolic diseases in Estonia: the application of new diagnostic methods. Tartu, 2012, 143 p.
16. **Monika Jürgenson.** A complex phenotype in mice with partial or complete deficiency of the NCAM protein. Tartu, 2012, 117 p.
17. **Ene Reimann.** Description of the cytokines and cutaneous neuroendocrine system in the development of vitiligo. Tartu, 2012, 117 p.

18. **Jürgen Innos.** Behavioural, pharmacological and neurochemical characterisation of limbic system-associated membrane protein (LSAMP) deficient mice. Tartu, 2013, 113 p.
19. **Kaili Anier.** The role of DNA methylation in the development of cocaine-induced behavioural sensitisation. Tartu, 2013, 147 p.
20. **Maarika Liik.** Cognitive functioning, perceived cognition, subjective complaints and symptoms of depression in patients with epilepsy: neuropsychological assessment and spet brain imaging study. Tartu, 2014, 124 p.
21. **Sten Ilmjärv.** Estimating differential expression from multiple indicators. Tartu, 2015, 125 p.
22. **Paula Reemann.** The effects of microenvironment on skin cells. Tartu, 2015, 146 p.
23. **Tanel Visnapuu.** Pharmacological and behavioral characterization of the monoaminergic and GABA-ergic systems of Wfs1-deficient mice. Tartu, 2015, 107 p.
24. **Indrek Heinla.** Behavioural and genetic comparison of B6 and 129Sv mouse lines focusing on the anxiety profile and the expression of *Lsamp* gene. Tartu, 2016, 115 p.
25. **Liina Haring.** Cognitive functioning after first psychotic episode. Tartu, 2017, 146 p.
26. **Triin Tekko.** Neurodevelopmental Approach in the Study of the Function of *Wfs1* and *Lsamp*, Potential Targets in the Regulation of Emotional Behaviour. Tartu, 2018, 194 p.
27. **Alina Altpere.** Targeting of mechanisms of elevated anxiety in female Wfs1-deficient mice. Tartu, 2018, 98 p.
28. **Maarja Toots.** Pharmacological challenge in rodent models of Wolfram syndrome with emphasis on diabetic phenotype. Tartu, 2018, 114 p.
29. **Katyayani Singh.** Neuropsychiatric endophenotypes – focusing on IgLON adhesion molecules in the mouse brain. Tartu, 2019, 148 p.
30. **Kattri-Liis Eskla.** Therapeutic strategies for ischemia reperfusion injury. Tartu, 2019, 138 p.
31. **Hardo Lilleväli**. Hyperphenylalaninaemias and neurophysiological disorders associated with the condition. Tartu, 2020, 134 p.
32. **Roman Balõtšev**. Interaction between the immune and metabolic systems in different stages of schizophrenia spectrum disorders. Tartu, 2020, 164 p.
33. **Mari Urb**. DNA methylation in the predisposition, expression and abstinence of cocaine addiction. Tartu, 2020, 147 p.
34. **Liisa Leppik.** Alterations in metabolomic profile of lipids, amino acids and biogenic amines in the early course of schizophrenia spectrum disorders. Tartu, 2021, 173 p.
35. **Kadri Seppa.** The neuroprotective effect of GLP-1 receptor agonist liraglutide in a rat model of Wolfram syndrome. Tartu, 2021, 154 p.
36. **Akbar Zeb.** The novel mechanisms of Parkin-dependent mitophagy. Tartu, 2022, 146 p.

37. **Aleksandr Bregin.** Alterations of emotional behaviour induced by the genetic invalidation of the limbic system associated membrane protein (Lsamp) – potential implications for neuropsychiatric disorders. Tartu, 2022, 176 p.
38. **Jane Varul.** Different stress coping strategies of 129Sv and C57/Bl6 mouse strains – evidence from behavioural, pharmacological, metabolomics and gene expression studies. Tartu, 2022, 177 p.
39. **Maria Kaare.** The involvement of NEGR1 and LSAMP in the psychiatric disorders are mediated through monoaminergic neurotransmission and changes in the systemic metabolism. Tartu, 2023, 164 p.
40. **Maria Piirsalu.** Effects of inflammation and diet on the metabolic profile and selected genetic parameters of Bl6 and 129Sv mouse lines. Tartu, 2023, 183 p.
41. **Taavi Vanaveski.** Modelling the quantitative nature of neuropsychiatric disorders in animal models: metabolic, behavioural, and genetic profiles. Tartu, 2023, 165 p.
42. **Keiu Heinla.** Effects of GLP-1 receptor agonists on pituitary and adrenal hormones. Tartu, 2023, 119 p.
43. **Ling Yan.** Stress-associated immune mechanisms of schizophrenia: the importance of region-specific microglia-neurovascular interaction. Tartu, 2023, 206 p.
44. **Fangling Xuan.** Regulation of stress response in first episode schizophrenia by monocytes and microglia. Tartu, 2024, 164 p.
45. **Katrin Tomson-Johanson.** Impulsivity, serum lipids and serotonin-related functional gene variants. Tartu, 2024, 145 p.
46. **Marite Punapart.** Effects of Valproate and Liraglutide in Rodent Models of Wolfram Syndrome: Emphasis on Transcriptomic Changes in the Renin–Angiotensin–Aldosterone System. Tartu, 2024, 166 p.